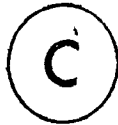


BULK ATTENUATION PROPERTIES  
OF  
TROPOSPHERIC AEROSOLS AS DETERMINED BY SURFACE MEASUREMENTS

By



TIMOTHY CHUKUEMEKA UBOEGBULAM

B.Sc., M.Sc.

A Thesis


Submitted to the School of Graduate Studies  
in Partial Fulfillment of the Requirements

for the Degree  
Doctor of Philosophy

MCMASTER UNIVERSITY

November 1981

BULK ATTENUATION PROPERTIES  
OF TROPOSPHERIC AEROSOLS

A handwritten signature or scribble consisting of several overlapping loops and lines, positioned in the upper left quadrant of the page.

Dedicated to my daughter Esther China

DOCTOR OF PHILOSOPHY (1981)  
(Geography)

MCMASTER UNIVERSITY  
Hamilton, Ontario

TITLE: Bulk Attenuation Properties of Tropospheric Aerosols as  
Determined by Surface Measurements

AUTHOR: Timothy Chukuemeka Uboegbulam,  
B.Sc., (Durham University, England),  
M.Sc., (McMaster University, Hamilton, Ontario)

SUPERVISOR: Professor J.A. Davies

NUMBER OF PAGES: xiii, 148

## ABSTRACT

Cloudless sky values of aerosol attenuation coefficient, scattering, absorption, recovery rate, bulk scattering albedo, and absorption to backscatter ratio were evaluated from surface measurements of global, diffuse, and direct beam irradiances for Montreal and Woodbridge (1968-78), Goose (1968 - 77), Charlottetown and Vancouver (1977 - 78), Winnipeg (1977), Hamilton (summer, 1977), and Sal (Cape Verde Islands, West Africa, summer, 1974).

The mean value of the coefficient ( $\sim 0.64$ ) indicates that turbidity of the Saharan dust at Sal is comparable to those of heavily industrialized cities of Europe and Eastern United States but in Canada, the mean values (0.10 - 0.20) for urban areas are less than those for similar cities in the world. The mean value at Goose ( $\sim 0.05$ ) is typical for the sub-Arctic. For the Canadian locations, maximum values of the coefficient ( $\sim 0.64$  for Montreal) occur in summer and the minimum (0.001) in winter but at Sal, maximum values ( $> 1.0$ ) are reached during the Saharan dust outbreaks that occur once in 4 to 5 days in summer.

Comparison of some meteorological parameters with the values of the coefficient for Montreal and Woodbridge show: a slight inverse relationship with windspeed; maximum values that are generally associated with winds from between southwest and southeast and minimum values associated with winds from between northwest and northeast; a direct positive corre-

lation with dew point temperature and also for relative humidity  $< 70\%$ ; that for visibility more than 10 km there is a strong linear relationship between turbidity and the inverse of visibility.

Mean annual values of the coefficient indicate significant downward trends in cloudless sky turbidity at Montreal and Woodbridge from 1968 to 1978 and at Goose from 1968 to 1977.

The amount of radiation scattered in a forward direction (downward) by aerosol is much larger at Sal (about 42% of global irradiance) than in Canada (6 - 13% of global irradiance). In Canada, aerosol absorption and backscatter are respectively 2-9% and 2-3% of global irradiance compared with 10% absorption and 7% backscatter at Sal. Aerosol recovery rates are least at Montreal. Estimates of bulk scattering albedo for Canadian urban sites (0.6 to 0.8) fall within the range of single scattering albedo values for American locations.

Mean values of the absorption to backscatter ratio indicate that, considering the solar radiation balance, aerosols over Montreal, Woodbridge, Hamilton and Goose could induce warming of the Earth-atmosphere system. Aerosols over Vancouver, Winnipeg, Charlottetown and Sal could induce cooling of the system.

## ACKNOWLEDGEMENTS

I appreciate the study-leave and bursary from the Alvan Ikoku College of Education, Owerri, Nigeria and also grants (through Dr. J.A. Davies) from the National Science and Engineering Research Council of Canada which made this study possible. I am also indebted to the Geography Department and the School of Graduate Studies, McMaster University and my friends at St. Cuthbert's Church, Hamilton for moral and material support during 'periods of crisis'.

My sincere gratitude goes especially to my supervisor Dr. J.A. Davies whose guidance and assistance went beyond the normal requirements and materials for this research. I would like also to acknowledge the helpful advise of Dr. W.R. Rouse and Dr. G.P. Harris, the other members of my supervisory committee. I am grateful to Dr. J.E. Hay of the Department of Geography, University of British Columbia for supplying the Vancouver data; to Dr. T.N. Carlson of the Department of Meteorology, Pennsylvania State University and Dr. J.M. Prospero of Rosenstiel School of Marine and Atmospheric Science, University of Miami, for providing data for Sal. I wish to thank Mr. Michael Yu for advice and help with the computer programmes and also Dr. P.D.M. Macdonald of the Department of Mathematical Sciences McMaster University for suggestions on the application of Cox's test for trend. My gratitude also extends to Mrs. Barbara Holdcroft for typing the manuscript,

Miss. Libby Ginn for cartographic assistance, and my past and present colleagues in the Climatology Laboratory for good company and meaningful discussions.

Finally, I am indebted to my parents for giving me the opportunity for education and my wife, Joyce, and my entire family for their patience in enduring limited attention from me.



## TABLE OF CONTENTS

	Page
ABSTRACT	iii
ACKNOWLEDGEMENTS	v
TABLE OF CONTENTS	vii
LIST OF DIAGRAMS	x
LIST OF TABLES	xii
1 INTRODUCTION	1
1.1 Relevance of the study	1
1.2 Aerosol studies and problems	2
1.3 Objective and outline of study	5
2 THEORETICAL BACKGROUND	7
2.1 Optical properties of aerosols	7
2.1.1 Evaluation of optical depth and single scattering albedo	8
2.1.2 Separation of aerosol absorption and scattering	11
2.2 MAC model (Davies, 1980)	13
2.3 Models used for aerosol turbidity	15
2.3.1 Unsworth and Monteith (1972) model	16
2.3.2 Linke's (1942) model	17
2.3.3 Polavarapu's (1978) model	18
2.3.4 Turbidity and visibility	19
2.4 Evaluation of aerosol scattering and absorption	22
2.4.1 Robinson's (1962) method	22
2.4.2 Recovery rate	23
2.4.3 Bulk scattering albedo $W_b$	26
2.5 Climatic impact of aerosols	26
2.5.1 Joseph and Wolfson (1975) method	27
3 DATA SELECTION AND CALCULATION OF PARAMETERS	30
3.1 Sources of data	30
3.1.1 Measured components of solar radiation and meteorological data	30

	Page	
3.1.2	Ozone	31
3.1.3	Radiosonde data and precipitable water	31
3.2	Processing of data	32
3.3	Calculation of parameters	33
3.3.1	Astronomical parameters	33
3.3.2	Ozone and molecular transmissions	35
3.3.3	Water vapour absorption	36
3.3.4	Correction for diffuse radiation	38
3.3.5	Diffuse radiation component (multiple reflection term) and Linke's turbidity parameters	39
4	TURBIDITY	41
4.1	Aerosol attenuation coefficient $\tau_a$	41
4.1.1	Diurnal and daily variation	46
4.1.1.1	Diurnal variation	46
4.1.1.2	Daily variation	51
4.1.2	Monthly and seasonal variation	52
4.1.2.1	Monthly variation	52
4.1.2.2	Seasonal variation	56
4.1.2.3	Charlottetown, Hamilton, Winnipeg and Vancouver	60
4.1.3	Sal - Tropical desert aerosol location	63
4.1.3.1	Mean $\tau_a$	63
4.1.3.2	Daily variation	65
4.1.4	Dependence of $\tau_a$ values on meteorological parameters	66
4.1.4.1	Dependence on surface windspeed and direction	68
4.1.4.2	Dependence on dew point temperature and relative humidity	70
4.2	Turbidity and visibility	74
4.2.1	$\tau_a$ and visibility	77
4.2.2	$\tau_{ak}$ calculated with Koschmieder formula	81
4.3	Turbidity trends	82
4.4	Turbidity coefficients compared	89

	Page	
5	BULK SCATTERING AND ABSORPTION PROPERTIES	93
5.1	Introduction	93
5.2	Scattering and absorption	94
5.3	Recovery rate $R_a$	103
5.4	Bulk scattering albedo $W_b$	108
5.5	Radiative significance of absorption and scattering	113
6	SUMMARY AND CONCLUSIONS	119
	APPENDIX 1 LIST OF SYMBOLS	123
	APPENDIX 2 TOTAL RECORDS AND DAYS OF DATA AT ALL STATIONS	128
	APPENDIX 3 THE EFFECT OF CHANGES IN OZONE TRANSMISSION ON $\tau_a$ AT WOODBRIDGE	129
	APPENDIX 4 MEAN MAXIMUM AND MINIMUM VALUES OF $\tau_a$ FOR CANADIAN LOCATIONS	130
	APPENDIX 5a SEASONAL FREQUENCY DISTRIBUTION OF THE NUMBER OF OCCURRENCES OF CORRESPONDING $\tau_a$ AND DRY BULB TEMPERATURE VALUES FOR MONTREAL (1968 - 78)	131
	APPENDIX 5b SEASONAL FREQUENCY DISTRIBUTION OF THE NUMBER OF OCCURRENCES OF CORRESPONDING $\tau_a$ AND WET BULB TEMPERATURE VALUES FOR MONTREAL (1968 - 78)	132
	APPENDIX 6 CORRELATION BETWEEN VALUES OF $\tau_a$ AND INVERSE OF VISIBILITY AT MONTREAL (1968 - 78)	133
	APPENDIX 7 ANNUAL CHANGES IN VALUES OF $\tau_a$ AT MONTREAL, WOODBRIDGE AND GOOSE	134
	APPENDIX 8 $T_{pm}/\tau_a$ FOR HAMILTON AND WOODBRIDGE	135
	APPENDIX 9 MEAN VALUES OF ABSORPTION, SCATTERING, AND SOLAR IRRADIANCES FROM OTHER SOURCES	136
	REFERENCES	137

LIST OF DIAGRAMS

FIGURE		Page
2.1	Aerosol forward-to-back scatter ratio	24
2.2	Schematic diagram of solar flux densities in a reflecting and absorbing aerosol layer above a surface	28
4.1	Cloudless sky direct beam irradiance at Woodbridge, 1976 - 78	42
4.2	Diurnal variation of mean hourly values of $\tau_a$ at Montreal, Woodbridge and Goose	47
4.3	Diurnal variation of mean hourly values of $\tau_a$ at Vancouver and Hamilton	49
4.4	Daily variations in $\tau_a$ values due to changes in air mass type	53
4.5	Mean monthly values of $\tau_a$ for Montreal, Woodbridge and Goose	54
4.6	Seasonal histograms of the frequency of occurrence of hourly values of $\tau_a$ at Montreal, Woodbridge and Goose	58
4.7	$\tau_a$ values compared with sunphotometer measurements at Sal (1974)	67
4.8	The inverse relationship between values of $\tau_a$ and windspeed: (a) at Montreal for two days; (b) at Montreal and Woodbridge, 1968 - 78	71
4.9	Polar plot of mean values of $\tau_a$ along the radial axis vs wind direction at Montreal, 1968-78	72
4.10	Polar plot of mean values of $\tau_a$ along the radial axis vs wind direction at Woodbridge, 1968 - 78	73
4.11	The inverse relationship between values of $\tau_a$ and visibility (km) for eight classes of wind direction at Montreal and Woodbridge, 1968 - 78	79
4.12	Two regime relationship between values of $\tau_a$ and the inverse of visibility at Montreal and Woodbridge, 1968 - 78	80

	Page
4.13 Values of $\tau_a$ and $\tau_{ak}$ compared for two sets of aerosol scale height and altitude for Montreal, 1968 - 78	83
4.14 Trends in monthly and seasonal values of $\tau_a$ at Montreal Woodbridge and Goose	86
4.15 Values of $\tau_a$ and $T_p$ compared	91
4.16 Ratios of $T_p/\tau_a$ , $T_{df}/T_{dfm}$ for 3 days at Hamilton	92
5.1 Aerosol recovery rates	107
5.2 Absorption to backscatter ratio as a function of surface albedo	117
5.3 Absorption to backscatter ratio as a function of zenith angle	118

LIST OF TABLES

TABLE		Page
1.1	Sources and estimates of global particle production	3
2.1	Ratio of forward-to-back scatter	23
3.1	Transmissivity after Rayleigh scattering	36
3.2	Shade ring correction factors for AES diffusograph	39
3.3	Range of surface albedo used at stations	40
3.4	P(m) values used for Linke's turbidity factor	40
4.1	Pyrheliometric measurements and residual estimates compared	41
4.2	Direct beam transmittance for the Braslau and Dave (1973) model B atmosphere (B + D) and MAC model compared	43
4.3a	Probable absolute error in $\tau_a$ values	44
4.3b	Relative error in $\tau_a$ values	45
4.4	Hourly $\tau_a$ percent departure from daily mean value at Montreal	50
4.5	Seasonal groups of $\tau_a$ values for Montreal and Woodbridge (1968 -78) and Goose (1968 - 77)	55
4.6	Monthly relative frequency of values of $\tau_a < 0.07$ and $\tau_a > 0.25$ at Montreal and Woodbridge (1968 - 78) and Goose (1968 - 77)	57
4.7	Monthly and seasonal $\tau_a$ values for the Canadian stations (1977 - 78)	61
4.8	Mean $\tau_a$ values for Hamilton and Woodbridge for the same days.	62
4.9	Values of $\tau_a$ for Sal and other locations compared	64
4.10	Mean seasonal $\tau_a$ and number of hourly values in four classes of windspeed at Montreal (1968 - 78)	69
4.11	Mean seasonal $\tau_a$ and number of hourly values in four classes of relative humidity at Montreal and Woodbridge (1968 - 78)	75

	Page	
4.12	Seasonal frequency distribution of the number of occurrences of corresponding $\tau_a$ and dew point temperature values for Montreal (1968 - 78)	76
4.13	Seasonal frequency distribution of the number of occurrences of corresponding $\tau_a$ and visibility values for Montreal (1968 - 78)	78
4.14	Correlation between values of $\tau_a$ and inverse of visibility at Montreal (1968 - 78)	81
4.15	Cox's test for $\tau_a$ trend at Montreal, Woodbridge and Goose	85
5.1	Global and diffuse irradiances for the Braslau and Dave (1973) model B atmosphere (B + D) and MAC model compared	94
5.2	Mean values (for specific zenith angles) of absorption, scattering and solar irradiances as fractions of extraterrestrial irradiance	96/97
5.3	Mean values of absorption, scattering and solar irradiances as fractions of extraterrestrial irradiance	98
5.4	Some days when absorption exceeds total scattering at Montreal and Woodbridge	100
5.5	Relative contributions of absorption, forward and backscattering to the extinction of global irradiance	101
5.6	Regression and mean hourly values of $R_a$ compared	106
5.7	Maximum and minimum values of hourly $R_a$ for Canadian sites	108
5.8	Range of $a/b \pm 5\%$ of the original value of 3.21 for $Z = 0^\circ$ and $\tau_a = 0.478$ at Sal (10.8.74)	109
5.9	Values of $W_b$ , $a/b$ and $g$ used in this study for Sal compared with those calculated with Delta-Eddington Approximation	111
5.10	Values of $W_b$ and $\omega_0$ compared	112
5.11	Sensitivity of $a/b$ to surface albedo at Vancouver (31 July, 1978)	113
5.12	Mean values of $a/b$ compared	116

INTRODUCTION

1.1 Relevance of the Study

Concern about possible changes in global climate (e.g., McCormick and Ludwig, 1967; Bryson, 1968; SCEP, 1970; SMIC, 1971; Daniel, 1980) and concomitant environmental, economic, and social consequence have stimulated interest in the radiative effects of aerosols (suspended particulates in the atmosphere) and carbon dioxide. Increasing carbon dioxide content is expected to warm the Earth-atmosphere system but the radiative effect of aerosols is still uncertain (e.g., Toon and Pollack, 1980; Charlock and Sellers, 1980).

In general, the amount of direct solar radiation which reaches the Earth's surface is reduced by aerosols through absorption and back-scattering while the amount of diffuse radiation received is increased. If other factors remain constant, increased aerosol absorption and diffuse radiation warm the system while increased backscattering cools it. Rational partitioning between aerosol absorption and scattering on the one hand, and between forward scattering and backward scattering on the other, have not been satisfactorily achieved and the amount of solar radiation attenuated by aerosols is a matter of conjecture.

The current energy crisis and the desire to have alternative energy sources have kindled new interest in solar energy studies for



industrial, agricultural, domestic, and commercial purposes. Therefore the calculation and analysis of solar energy reaching the Earth's surface requires the proper knowledge of the effects of aerosols.

## 1.2 Aerosol Studies and Problems

The problem of specifying correctly the effects of aerosols on solar radiation can be attributed to the nature of aerosols and the limitations in the practical sampling and modelling of aerosols in real atmospheres.

The sources (Table 1.1), sizes and time of residence of aerosols in the atmosphere vary enormously on local and regional scales over short or long time periods. This variation is compounded by the diffusion processes in the atmosphere resulting from frequent changes in wind speed and direction, and also by chemical processes in the atmosphere and the changes in the physical state of atmospheric water vapour in the troposphere.

Direct measurements of aerosols in the free atmosphere to obtain data on particle size distribution, concentration, chemical composition, scattering effects, and attenuation of radiation have been carried out by a number of scientists (e.g., Elterman, 1968; Volz, 1969; McClatchey et al., 1970; Bullrich, 1964; Junge, 1963; Prospero et al., 1976; DeLuisi et al., 1976) using optical and microphysical methods with various instruments mounted on balloons, aircraft, and rockets (Kondratyev, 1972). Because the experiments have not been carried out systematically,

TABLE 1.1 SOURCES AND ESTIMATES OF GLOBAL PARTICLE PRODUCTION  
(After Bach, 1976)

Source		All Sizes [ $10^6$ tons/yr.]
Total	Man-Made	408
Subtotal	Direct Particle Production	133.2
	Transportation	2.2
	Stationary Fuel Service	43.4
	Industrial Processes	56.4
	Solid Waste Disposal	2.4
	Miscellaneous	28.8
Subtotal	Particles Formed From Gases	275
	Converted Sulfates	220
	"    Nitrates	40
	"    Hydrocarbons	15
Total	Natural	2115
Subtotal	Direct Particle Production	1545
	Sea Salt	1000
	Windblown Dust	500
	Volcanic Emissions	25 (Particle < 5 m)
	Meteoric Debris	10
	Forest Fires	35
Subtotal	Particles Formed from Gases	570
	Converted Sulphates	420
	"    Nitrates	75
	"    Hydrocarbons	75
Grand total	Man-Made and Natural	2523

intercomparison of results is not easy and the data must be used with caution. The variability of aerosols in time and space, the high cost of direct in situ measurements of atmospheric aerosols, and the need to obtain reliable standard data, necessitate well co-ordinated programmes for comprehensive study of aerosols. Two programmes - the Complete Atmospheric Energetics Experiment (CAENEX:- Russian) and Global Atmospheric Aerosol and Radiation Study (GAARS:- American) - have been mounted in recent years (DeLuisi et al., 1976; Kondratyev, 1977).

Modelling the radiative effects of aerosols is more common than direct measurement. However, since there are many aerosol species and direct measurements are limited, theorists provide different solutions to the problem of the impact of aerosols on radiative transfer. Two groups of models are used to characterize the effects of aerosols on solar radiation. The first group uses the physical properties of aerosols, such as size, shape, refractive index, and concentration in the atmosphere to evaluate three fundamental optical properties - optical depth, single scattering albedo, and asymmetry factor, using Mie theory or modifications of it (e.g., Ensor et al., 1971; Carlson and Caverly, 1977; McCartney, 1975). The drawback in using these models is that data on the physical properties, especially the refractive index which determines the extent of absorption, are difficult to obtain. The models in this group are therefore limited in application.

The second group of models infer aerosol properties from measure-

ments of solar radiation in a cloudless atmosphere. Even though the models are less sophisticated they have proved useful in describing the effects of aerosols on solar radiation (e.g., Robinson, 1962; Unsworth and Monteith, 1972; Wesely and Lipschutz, 1976; DeLuigi et al., 1977; Davies, 1980). Since these models use solar radiation measurements which are easier to obtain than measurements of the physical properties of aerosols, they are capable of application over a wider area, for determining bulk properties of aerosols.

### 1.3 Objective and Outline of Study

This study uses simple models and surface measurements of solar radiation and meteorological elements in cloudless sky for contrasting atmospheric conditions, from 'clean' sub-Arctic to very dusty Tropical Saharan air, to investigate and categorize: (a) the variability of aerosol loading in time and space, (b) the bulk absorption and scattering properties of aerosols, and (c) the possible radiative effects of aerosols. The study also tests the performance of the models and where possible their compatibility with similar models.

Although complete assessment of the radiative and climatic effects of aerosols in the Earth-atmosphere system requires the consideration of the interactions between aerosols and both short wave and long wave radiation not only in the troposphere but also in the stratosphere, this study concentrates only on the interactions between aerosols and short wave radiation at the Earth's surface because few long wave irradiance measurements are available. This neglect is unlikely to be

serious since aerosol effects are larger on short wave radiation than on long wave radiation. According to Coakley (1977) the maximum change in the net solar radiative flux due to the presence of aerosols is about 8% and the maximum change in the net flux of terrestrial radiation is 2%. Paltridge and Platt (1976) also estimate that aerosol extinction optical depth in the visible region is about 10 times the extinction optical depth in the long wave region.

The models used in this study have received little attention from previous workers even though they are capable of large scale application with existing data. Aerosol loading is determined mainly with Unsworth and Monteith's (1972) model. Bulk absorption and scattering properties of aerosol are examined using the models of Robinson (1962), Wesely and Lipschutz (1976) and Davies (1980). Possible radiative effects are studied using the ratio of absorption to backscatter (Joseph and Wolfson, 1975).

## THEORETICAL BACKGROUND

2.1 Optical Properties of Aerosols

Radiative transfer in the atmosphere is given by

$$\frac{\mu \, dI_{\lambda}(\tau_{\lambda}, \mu, \phi)}{d\tau_{\lambda}} = -I_{\lambda}(\tau_{\lambda}, \mu, \phi) + \frac{\omega_{0\lambda}}{4\pi} \int_0^{2\pi} \int_0^1 I_{\lambda}(\tau_{\lambda}, \mu', \phi') \, d\mu' \, d\phi'$$

$$p_{\lambda}(\tau_{\lambda}, \mu', \phi' \rightarrow \mu, \phi) \, d\mu' \, d\phi' \tag{2.1}$$

Here,  $\tau$  is optical depth,  $\mu$  the cosine of the zenith angle,  $\omega_0$  the single scattering albedo,  $I_{\lambda}$  the spectral radiant intensity at wavelength  $\lambda$ , and  $p_{\lambda}$  the spectral scattering phase function which specifies the fraction of unpolarized incident radiation scattered from the direction  $\mu', \phi'$  into the direction  $\mu, \phi$ . The optical depth varies with atmospheric aerosol loading and is used to determine the total extinction of the solar beam. The single scattering albedo defines the fraction of the total extinction which is due to scattering by a single particle. If  $k_{\lambda}$  and  $\sigma_{\lambda}$  are mass absorption and scattering coefficients, the optical depth and single scattering albedo are given by

$$\tau_{\lambda} = \int_0^Z T(k_{\lambda} + \sigma_{\lambda}) \, dz \tag{2.2}$$

and

$$\omega_{0\lambda} = \sigma_{\lambda} / (k_{\lambda} + \sigma_{\lambda}) \tag{2.3}$$

where  $Z_T$  is the height of the aerosol atmosphere. The phase function can be usefully characterized by the asymmetry factor  $g_\lambda$  which is defined by

$$g_\lambda = \langle \cos \psi \rangle = \int_{-1}^{+1} p_\lambda(\cos \psi) \cos \psi \, d \cos \psi \quad (2.4)$$

where  $\psi$  is the scattering angle. Physically  $g$  is the difference between flux densities in the forward direction and backward direction arising from the scattering by a particle when the incident flux is normalized to 1 (Paltridge and Platt, 1976).

#### 2.1.1 Evaluation of Optical Depth and Single Scattering Albedo

Optical depth, single scattering albedo, and asymmetry factor are important optical properties which define the interaction of aerosols with solar radiation.  $\tau_\lambda$  can be directly measured in real atmosphere by photometry and lidar methods but the accuracy of these measurements are yet to be ascertained. Values of  $\omega_{0\lambda}$  and  $g_\lambda$  are not measured directly. Using measurements of solar radiation only,  $\tau_\lambda$  may be calculated by solving equation 2.1.

For direct beam radiation, the scattering integral in equation 2.1 can be neglected and integration gives

$$I_{\lambda}(\tau_{\lambda}) = I_{\lambda}(0)\exp(-\tau_{\lambda}/\mu) \quad (2.5)$$

where

$$\tau_{\lambda} = -\frac{1}{m} \ln[I_{\lambda}/I_{\lambda}(0)] \quad (2.6)$$

Here  $I_{\lambda}(0)$  is the spectral irradiance at the top of the atmosphere where  $\tau_{\lambda} = 0$ , and  $m = \frac{1}{\mu}$  is the optical air mass.

Values of  $\tau_{\lambda}$ ,  $\omega_{0\lambda}$ , and  $g_{\lambda}$  can be calculated from Mie theory if particle radius  $r$ , the complex index of refraction  $\eta = n_r - n_i$  ( $n_r$  = real part,  $n_i$  = imaginary part), and  $n(r)$  the size distribution function which depends on the particle concentration are known. There is no agreement as to the best distribution function, but three functions are commonly used: Junge (1963) power-law distribution function, Deirmendjian (1969) exponential (modified gamma) distribution function, and zero-order logarithmic distribution (Zold) function (Espencheid et al., 1964). The Junge function is normally used in turbidity calculation (Section, 2.3) and is given by

$$n(r) = Cr^{-v} \quad (2.7)$$

Here  $C$  is a constant that depends on the particle concentration and  $v$  is the slope of the size distribution curve. For a given wavelength  $\lambda$  and spherical particle of radius  $r$ , the Mie size parameter is defined by  $x = 2\pi r/\lambda$ .

Using the Mie extinction and scattering efficiencies,  $Q_{\text{ext}}$  and  $Q_{\text{sca}}$ , the



volume extinction and scattering coefficients:  $\beta_{\text{ext}}$  and  $\beta_{\text{sca}}$ , and the extinction and scattering cross-sections:  $\sigma_{\text{ext}}$  and  $\sigma_{\text{sca}}$ , can be evaluated from

$$\beta_{\text{ext}_\lambda} = \int_0^\infty \pi r^2 Q_{\text{ext}_\lambda}(x, \eta) n(r) dr \quad (2.8)$$

$$\beta_{\text{sca}_\lambda} = \int_0^\infty \pi r^2 Q_{\text{sca}_\lambda}(x, \eta) n(r) dr \quad (2.9)$$

$$\sigma_{\text{ext}_\lambda} = Q_{\text{ext}_\lambda}(x, \eta) \pi r^2 \quad (2.10)$$

$$\sigma_{\text{sca}_\lambda} = Q_{\text{sca}_\lambda}(x, \eta) \pi r^2 \quad (2.11)$$

The aerosol optical depth  $\tau_{a_\lambda}$  is obtained by integrating equation 2.8 from the surface to the top of the atmosphere  $Z_T$

$$\tau_{a_\lambda} = \int_0^{Z_T} \beta_{\text{ext}_\lambda} \quad (2.12)$$

The single scattering albedo is calculated from

$$\omega_{0\lambda} = \beta_{\text{sca}_\lambda} / \beta_{\text{ext}_\lambda} = \sigma_{\text{sca}_\lambda} / \sigma_{\text{ext}_\lambda} = Q_{\text{sca}_\lambda} / Q_{\text{ext}_\lambda} \quad (2.13)$$

### 2.1.2 Separation of Aerosol Absorption and Scattering

Although  $\omega_0$  gives an idea of how much scattering and absorption takes place, it does not separate absorption from backscatter or forward scatter. Aerosol backscatter and aerosol absorption to total scatter ratios are hard to measure in real atmospheres and no reliable method has yet been developed for their rational partitioning (Paltridge and Platt, 1976). The main problem is that the imaginary part of the complex index of refraction which determines the absorption characteristics of a particle is not well known. The problem is compounded by the temporal and spatial variability of aerosol sources, types, physical, and chemical properties. The partitioning is also affected by the complexities of multiple and anisotropic scattering; differences between scattering characteristics of molecules and those of particles; and variation with altitude of the amount of scattering of the direct beam (Wesely and Lipschutz, 1976).

Assuming the Junge (1963) power law size distribution function, the backscatter coefficient  $b_{bs}$  can be defined using Mie theory as

$$b_{bs} = \int_{r_1}^{r_2} Q_{bs} \pi r^2 n(r) dr \quad (2.14)$$

where  $Q_{bs}$  the Mie backscatter efficiency factor is obtained from

$$Q_{bs} = \frac{1}{x^2} \int_{\pi/2}^{\pi} [i_1(\psi) + i_2(\psi)] \sin \psi d\psi \quad (2.15)$$

Here  $i_1(\psi)$  and  $i_2(\psi)$  are the intensity of scattered light per solid angle polarized perpendicular or parallel, respectively, to the plane of scattering.

The absorption coefficient  $b_{\text{abs}}$  is related to the Mie absorption efficiency factor  $Q_{\text{abs}}$  by

$$b_{\text{abs}} = \int_{r_1}^r 2Q_{\text{abs}} \pi r^2 n(r) dr \quad (2.16)$$

In a 'two stream' approximation in which the diffuse radiation is assumed hemispherically isotropic,  $g$  becomes useful in separating aerosol backscatter from forward scatter.  $g$  is equal to  $+1$  and  $-1$  for complete scatter into the forward and backward directions respectively. From equation 2.4, the backscattered and forward scattered fractions  $B$  and  $F$  of the total scatter can be approximated (Paltridge and Platt, 1976) in terms of  $g$  as

$$B = (1 - g)/2 \quad (2.17)$$

and

$$F = (1 + g)/2 \quad (2.18)$$

Evaluation of  $\tau$ ,  $\omega_0$ , and  $g$  for the whole solar spectrum involves considerable calculation since the spectrum must be divided into a large number of parts. The Mie theory calculations involve not only the knowledge of the physical properties of the aerosols spectrally but also the application of series of complex equations. If the aim of using simple

models with readily available data to characterize aerosol effects on solar radiation is to be achieved, then the methods discussed above of evaluating the fundamental optical properties of aerosols must be modified or changed but with minimum loss of accuracy. Models used in this study set out to achieve this.

## 2.2 MAC Model (Davies, 1980)

The model calculates direct beam irradiance at the Earth's surface after allowing for transmission by molecules and gases and also absorption by water vapour. The diffuse radiation is calculated as the sum of three components due to Rayleigh scattering, aerosol scattering, and multiple reflections between the surface and the atmosphere. This treatment of the diffuse radiation is a unique feature of the model because previous studies have not explicitly separated the components especially on cloudless days. Global radiation is the sum of the direct beam and the three components of the diffuse radiation.

The model has been developed assuming:

- (a) horizontal plane-parallel atmosphere,
- (b) isotropic single scattering within a given hemisphere,
- (c) that water vapour only absorbs the direct beam irradiance, and its absorptance is additive (Paltridge, 1972),
- (d) that Beer's law can be applied to the whole solar spectrum.

Assumptions (a) and (b) allow the application of the two-stream approxi-

mation. Coakley and Chýlek (1975) have demonstrated the adequacy of the approximation especially for optically thin layers as is the case with most aerosol atmospheres.

The single scattering assumption gets round the problem of solving the phase function. The validity of the single scattering approximation depends primarily on the optical depth of the aerosol atmosphere. If the optical depth is small, it is assumed that radiation passing through the layer is scattered only once by the particles provided the interest is solar radiation reaching the surface. Twomey (1977) suggested that for many practical applications,  $\tau \ll 1$  can be regarded as thin and for most applications  $\tau < 0.10$  ensures that thin-layer approximations are accurate. Wesely and Lipschutz (1976) assumed that single scattering is dominant for surfaces with albedo less than 0.25. Davies and Hay (1980) have shown however that the MAC model yields results which are very similar to those obtained by Braslau and Dave (1973) for a model atmosphere which contains a scattering aerosol (Mie scattering optical depth = 0.10) and surface albedo values between 0.0 and 0.8.

Since the model is used in this study to calculate only the parameters in an aerosol-free atmosphere, the aerosol terms have been omitted. The direct beam is calculated from

$$I_o = I_*(T_{oz} \cdot T_R - a_w) \quad (2.19)$$

Here  $I_*$  is the extraterrestrial irradiance on a horizontal surface corrected for the Sun-Earth distance;  $T_{oz}$ ,  $T_R$  are transmittances due to gases (e.g., ozone) and molecules and are applied multiplicatively because both occur at similar wavelengths in the ultraviolet and visible parts of the solar spectrum;  $a_w$  is the water vapour absorption which is additive because it occurs in the near infrared not affected by  $T_{oz}$  and  $T_R$ .

The diffuse component  $D_R$  due to molecular scattering is calculated assuming that half of the radiation scattered by molecules reaches the surface (isotropic assumption).  $D_R$  is given by

$$D_R = I_* (1 - T_R) T_{oz} / 2 \quad (2.20)$$

The diffuse component  $D_S$  due to multiple reflections between the surface and the atmosphere is calculated from

$$D_S = \alpha_R \cdot \alpha_s (I_o + D_R) / (1 - \alpha_R \cdot \alpha_s) \quad (2.21)$$

Here,  $\alpha_R$  is the albedo of molecular atmosphere, and  $\alpha_s$  the surface albedo.

The diffuse radiation  $D_o$  is the sum of equations 2.20 and 2.21 i.e.,

$$D_o = D_R + D_S \quad (2.22)$$

The global radiation  $G_o$  is the sum of equations 2.19 and 2.22 i.e.,

$$G_o = I_o + D_o \quad (2.23)$$

### 2.3 Models used for Aerosol Turbidity

Turbidity refers to the total extinction of the solar beam by

aerosols at specific short wavelengths usually 0.55  $\mu\text{m}$  and 0.38  $\mu\text{m}$  but more commonly at 0.55  $\mu\text{m}$ . Turbidity models, for example, Ångström (1961) and Schüepp (1949) have been used for a long time. They give a satisfactory measure of total extinction of the solar beam in areas of high pollution but are not suitable for areas with "background" aerosol (Paltridge and Platt, 1976).

In this study, the models used refer to the whole solar spectrum and so may be called "integral turbidity" models.

### 2.3.1 Unsworth and Monteith (1972) Model

The model starts with Beer's law (equation 2.5) and arrives at an analogous form suitable for the whole solar spectrum. The optical depth  $\tau_\lambda$  may be written as the sum of four components representing gaseous absorption  $g$ , water vapour absorption  $w$ , Rayleigh scattering  $R$ , and aerosol extinction  $a$ .

$$\tau_\lambda = \tau_{g\lambda} + \tau_{w\lambda} + \tau_{R\lambda} + \tau_{a\lambda} \quad (2.24)$$

To isolate aerosol attenuation of solar radiation, equation 2.5 is put in a form in which the measured flux  $I_\lambda$  is compared with the model estimate  $I_{o\lambda}$  for clean atmosphere with the same amount of water vapour, gaseous absorbers and Rayleigh scatterers.  $I_\lambda$  is then expressed as

$$\begin{aligned} I_\lambda &= I_\lambda(o) [\exp-(\tau_{g\lambda} + \tau_{w\lambda} + \tau_{R\lambda})^m] [\exp-(\tau_{a\lambda})^m] \\ &= I_{o\lambda} \exp-(\tau_{a\lambda}^m) \end{aligned} \quad (2.25)$$

and

$$\tau_{a\lambda} = -\frac{1}{m} \ln(I_{\lambda}/I_{0\lambda}) \quad (2.26)$$

For the whole solar spectrum, Unsworth and Monteith defined an aerosol attenuation coefficient  $\tau_a$  as

$$\tau_a = -\frac{1}{m} \ln(I/I_0) \quad (2.27)$$

Here  $I$  and  $I_0$  are the measured and calculated values of direct beam irradiance measured normal to the horizontal surface. The main criticism of the model is the application of Beer's law to spectrally integrated quantities.

### 2.3.2 Linke's (1942) Model

This model also has its origin in Beer's law and calculates a turbidity factor  $T$ . Following equation 2.5,  $T$  is defined as

$$I = I_* \exp\{-T \cdot \tau_R(m)m\} \quad (2.28)$$

and  $T$  is evaluated from

$$T = P(m)(\log I_* - \log I) \quad (2.29)$$

Here  $P(m) = (m\tau_R(m)\log e)^{-1}$  and  $\tau_R(m)$  is the integral optical depth for Rayleigh atmosphere. Physically,  $T$  is the number of Rayleigh atmospheres needed to produce the same attenuation as the real atmosphere containing water vapour and aerosol.  $T$  is always greater than one since



$$\begin{aligned}
 T &= (\tau_g + \tau_R + \tau_a + \tau_w)m/\tau_R(m) \\
 &= 1 + (\tau_g + \tau_a + \tau_w)m/\tau_R(m)
 \end{aligned}
 \tag{2.30}$$

### 2.3.3 Polavarapu's (1978) Model

The model first calculates Linke's turbidity factor for an actual atmosphere and then corrects the result for water vapour absorption by subtracting from it Linke's turbidity factor for an ideal dust-free atmosphere with the same amount of water vapour. This involves applying an aerosol transmission factor to replace I in equation 2.29.

Following Yamamoto et al. (1968), the spectral transmission due to aerosols is given by

$$T_{a\lambda} = e^{-\beta\lambda^{-1}} \tag{2.31}$$

Here  $\beta$  is an aerosol turbidity coefficient obtained by assuming  $v = 4$  in the Junge size distribution function (equation 2.7) and integrating equation 2.8 with respect to the size parameter  $x$

$$\beta = 2\pi^2 C \int_0^{\infty} Q_{\text{ext}}(x, \eta) x^{-2} dx \tag{2.32}$$

An analogous expression to equation 2.31 is defined as the mean transmission  $T_a$  due to aerosols for the whole spectrum.

$$T_a(m, m\omega, m\beta) = I/I_0 \quad (2.33)$$

hence

$$I = I_0 T_a(m, m\omega, m\beta) \quad (2.34)$$

Linke's turbidity factor for dust free atmosphere  $T_{df}$  is calculated by assuming  $\beta = 0$ , hence  $T_a(m, m\omega, m\beta) = 1$ . Polavarapu's turbidity coefficient  $T_p$  is determined from

$$T_p = T - T_{df} \quad (2.35)$$

The relationship between Unsworth and Monteith model and Polavarapu Model can be established by re-writing equation 2.27 in the form

$$\tau_a = -\frac{1}{m} \ln(T_a)$$

where

$$T_a = e^{-m\tau_a} \quad (2.36)$$

#### 2.3.4 Turbidity and Visibility

Visibility is the distance that the human eye can see and therefore applies only to the visible part of the spectrum. In all conditions, scattering is the dominant determinant of visibility. The relationship between visibility and scattering is therefore given by the Koschmieder formula (McCartney, 1976)

$$v = \frac{1}{\beta_{sca}} \ln \frac{C}{\epsilon} \quad (2.37)$$

Here  $v$  is the visibility (km),  $C$  is the inherent contrast of the target against the background,  $\epsilon$  is the threshold contrast of the observer. If the target for specifying visibility is black, its inherent contrast against the sky is unity, i.e.,  $C = 1$ .  $\epsilon$  is taken equal to 0.02 and equation 2.37 becomes

$$v = 3.912/\beta_{sca} \quad (2.38)$$

The use of volume total scattering coefficient  $\beta_{sca}$  instead of the volume total extinction coefficient  $\beta_{ext}$  implies that absorption by atmospheric particles in the visible wavelengths is negligible (McCartney, 1976). In polluted atmospheres, this view may not be justified. However in conditions of low visibility, Patterson and Gillete (1977) suggested that  $\beta_{ext}$  is a valid substitute for  $\beta_p$  the volume total scattering coefficient for particles. It means that even  $\beta_{sca}$  is a better substitute for  $\beta_p$  since  $\beta_{sca}$  and  $\beta_p$  are more closely related as suggested by the following equations

$$\beta_{sca} = \beta_m + \beta_p \quad (2.39)$$

and

$$\beta_{ext} = \beta_m + \beta_p + \beta_{abs} \quad (2.40)$$

where  $\beta_m$  is the volume total scattering coefficient for molecules.

When only single scattering is involved, the attenuation coefficient  $\tau_a$  is independent of the spatial distribution of the particles and only their total number and scattering characteristics need be considered, hence the average particle concentration  $N_z$  at altitude  $Z$  may be represented (McCartney, 1976) by

$$N_z = N_0 \exp(-Z/H_p) \quad (2.41)$$

Here  $N_0$  is the concentration at ground level and  $H_p$  is the scale height for aerosol.  $H_p$  which can also be interpreted as the height of the homogeneous aerosol layer is independent of wavelength (Kriebel, 1978).

⇔

$\tau_a$  can be expressed in terms of  $Z$ ,  $H_p$ , and  $\beta_{sca}$  as

$$\tau_{ak} = \beta_{sca} \int_0^Z \exp(-Z/H_p) dZ \quad (2.42)$$

Integrating the equation yields

$$\tau_{ak} = H_p \beta_{sca} [1 - \exp(-Z_T/H_p)] \quad (2.43)$$

By substituting for  $\beta_{sca}$  from equation 2.38,  $\tau_{ak}$  can be expressed in terms of visibility.

$$\tau_{ak} = \frac{3.912 H_p}{v} [1 - \exp(-Z_T/H_p)] \quad (2.44)$$

Previous studies have concentrated mainly on the relationship between visibility and aerosol mass concentration (e.g., Charlson et al., 1968; Patterson and Gillette, 1977). Assuming that  $\tau_a$  at visible wavelength can represent the whole spectrum, the real problem in applying equation 2.44 lies in the uncertainties in values of visibility, scale height, and Z. The present study is one of the few, specifically, relating visibility and aerosol attenuation coefficient.

## 2.4 Evaluation of Aerosol Scattering and Absorption

### 2.4.1 Robinson's (1962) Method

Essentially the method defines aerosol scattering and absorption by comparing measured values of global and diffuse radiation with model values for an aerosol-free atmosphere.

Forward scatter  $f$  is defined as

$$f = D - D_0 \quad (2.45)$$

Where  $D$  is the measured diffuse and  $D_0$  the calculated diffuse for a model aerosol-free atmosphere.

Backscatter  $b$  was estimated by Robinson (1962) from numerically integrated values of Waldram's (1945) measured angular distributions of scattered radiation. The ratio  $f/b$  is tabulated by Robinson (his Table 2) as a function of zenith angle. A recent survey by Wiscombe and Grams

(1976) of the backscattered fraction in two-stream approximation, shows a diversity of methods and definitions of 'backscatter'. Values range from 0.01 to 0.20. Some of the values are assumed, a few are estimated from measurements (e.g., Robinson, 1962), and others calculated. Values are either given for a fixed zenith angle or as a function of zenith angle (e.g., Robinson, 1962, Table 2.1). Figure 2.1 indicates that Robinson's  $f/b$  compares well with ratios from other workers.

TABLE 2.1: RATIO OF FORWARD-TO-BACK SCATTER  
 $f/b$  (after Robinson, 1962)

solar zenith angle	0	25.8	36.9	45.6	53.1	60	66.4	72.5	78.5
$f/b$	12	10	8	6	5	3.5	2.5	2.0	1.5

Absorption by aerosols  $a$  is defined by

$$a = G_0 - G - b \quad (2.46)$$

Here  $G$  is the measured global and  $G_0$  the model global radiation.

By adopting Robinson's method, the uncertainties in the calculation of  $\omega_0$  and  $g$  in order to define scattering and absorption have been avoided.

#### 2.4.2 Recovery Rate

Aerosol recovery rate is defined as the fraction of the direct beam solar irradiance that is removed by aerosols and regained as diffuse

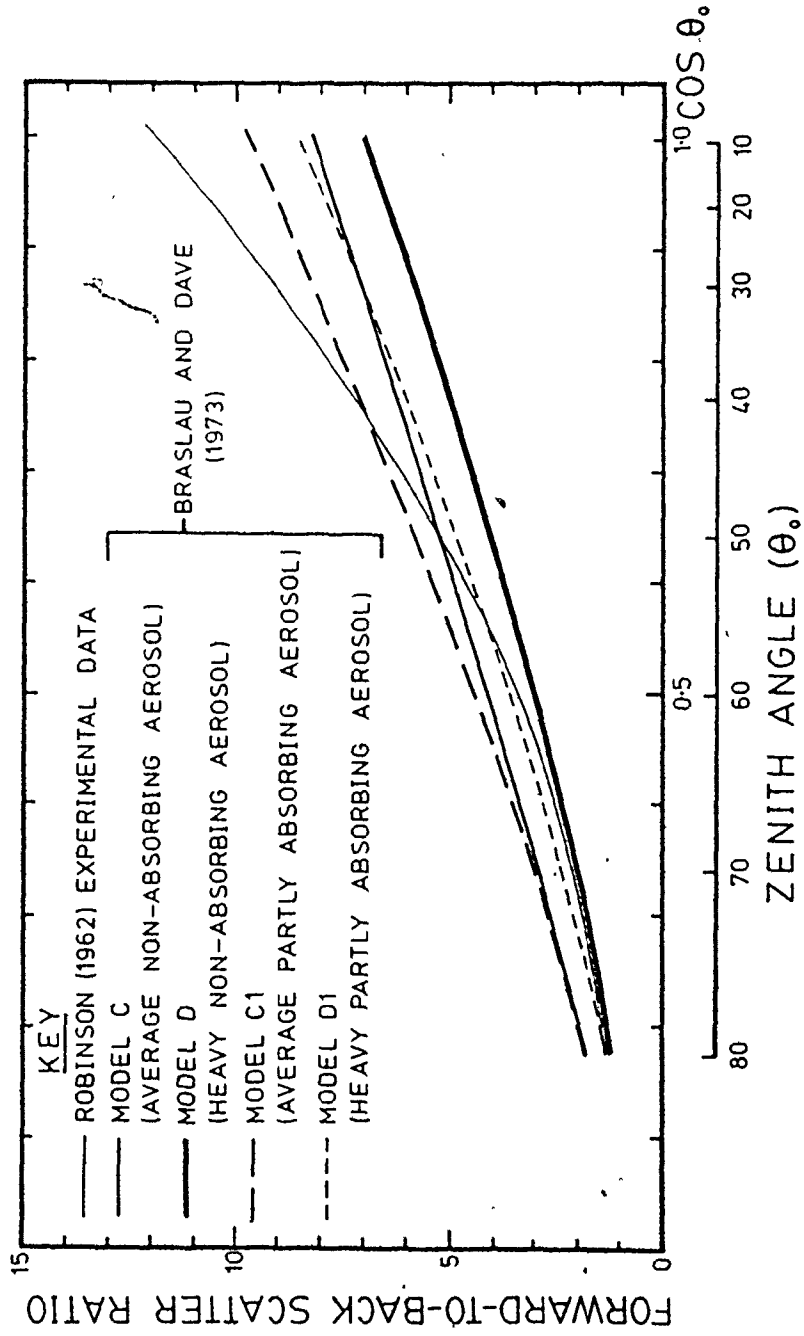


Figure 2.1. Aerosol forward-to-back scatter ratio.

radiation. The concept was applied by Unsworth and Monteith (1972) and elaborated by Wesely and Lipschutz (1976). It is important because,

- (a) the ratio of diffuse to direct beam irradiance is a sensitive indicator of turbidity since the effect of increased airborne particulates on solar radiation is to increase the amount of radiation absorbed, backscattered to space, and scattered forwards to the Earth's surface;
- (b) it assesses the extent to which the loss from the direct beam is compensated by increase in diffuse radiation.

The Wesely and Lipschutz method is based on a regression of measured diffuse irradiance  $D$  against measured direct beam irradiance  $I$  for a specified zenith angle over a period of time. The regression equation is of the form

$$D = A - B \cdot I \quad (2.47)$$

$$R_a = -dD/dI = B \quad (2.48)$$

Here  $R_a$  is the recovery rate,  $A$  and  $B$  are regression parameters.

Recovery rate can be evaluated for an instantaneous time or integrated short period, say an hour for a specified zenith angle. In this case  $R_a$  is defined as

$$R_a = (D - D_0)/(I_0 - I) \quad (2.49)$$



### 2.4.3 Bulk Scattering Albedo $W_b$

The MAC model can be used to calculate  $W_b$  as a residual. A similar approach was adopted by DeLuisi et al. (1977).  $W_b$  is analogous to  $\omega_0$  but while  $\omega_0$  represents the fractional extinction due to scattering by a single particle,  $W_b$  represents a spectrally integrated value that is due to the total aerosol above the site of measurement.  $W_b$  is defined using  $R_a$  by

$$W_b = R_a / F \quad (2.50)$$

Here  $F$  is the ratio of forward scatter to total scatter, i.e.,  $F = f / (f + b)$ .

### 2.5 Climatic Impact of Aerosols

The direct radiative effect of tropospheric aerosols on the Earth-atmosphere system is expressed mainly in terms of changes in surface temperature or simply in terms of warming and cooling. The relationship between surface temperature and aerosols is studied by examining the relationships between  $\tau$ ,  $\omega_0$ , and aerosols; the absorption to backscatter ratio; or by comparing the surface albedo and the Earth's effective albedo.

### 2.5.1 Joseph and Wolfson (1975) Method

The method uses the absorption-backscatter ratio  $a/b$  and the surface albedo  $\alpha_s$  to establish limits of the ratio which lead to warming or cooling of the EAS. This approach has been used by several authors (Charlson and Pilat, 1969; Ensor et al., 1971; Chýlek and Coakley, 1974; Russell and Grams, 1975; and Joseph and Wolfson, 1975). The method of Joseph and Wolfson is based on the premise that  $b_{bs}$  (equation 2.14) and  $b_{abs}$  (equation 2.16) can be replaced with  $b$  and  $a$  obtained using Robinson's (1962) analysis (Section 2.4.1).

From equations 2.45 and 2.46

$$\frac{G_o - G}{D - D_o} = \frac{a + b}{f} = \frac{b}{f} [(a/b) + 1] \quad (2.51)$$

$$a/b = \frac{f}{b} \cdot \frac{\delta G}{\delta D} - 1 \quad (2.52)$$

where  $\delta G = G_o - G$  and  $\delta D = D - D_o$ .

If the recovery rate is used, equation 2.52 becomes

$$a/b = f/(b \cdot R_a) - 1/b = (f - R_a)/(b \cdot R_a) \quad (2.53)$$

Considering multiple reflections between an aerosol layer and the Earth's surface (Figure 2.2) and following Schneider (1971), the Earth's effective albedo  $\alpha_E$  for clear skies can be written as

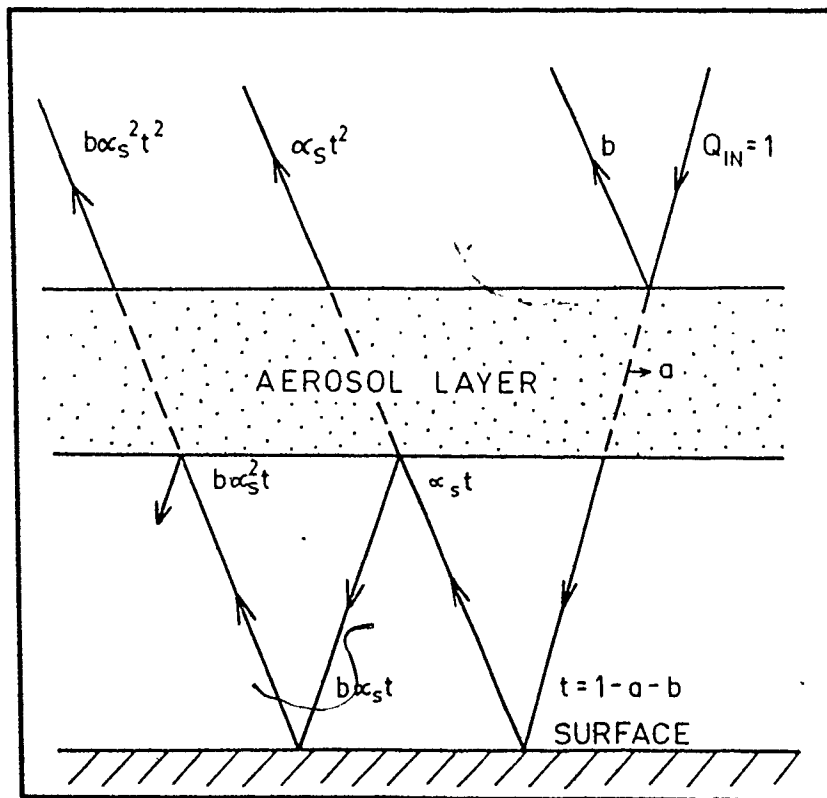


Figure 2.2. Schematic diagram of solar flux densities in a reflecting and absorbing aerosol layer above a surface.  $Q_{IN}$  = incoming solar irradiance.

$$\alpha_E = b + \alpha_s t^2 / (1 - \alpha_s b) \quad (2.54)$$

and

$$a/b = \alpha_E - \alpha_s \quad (2.55)$$

Using equations 2.54 and 2.55,  $(a/b)_{\text{crit}}$  (i.e.,  $\alpha_E = \alpha_s$ ) is defined by

$$(a/b)_{\text{crit}} = \frac{(1 - \alpha_s)^2 + 2 a \alpha_s}{\alpha_s (2 - a)} \quad (2.56)$$

For weak extinction by aerosol,  $a \rightarrow 0$  and for strong extinction  $a \rightarrow 1$  and equation 2.56 tends to

$$(a/b)_{\text{crit}} = (1 - \alpha_s)^2 / 2 \alpha_s \quad (2.57)$$

and

$$(a/b)_{\text{crit}} = (1 + \alpha_s^2) / \alpha_s \quad (2.58)$$

Equation 2.57 was also derived by Coakley and Chýlek (1975) using a two-stream approximation, Russell & Grams (1975), and Paltridge and Platt (1976). The significance of equation 2.57 is that an aerosol layer is considered warming if  $a/b > (a/b)_{\text{crit}}$  and cooling if  $a/b < (a/b)_{\text{crit}}$ .

## CHAPTER 3

### DATA SELECTION AND CALCULATION OF PARAMETERS

#### 3.1 Sources of Data

##### 3.1.1 Measured Components of Solar Radiation and Meteorological Data

Integrated hourly measurements of global and diffuse radiation on a horizontal surface plus dew point temperature, cloud amount, sunshine, windspeed and direction, visibility, relative humidity, air temperature, and atmospheric pressure were obtained from the Atmospheric Environment Service (AES), Toronto for five stations. These were: Montreal (Jean Brebeuf: 1968-78), Toronto (Woodbridge-Meteorological Research Station: 1968-78), Goose (1968-77), Charlottetown (Central Business District: June 1977-Dec. 1978), and Winnipeg (International Airport: Dec. 1976-77). Both global and diffuse radiation were measured mostly with Kipp pyranometers and sometimes with Eppley sensors. Diffuse radiation was measured beneath a shade ring. Direct beam radiation was obtained as the difference between global and diffuse radiation.

Integrated hourly measurements of global and diffuse radiation on a horizontal surface and direct beam (normal incidence) radiation were supplied for Vancouver, University of British Columbia (Jan. 1977-July 1978) by Professor John Hay.

Half hourly instantaneous measurements of global and direct beam

(normal incidence) radiation for Hamilton (5 days, May-June, 1977) were supplied by Professor John Davies. Measurements were made with Eppley sensors.

The averaged values of global and direct beam radiation over five to ten minute intervals for Sal (7 days, July-August, 1974) were obtained from published measurements by Carlson (1975). Sal is one of the Cape Verde islands off the northern coast of West Africa. Measurements were made with Eppley sensors. Diffuse radiation was obtained as the difference between global and direct beam radiation.

### 3.1.2 Ozone

Daily measurements of ozone are published in 'World Ozone Data' by the Atmospheric Environment Service, Toronto. In Canada, measurements are made only at Toronto, Goose and Edmonton. Because ozone amount does not vary significantly over large areas, Toronto data have been used in this study for Montreal, Hamilton and Charlottetown. Edmonton data have been used for Vancouver and Winnipeg.

For Sal, ozone depth of 2.5 mm STP is assumed (Carlson, 1974; Carlson and Caverly, 1977).

### 3.1.3 Radiosonde Data and Precipitable Water

Of all the stations only Goose has some records of precipitable water calculated from radiosonde data. For a few days in Toronto and for

Hamilton, precipitable water was calculated from radiosonde data for 1200 GMT at Buffalo International Airport. For Sal, an average of 28 mm (Carlson and Caverly, 1977) was used.

The daily average precipitable water calculated from radiosonde data for Port Hardy was used for Vancouver. Hourly precipitable water was also calculated from surface humidity for Vancouver (using data from the International Airport) and for the rest of the stations where no radiosonde data were available. Errors arising from this procedure are discussed in section 4.1.

### 3.2 Processing of Data

The total number of hours and days of data used are shown in Appendix 2. Cloud amount was first used to identify cloudless hours. Sunshine data were used to cross-check.

All cloudless hours with zenith angle larger than  $78.5^\circ$  were eliminated since this angle is the upper limit for aerosol forward to backscatter ratio given by Robinson (1962).

For analysis requiring the examination of the relationship between optical air mass and other parameters, days with at least 5 consecutive cloudless hours were chosen. Furthermore, plots of direct beam radiation versus zenith angle were made to eliminate days with obvious poor symmetry.

To facilitate the choice of appropriate surface albedos, snow cover records were checked for Canadian stations.

### 3.3 Calculations of Parameters

#### 3.3.1 Astronomical Parameters

Following Thekaekara and Drummond (1971),  $1353 \text{ W/m}^2$  is adopted as the solar constant. Because this value refers to the mean Sun-Earth distance  $\bar{R}$ , it should be corrected to account for the departure of the actual distance  $R$  from  $\bar{R}$ . The corrected solar constant  $I(o)$  is given by

$$I(o) = 1353(\bar{R}/R)^2 \quad (3.1)$$

The extraterrestrial irradiance  $I_*$  which refers to a horizontal surface is defined by

$$I_* = I(o)\mu_o \quad (3.2)$$

Where  $\mu_o$ , the cosine of the zenith angle  $\theta$ , is calculated from

$$\mu_o = \sin \phi \sin \delta + \cos \phi \cos \delta \cos H \quad (3.3)$$

in which  $\phi$  is latitude,  $\delta$  solar declination, and  $H$  the solar hour angle (degree).  $H$  is obtained from

$$H = 15|12.5 - \text{LAT}| \quad (3.4)$$



Where LAT is the local apparent (true solar) time. LAT is determined from local standard time LST, equation of time ET (in minutes), and the longitudes LS of the station and LSM of the standard meridian appropriate to the time zone. LAT is given by

$$\text{LAT} = \text{LST} + \text{ET}/60 + (\text{LSM} - \text{LS})/15 \quad (3.5)$$

Following Paltridge and Platt (1976), Spencer's (1971) method has been used to calculate values of  $(\bar{R}/R)^2$ ,  $\delta$ , and ET from day number  $d_n$  (= Julian day - 1). This is used to define the angle  $\theta_o$  (radians)

$$\theta_o = 2\pi d_n / 365 \quad (3.6)$$

then

$$\begin{aligned} (\bar{R}/R)^2 = & 1.00011 + 0.034221 \cos \theta_o + 0.00128 \sin \theta_o \\ & + 0.000719 \cos 2\theta_o + 0.000077 \sin 2\theta_o \end{aligned} \quad (3.7)$$

$$\begin{aligned} \delta = & 0.006918 - 0.399912 \cos \theta_o + 0.070257 \sin \theta_o \\ & - 0.006758 \cos 2\theta_o + 0.000907 \sin 2\theta_o - 0.002697 \cos 3\theta_o \\ & + 0.00148 \sin 3\theta_o \end{aligned} \quad (3.8)$$

$$\begin{aligned} \text{ET} = & 0.000075 + 0.001868 \cos \theta_o - 0.032077 \sin \theta_o \\ & - 0.014615 \cos 2\theta_o - 0.040849 \sin 2\theta_o \end{aligned} \quad (3.9)$$

According to Paltridge and Platt (1976), the maximum error for  $(\bar{R}/R)^2$  is less than 0.0001,  $\delta$  less than 0.05 degree, and ET less than 35 seconds in time.

Optical air mass  $m$  was evaluated from Kasten's (1966) formula

$$m = 1/[\cos \theta + 0.15(93.885 - \theta)^{-1.253}] \quad (3.10)$$

### 3.3.2 Ozone and Molecular Transmissions

Transmissivity after ozone absorption  $a_{oz}$  is defined by

$$T_{oz} = 1 - a_{oz} \quad (3.11)$$

Following Lacis and Hansen (1974),  $a_{oz}$  is calculated by

$$\begin{aligned} a_{oz}(x) = & 0.002118x/(1 + 0.0042x + 0.0000323x^2) \\ & + 0.1082x/(1 + 13.86x)^{0.805} \\ & + 0.00658x/[1 + (10.36x)^3] \end{aligned} \quad (3.12)$$

Here  $x$  is the vertical length for ozone which is the product of ozone depth  $U_{oz}$  (mm) in the atmosphere and the optical air mass. Since ozone transmission is rather insensitive to errors in  $x$  (Appendix 3), a fixed value of 3.5 was used for  $U_{oz}$  in calculating  $\tau_a$  for Montreal, Woodbridge and Goose for the trend analysis discussed in section 4.3. The first term in equation 3.12 represents ozone absorption in the visible wave-

length (Chappuis band) and the other two terms represent the absorption in the ultraviolet (Hartley and Huggins band) Maximum error due to equation 3.12 is  $< 0.5\%$  for  $U_{oz} = 10^{-3} - 10\text{mm}$  (Paltridge and Platt, 1976).

TABLE 3.1: TRANSMISSIVITY AFTER RAYLEIGH SCATTERING

Relative Optical Air Mass	Rayleigh Transmission
0.5	0.9385
1.0	0.8973
1.2	0.8830
1.4	0.8696
1.6	0.8572
1.8	0.8455
2.0	0.8344
2.5	0.8094
3.0	0.7872
3.5	0.7673
4.0	0.7493
4.5	0.7328
5.0	0.7177
5.5	0.7037
6.0	0.6907
10.0	0.6108
30.0	0.4364

The transmissivity after Rayleigh scattering is obtained from Davies (1980) as a function of optical air mass (Table 3.1). His calculations were based on Elterman's (1968) procedure using the extraterrestrial solar spectrum of Thekaekara and Drummond (1971). Errors due to Rayleigh transmission are negligible as the main features of Rayleigh's law may be regarded as well established (Robinson 1966).

### 3.3.3 Water Vapour Absorption

The water path length  $U'_w$  is calculated using radiosonde data

from Buffalo and also using Won's (1977) empirical formula derived from Canadian data. Using radiosonde data, the water path can be determined from

$$U'_w = \frac{1}{g} \sum_{i=0}^{i=n} \bar{q}_i \Delta p_i \quad (3.13)$$

Here  $\bar{q}_i$  is the mean specific humidity and  $\Delta p_i$  the pressure difference between two pressure levels.  $q$  is expressed as

$$q = 0.622e/(p - 0.378e) \quad (3.14)$$

where  $e$  the vapour pressure is given by

$$e = e_s(T_d) - \gamma(T - T_d) \quad (3.15)$$

The saturation vapour pressure  $e_s(T_d)$  is calculated using Tetten's (1930) formula (Professor John Davies, private communication)

$$e_s(T_d) = \alpha \exp[\beta T/(T + \phi)] \quad (3.16)$$

$T$  and  $T_d$  are surface air temperature and dew point temperature in Celsius. The constants  $\gamma$ ,  $\alpha$ ,  $\beta$ , and  $\phi$  are given by  $\gamma = 0.066$  (kPa),  $\alpha = 0.61078$  (kPa),  $\beta = 17.269$ , and  $\phi = 237.3$ .

Won's formula is given by

$$U'_w = \exp(2.2572 + 0.05454 T_d) \quad (3.17)$$

Because water vapour absorption is temperature and pressure dependent,  $U'_w$  is corrected as suggested by Paltridge and Platt (1976)

$$U_w = U'_w (p/p_0)^{0.75} (T_0/T)^{0.5} \quad (3.18)$$

where  $T$  and  $T_0 = 273$ , the surface and standard surface air temperatures, are in degrees Kelvin. Water vapour absorption  $a_w$  is calculated from Yamamoto's (1962) formula modified by Lacis and Hansen (1974).

$$a_w = 0.29 U_w \cdot m / [(1 + 14.15 U_w \cdot m)^{0.635} + 0.5925 U_w \cdot m] \quad (3.19)$$

#### 3.3.4 Correction for Diffuse Radiation

Diffuse irradiance is measured by the Atmospheric Environment Service (AES) using a shade ring and so the measurements must be increased in summer by up to 17% (Davies et al., 1970) to account for depletion by the ring. The correction factor  $D_{SR}$  applied to the measurements is calculated from (Davies et al., 1970; Latimer, 1972)

$$D_{SR} = 1/(1 - F/D) \quad (3.20)$$

where  $F$  the radiation intensity from the portion of the hemisphere screened off by the ring is given by

$$F = \frac{2I}{\gamma} W \cos^3 \delta (H_0 \sin \phi \cdot \sin \delta + \cos \phi \cdot \cos \delta \cdot \sin H_0) \quad (3.21)$$

in which  $W$  is the width of the shade ring,  $\gamma$  the radius,  $H_0$  the solar hour angle at sunset. Calculation from equation 3.21 is increased by an experimental factor of 4% to relate isotropic to real sky conditions and the final correction factor (Table 3.2) yields the desired evaluation of diffuse sky radiation within  $\pm 2\%$  accuracy (Latimer, 1972).

TABLE 3.2: SHADE RING CORRECTION FACTORS FOR AES DIFFUSOGRAPH  
(After Latimer, 1972)

Lat°N	Jan	Feb	Mar	Apr	May	Jun	Jul	Aug	Sep	Oct	Nov	Dec
30	1.11	1.13	1.15	1.16	1.17	1.16	1.17	1.17	1.20	1.15	1.12	1.10
40	1.09	1.11	1.13	1.15	1.17	1.16	1.17	1.17	1.18	1.13	1.11	1.09
50	1.07	1.08	1.11	1.14	1.16	1.16	1.16	1.16	1.15	1.12	1.09	1.07
60	1.05	1.06	1.08	1.11	1.15	1.16	1.15	1.14	1.13	1.09	1.07	1.05

### 3.3.5 Diffuse Radiation Component (Multiple Reflection Term) and Linke's Turbidity Parameters

The multiple reflection term of the diffuse radiation component in MAC model requires surface albedo  $\alpha_s$  and Rayleigh backscatter coefficient  $\alpha_R$ . The choice of  $\alpha_s$  is based on the season (in the case of Canadian Stations), the typical landscape of the area in and around the measurement site and also on surface estimates by Oke (1978). Information by Carlson (1975) was used for Sal. Table 3.3 shows the range of  $\alpha_s$  used in this study. The Rayleigh backscatter coefficient is fixed at 0.0685 (Lacis and Hansen, 1974).

TABLE 3.3: RANGE OF SURFACE ALBEDO USED AT STATIONS

Station	Summer	Winter
Montreal	0.15	0.25 - 0.50
Woodbridge	0.15	0.25 - 0.50
Goose	0.15	0.25 - 0.70
Hamilton	0.15	-
Charlottetown	0.10	-
Winnipeg	0.15	-
Vancouver	0.15	-
Sal	0.20	-

Linke's model (equation 2.29) uses  $p(m)$  which is a function of molecular transmission. To enable fair comparison of results, the  $p(m)$  values used by Polavarapu (Table 3.4) have been used also.

TABLE 3.4:  $p(m)$  VALUES USED FOR LINKE'S TURBIDITY FACTOR

Optical air mass	$p(m)$
1.0	23.2
1.4	17.3
1.8	14.0
2.2	11.91
2.6	10.43
3.0	9.33
3.4	8.51
3.8	7.84
4.2	7.30
4.6	6.84
5.0	6.46

Values of Linke's turbidity factor for dust-free atmosphere  $T_{df}$  as a function of optical air mass and precipitable water are plotted in Polavarapu's (1978) Figure 3. The values of  $T_{df}$  used in this study have been derived from these data.

## TURBIDITY

4.1 Aerosol Attenuation Coefficient  $\tau_a$ 

Values of  $\tau_a$  are sensitive to the accuracy of measured and calculated direct beam irradiances. Measured irradiance was obtained as the difference between measured global and diffuse irradiances. Secrest and Dirmhirn (1979) concluded that residual estimates of direct beam irradiance are within 2% when corrections are applied for sensor cosine response and the effect of the shade ring on diffuse irradiance. The Atmospheric Environment Service only corrects for shade ring error (section 3.3.4). To assess the accuracy of the direct beam irradiance used in this study, hourly residual estimates and pyrheliometric measurements for all cloudless hours at Woodbridge (1976-78) were compared. The two sets of values are well correlated (Table 4.1) with a standard deviation of 3% for the differences. In 90% of the cases, they compared to within 5% (Figure 4.1).

TABLE 4.1: PYRHELIOMETRIC MEASUREMENTS AND RESIDUAL ESTIMATES COMPARED

	Mean I (MJ/m <sup>2</sup> /hr)	Standard deviation	Sample Size
Pyrheliometric measurements	2.84	0.53	233
Residual estimates	2.86	0.50	233
	Slope	Intercept	Correlation Coefficient
	0.94	0.20	0.99
			Standard Error of Estimate
			0.02



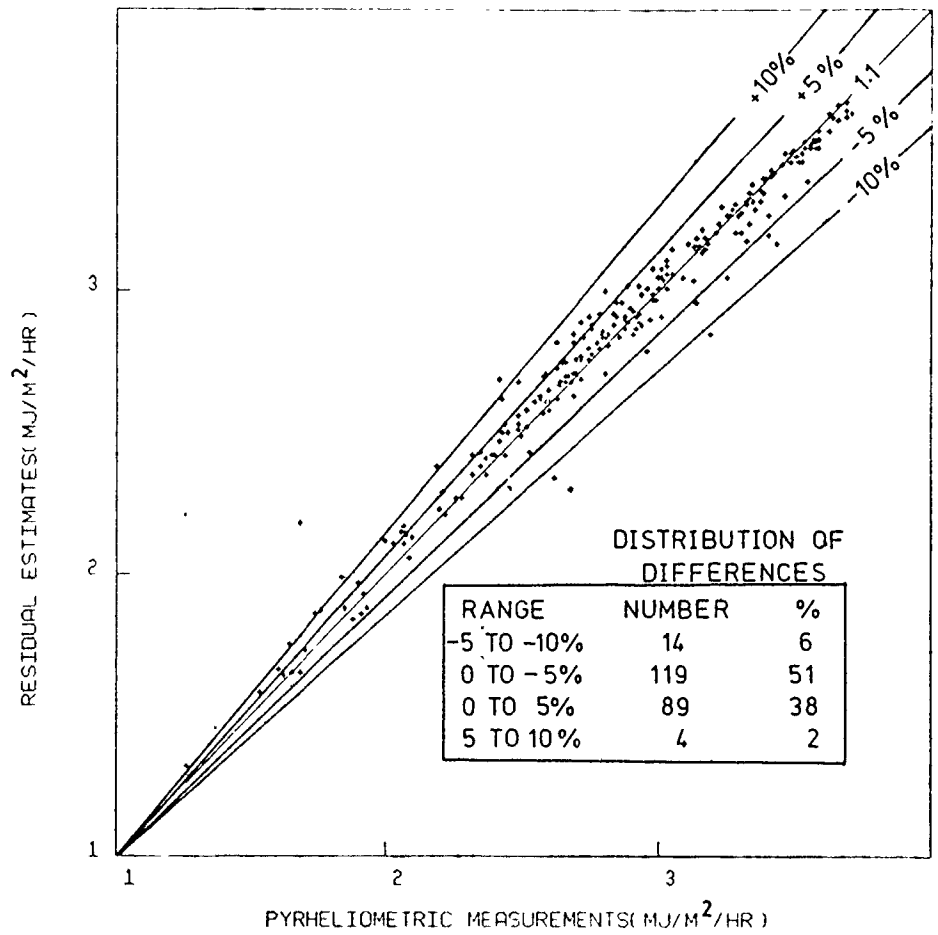


Figure 4.1. Cloudless sky direct beam irradiance at Woodbridge, 1976-78.

Direct beam irradiance  $I_0$  for cloudless, aerosol-free atmospheric condition was calculated with the MAC model (section 2.2). To test the appropriateness of the model to provide cloudless sky irradiance, it was applied to the Braslau and Dave (1973) model B atmosphere. This is an aerosol-free atmosphere with 0.318 cm-atm of ozone and a water vapour content of  $2.383 \text{ gm/cm}^2$  (scaled with pressure and temperature). The results compare to within 1% (Table 4.2; Davies and Hay, 1980) with detailed exact calculations by Braslau and Dave (1973). This agreement demonstrates that molecular absorption and scattering are adequately treated in the MAC model.

TABLE 4.2: DIRECT BEAM TRANSMITTANCE FOR THE BRASLAU AND DAVE (1973) MODEL B ATMOSPHERE (B+D) AND MAC MODEL COMPARED

Zenith angle (degrees)	B+D	MAC
0	0.76	0.75
30	0.74	0.73
60	0.67	0.66
80	0.49	0.47

Since  $I_*$  is equal to  $S(\bar{R}/R)^2$  in equation 2.19, it is clear that  $I_0$  is sensitive to uncertainties in the solar constant  $S$ , the radius vector  $(\bar{R}/R)^2$ , water vapour absorption, ozone and Rayleigh scattering transmissions for a given optical air mass. Errors due to the radius vector (section 3.3.1), Rayleigh scattering (section 3.3.2), and ozone (Appendix 3) transmissions are negligible. The value and temporal variation of  $S$  are uncertain (London, 1977). The value of  $1353 \text{ W/m}^2$  used in this study is accurate to within 1% (Thekaekara and Drummond, 1971). Because of its variability, errors due to water vapour absorption are

probably the most important. Differentiating equation 3.19 with respect to water vapour path  $mU_w$  shows that errors in direct beam transmittance per unit  $dx(x = mU_w)$  decrease with increase in  $x$  from 0.6% at  $x = 5\text{mm}$  (rarely encountered in real atmosphere) to 0.1% at  $x = 50\text{ mm}$ .

From equations 2.19 and 2.27 the probable absolute and relative errors in  $\tau_a$  are given by

$$d\tau_a = \{(dS/S)^2 + (dI_t/I_t)^2 + (-dI/I)^2\}^{1/2} \quad (4.1)$$

and

$$d\tau_a/\tau_a = \{(dS/S)^2 + (dI_t/I_t)^2 + (-dI/I)^2\}^{1/2}/\ln(I_0/I) \quad (4.2)$$

Here,  $I_t = T_{oz} \cdot T_R - a_w$ . Root sum square errors (RSSE) for given optical air mass and typical values of  $I/I_0$  are shown in Table 4.3. The calculations were made for errors of 1% in  $dS/S$  and  $dI_t/I_t$  and of 2% in  $dI/I$ . These produce an absolute error of 0.02 in  $\tau_a$ . Relative errors decrease with  $I/I_0$  as  $\tau_a$  increases.

TABLE 4.3a: PROBABLE ABSOLUTE ERROR IN  $\tau_a$

Optical air mass	RSSE
1.0	0.024
1.15	0.021
2.0	0.012
5.0	0.005

TABLE 4.3b: RELATIVE ERROR IN  $\tau_a$  VALUES

Optical air mass	$I/I_0$	$I_0/I$	$\tau_a$	RSSE(%)
1.07	0.93	1.08	0.068	40.3
1.08	0.90	1.11	0.098	29.4
1.10	0.85	1.18	0.150	18.2
1.07	0.79	1.26	0.219	13.4
1.10	0.76	1.31	0.248	11.2
1.10	0.72	1.39	0.300	9.2
1.08	0.61	1.65	0.467	6.1
1.09	0.57	1.76	0.519	5.4
1.49	0.44	2.29	0.558	2.7

The attenuation coefficient  $\tau_a$  has been little used in North America probably because of lack of direct beam and radiosonde data. The writer is only aware of McArthur's (1976) study at Hamilton. The present study is the first application of the method to several locations over long time periods. Values have been calculated for all the eight stations used in this study. Because the amount of data and time period that they represent are different (Appendix 2), it is inappropriate to compare and classify the Canadian stations using mean values. However, the values were analyzed for diurnal, daily, and seasonal variations. Montreal, Woodbridge (Toronto), and Goose with larger data sets (10 to 11 years) were also examined for annual variations and dependence of the values on meteorological parameters. Sal, being directly in the path of Saharan dust, is so different from the Canadian stations that it is discussed separately.

#### 4.1.1 Diurnal and Daily Variation

##### 4.1.1.1 Diurnal Variation

From the AES and Vancouver radiation data, presented as hourly integrated values (section 3.1.1), hourly  $\tau_a$  values were calculated for Montreal, Woodbridge, Goose, Charlottetown, Winnipeg, and Vancouver. Half-hourly values were calculated for Hamilton. For those days with at least five cloudless hours of values (including midday values), each hourly value was expressed as a percentage departure from midday (1130 and 1230) and daily means. The hourly values and departures were averaged for three seasonal groupings (section 4.1.2.2): November-March (winter), May - August (summer), and April, September and October (spring/autumn). This analysis ignored the effects of changes in synoptic air mass on diurnal  $\tau_a$  values.

Various diurnal variations occur at all stations. At Montreal and Woodbridge (Figure 4.2) the general trend, for all seasons, is for values to increase from early morning to a maximum between 1100 and 1500 and then decrease for the rest of the day. Hamilton with some days in May and June illustrates this pattern well (Figure 4.3) with the maximum occurring between 1100 and 1300 hours. This trend is similar to that shown by Yamashita (1974) for Woodbridge using Linke's turbidity factor and by Peterson et al. (1981) for Raleigh, United States using Volz sun-photometer optical depths.

In winter at Goose (Figure 4.2)  $\tau_a$  values show an afternoon mini-

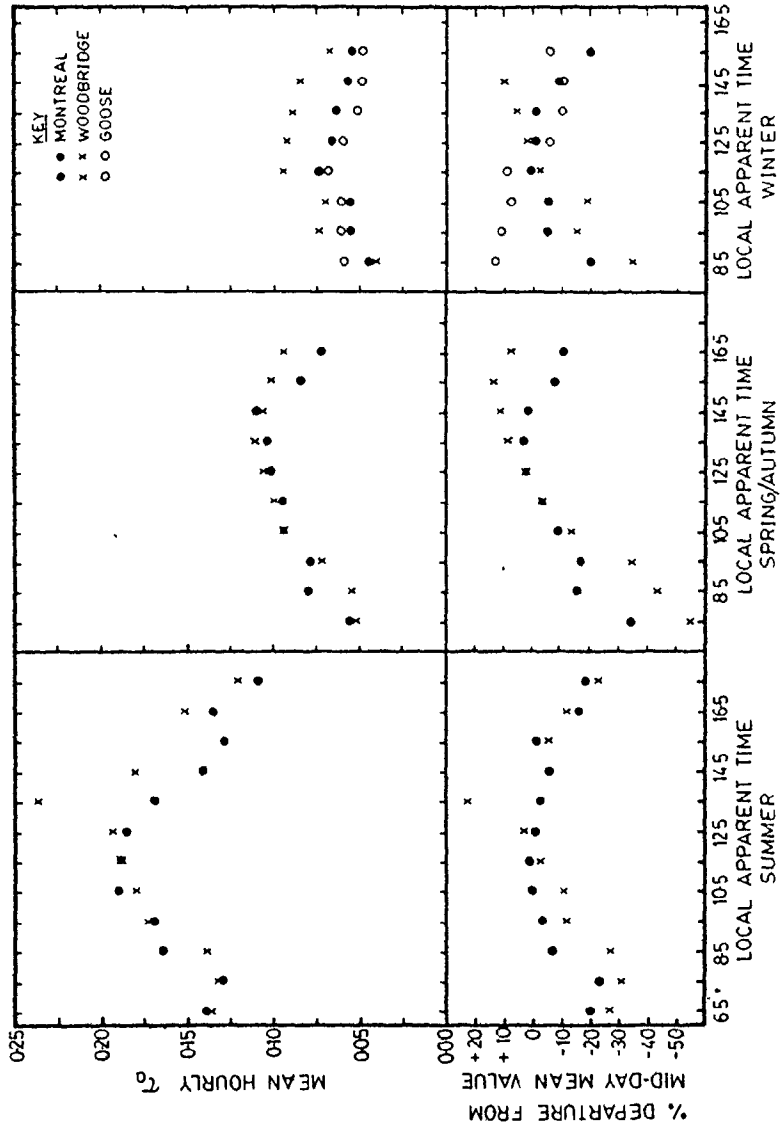


Figure 4.2. Diurnal variation of mean hourly values of  $\tau_a$  at Montreal, Woodbridge and Goose.

mum. Summer values at Vancouver (Figure 4.3) indicate a similar pattern to that of Goose but in addition show slight rise around midday.

The diurnal cycle with midday maximum shown at Montreal, Woodbridge, and Hamilton is typical of locations influenced by local sources of particulates. Peterson et al. (1981) suggest that it is due to the following:

- (a) most pollutant emissions and other human activities which eject particulates into the atmosphere, have a daytime maxima;
- (b) solar irradiance and consequently air temperature, both of which encourage the formation of photochemically generated particulates, have daytime maxima (Whitby et al., 1972; Peterson et al., 1978);
- (c) atmospheric mixing height increases with temperature and afternoon convection disperses the particulates;
- (d) direct measurements of Aitken nuclei (Hogan, 1968) and theoretical modelling studies of aerosol growth and light scattering (Middleton and Brock, 1977), indicate midday maxima.

Variability is present at all stations. Three typical days at Montreal (Table 4.4) reveal the variability of the hourly means within the diurnal cycle.

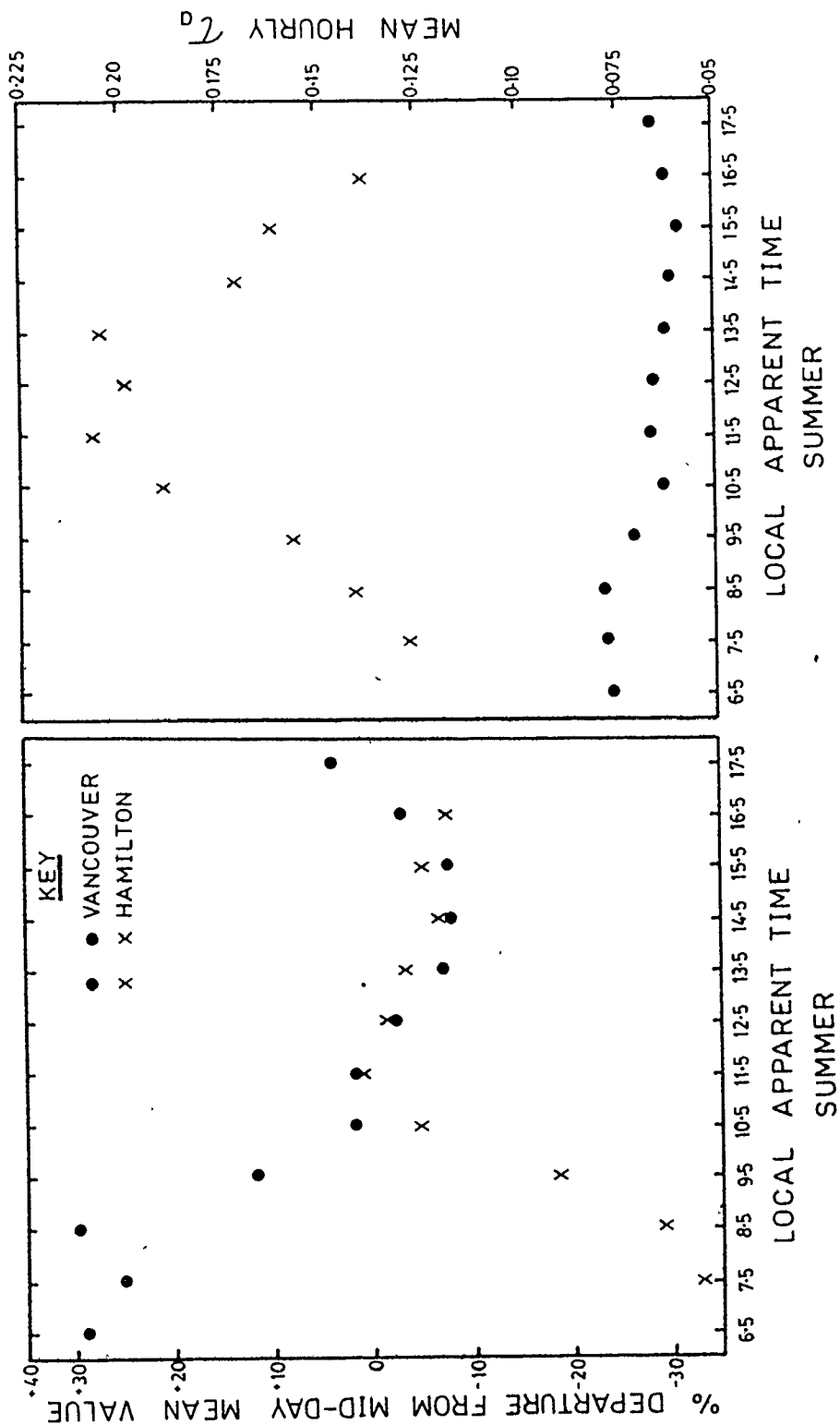


Figure 4.3. Diurnal variation of mean hourly values of  $\tau_a$  at Vancouver and Hamilton.



The winter pattern at Goose is perhaps typical of a rural area without urban influence. During early morning, temperature inversions may occur and relative humidity is high and so particulates increase in size due to condensation, coagulation and coalescence processes (Hänel, 1976). This results in a large value of  $\tau_a$ . As the day becomes relatively warmer, relative humidity decreases and particulates consequently reduce in size. Since there are no local sources of particulates, values of  $\tau_a$  become smaller and may increase later in the afternoon if the relative humidity increases again. Polavárapu (1978) noted a similar diurnal variation in turbidity within Arctic air in June at Goose.

TABLE 4.4: HOURLY  $\tau_a$  PERCENT DEPARTURE FROM DAILY MEAN VALUE AT MONTREAL

Date	Time of day										
	7.5	8.5	9.5	10.5	11.5	12.5	13.5	14.5	15.5	16.5	17.5
22.5.72	-21	-34	-10	6	20	2	15	21	29	2	-31
27.5.72	-20	4	3	7	9	11	4	10	10	-5	-
10.7.77	-44	-34	0	13	23	28	44	21	-2	-17	-33

The limited data for Vancouver suggest that the local topography and the maritime influence are important. Largest  $\tau_a$  values in the morning may be due to particulates transported into the city from the mountain valleys by the nocturnal land breeze. The stronger sea breeze during the day brings in cleaner marine air and 'flushes' much of the particulates up valley and into the mountains hence the reduction in  $\tau_a$  values. The slight rise in midday values is due to additional local sources.

Vancouver, like the Los Angeles basin (Leighton, 1966), may be an example where local aerosol sources are more important than foreign sources.

#### 4.1.1.2 Daily Variation

Mean daily  $\tau_a$  values were calculated for each station as the average of hourly values. The averages exhibit large variation within the year. Maximum and minimum values were selected (Appendix 4) for days with no less than 6 hours (winter) and 8 hours (rest of the year) of data symmetrically arranged around midday. The smallest mean values (0.007, Montreal and Charlottetown) occurred during winter and the largest (0.478, Montreal) in summer. For the periods covered in this study, the difference between maxima and minima is, in general, largest between May and August when  $\tau_a$  values are largest. The major cause of daily varia-

tion in turbidity is due to changes in the synoptic situation involving contrasting air mass types. The dramatic variations at Winnipeg and Hamilton (Figure 4.4) illustrate this influence.

The daily mean values reveal the similarity between Montreal and Woodbridge and the contrast between them and Goose except during winter when values are similar at all three locations because clean Arctic air dominates the region.

#### 4.1.2 Monthly and Seasonal Variation

##### 4.1.2.1 Monthly Variation

Values of  $\tau_a$  were calculated hourly when no cloud cover was reported and 100% sunshine was recorded (section 3.2). Mean monthly values were calculated for Montreal and Woodbridge (1968-78) and for Goose (1968-77). The values and standard deviations are plotted in Figure 4.5. An annual cycle is evident at Montreal and Woodbridge with minimum and maximum in winter and summer respectively. Similar cycles in Canada have been reported by Polavarapu (1978) for Montreal and Woodbridge; Yamashita (1974) for Woodbridge, Toronto City, and Scarborough; and in the United States by Peterson et al. (1981) for Raleigh; and by Flowers et al. (1969). The largest standard deviations of 0.15 for Montreal and Woodbridge occur in July and June and the smallest (0.04 and 0.03) in December. Considering the coefficient of variability (standard deviation divided by the mean), the months of greatest and least

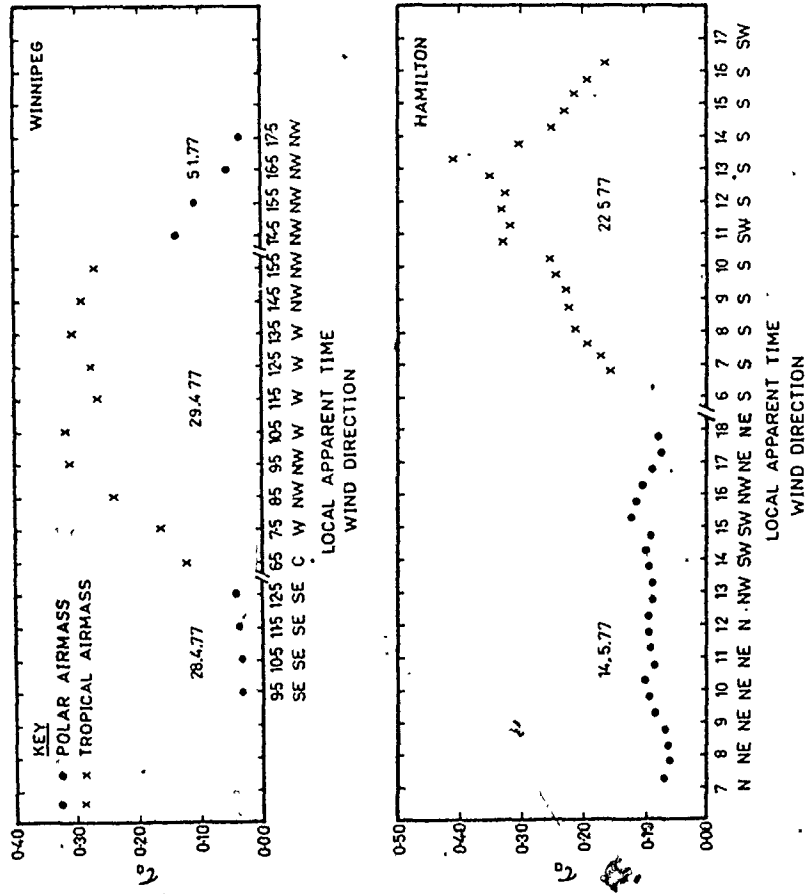


Figure 4.4. Daily variations in  $\tau_a$  values due to changes in air mass type.

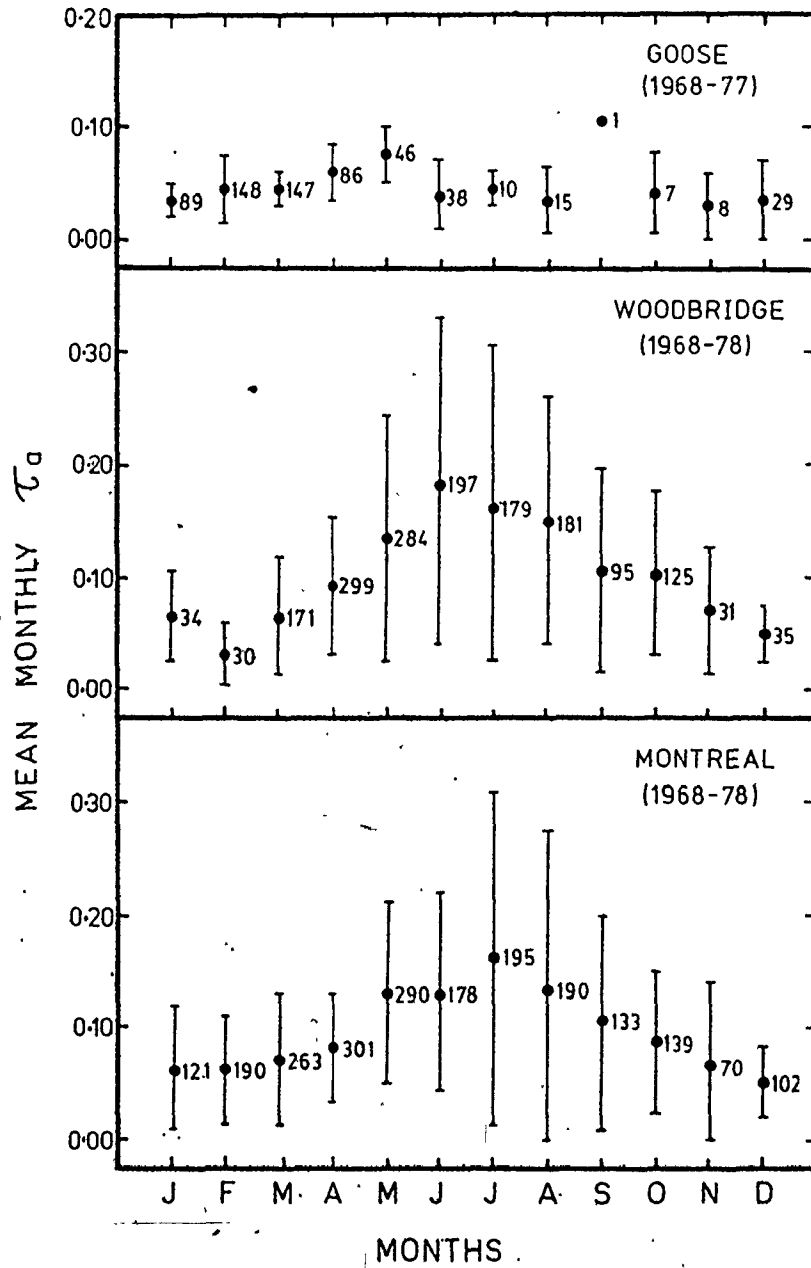


Figure 4.5. Mean monthly values of  $\tau_a$  and  $\pm$  one standard deviation about the mean for Montreal, Woodbridge and Goose. The numbers indicate sample size.

TABLE 4.5: SEASONAL GROUPS OF  $\tau_a$  VALUES FOR MONTREAL AND WOODBRIDGE (1968-78) AND GOOSE (1968-77)

summer	summer*	spring	autumn	spring/ autumn*	winter	winter*	All Season
Jun/ Aug	May/ Aug	Mar/ May	Sep/ Nov	Apr/Sep/ Oct	Dec/ Feb	Nov/ Mar	
$\tau_a$							
Montreal							
0.146	0.141	0.098	0.094	0.092	0.062	0.067	0.103
Woodbridge							
0.166	0.155	0.104	0.101	0.116	0.050	0.062	0.121
Goose							
0.040	0.054	0.055	0.040	0.061	0.041	0.043	0.047
Size							
Montreal							
563	853	854	342	573	413	746	2172
Woodbridge							
557	841	757	252	523	99	301	1665
Goose							
63	109	279	16	94	266	421	624

\* indicates the three seasonal groupings

variability at Montreal (November and April/May) are close to October and March reported for Raleigh by Peterson et al. (1981). February and December are the months of greatest and least variability for Woodbridge.

Mean monthly values at Goose (Figure 4.5) do not show much variation. However there was only one data point for September and data for some other months are limited. Polavarapu (1978) also using limited data suggested a maximum in July and a minimum in February. The largest and smallest standard deviations occur in October/November and March/July respectively. The variability is similar to that at Montreal - greatest in October/November and least in May.

#### 4.1.2.2 Seasonal Variation

Monthly values were pooled into three seasonal groups for the year -- summer (May - August), winter (November - March), and spring/autumn (April, September, and October). Values obtained by this grouping are very close to those obtained by the usual four seasonal grouping (Table 4.5). The use of three seasonal divisions, ensures that mean values are calculated from larger data sets than four or more divisions.

The seasonal means emphasize again the similarity between Montreal and Woodbridge and their differences with Goose.

The monthly relative frequency of occurrence of hourly values  $< 0.07$  and  $> 0.25$  are presented in Table 4.6 while the seasonal frequency of all values are shown in Figure 4.6.

TABLE 4.6: MONTHLY RELATIVE FREQUENCY OF VALUES OF  $\tau_a < 0.07$  AND  $\tau_a > 0.25$  AT MONTREAL AND WOODBRIDGE (1968-78) AND GOOSE (1968-77) (AS PERCENT OF TOTAL FREQUENCY FOR THE MONTH OR SEASON)

	Montreal		Woodbridge		Goose	
	$\tau_a < 0.07$	$\tau_a > 0.25$	$\tau_a < 0.07$	$\tau_a > 0.25$	$\tau_a < 0.07$	$\tau_a > 0.25$
January	71	0	60	0	96	0
February	66	1	86	0	84	0
March	60	3	67	3	95	0
April	54	3	43	4	69	0
May	23	13	32	12	52	0
June	39	19	28	28	84	0
July	40	27	36	21	100*	0
August	49	22	34	23	88	0
September	51	10	53	13	—*	0
October	52	4	41	6	86*	0
November	71	3	68	0	88*	0
December	79	0	80	0	83	0
Winter	67	2	70	2	90	0
Summer	36	19	70	20	72	0
Spring/ Autumn	53	5	44	6	69	0
All Season	51	9	43	12	84	0

\* Sample size < 10



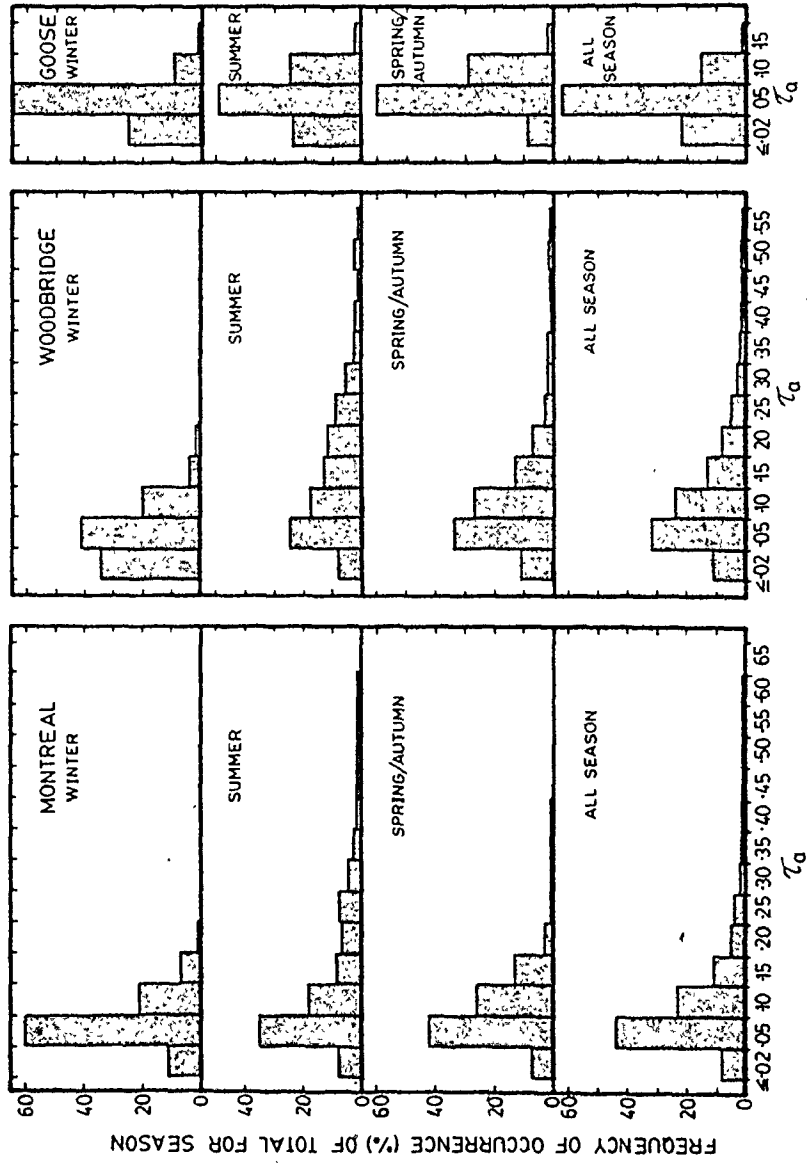


Figure 4.6. Seasonal histograms of the frequency of occurrence of hourly values of  $\tau_a$  at Montreal, Woodbridge and Goose.

Table 4.6 clarifies the relative 'cleanliness' of the locations and further justifies the 3 seasonal groupings for Montreal and Woodbridge. It can be inferred that Goose has cleaner atmosphere than the other locations. Figure 4.6 shows that for all locations in all seasons values  $\sim 0.05$  dominate.

The winter mean values (1968-78) for Woodbridge and Montreal ( $\sim 0.06$ ) are the smallest seasonal means and are much lower than the value of 0.25 given by Unsworth and Monteith (1972) for British urban sites affected by Polar air mass. The December and January averages for Montreal and Woodbridge ( $\sim 0.05$ ) are also smaller than the spectral value of 0.13 for Raleigh (Peterson et al., 1981). Winter minimum hourly values are also lower (0.001) at both stations than values for Raleigh ( $\sim 0.023$ ) which further emphasizes the cleaner air at Montreal and Woodbridge.

The summer average values ( $\sim 0.15$ ) at Montreal and Woodbridge are the largest seasonal values. These are smaller than the value (0.55) suggested by Unsworth and Monteith (1972) for an urban site affected by continental air mass, and the average of 0.30 for world cities (WMO, 1974) but lie close to the lower end of the range (0.125 to 0.75 at wavelength of  $0.5 \mu\text{m}$ ) given by Toon and Pollack (1976). Largest monthly means (0.16 - 0.19) and largest daily means (0.4 - 0.48) are smaller than the Raleigh spectral values of 0.74 (July average) and 1.6 daily average. Largest hourly values (0.59 - 0.64) also occur in summer. They are smaller than the largest spectral value of  $\sim 2.3$  at Raleigh.

For Goose, the monthly and seasonal means (Figure 4.5 and Table 4.5) change so little that annual mean value of 0.05 for the 10 year period is appropriate. This value agrees with that proposed for the North Atlantic by Unsworth and Monteith (1972) and with the spectral value of 0.06 given by Toon and Pollack (1976) as the average for 60°-90°N.

Annual average  $\tau_a$  values for the 11-year period were determined from the hourly values. Values for Montreal (0.103) and Woodbridge (0.121) are much lower than the spectral value of 0.336 reported for non-urban areas along the southern Appalachians by Valente and Robinson (Peterson et al., 1981) but near the global average of  $\sim 0.1$  at visible wavelengths (Toon and Pollack, 1976).

#### 4.1.2.3 Charlottetown, Hamilton, Winnipeg and Vancouver

Since data for 1977 and 1978 are represented for all the Canadian stations, monthly and seasonal averages were calculated from the hourly values and presented in Table 4.7.

Values for Charlottetown are on the average similar to those for Montreal and Woodbridge for the appropriate periods. Even though the measurement site is downtown, Charlottetown is a relatively small urban area with few industries. Hence, local influence on  $\tau_a$  values is not comparable with Montreal or Toronto. The result indicates that imported particulates have considerable effects on the values of  $\tau_a$  in both large and small urban locations in Eastern Canada. The position of Charlotte-

TABLE 4.7: MONTHLY AND SEASONAL  $\bar{\tau}_a$  VALUES FOR THE CANADIAN STATIONS (1977-78)

Period	Woodbridge $\bar{\tau}_a$	No. of hrs.	Montreal $\bar{\tau}_a$	No. of hrs.	Charlottetown $\bar{\tau}_a$	No. of hrs.	Vancouver $\bar{\tau}_a$	No. of hrs.	Winnipeg $\bar{\tau}_a$	No. of hrs.	Goose $\bar{\tau}_a$	No. of hrs.	Hamilton $\bar{\tau}_a$	No. of hrs.
1977														
Jan.	0.074	7	0.131	8	-	-	-	-	0.069	17	-	-	-	-
Feb.	0.033	6	0.063	14	-	-	-	-	0.030	22	0.034	21	-	-
Mar.	0.096	48	0.063	18	-	-	-	-	0.036	43	0.018	16	-	-
Apr.	0.098	42	0.074	42	-	-	-	-	0.086	50	0.084	7	-	-
May	0.126	50	0.115	62	-	-	-	-	0.057	18	0.063	5	0.178	38
Jun.	0.108	15	0.094	20	0.156	10	0.073	38	0.045	22	0.012	11	0.139	6
Jul.	0.136	18	0.086	28	0.075	10	0.105	11	0.032	26	-	-	-	-
Aug.	0.162	9	0.085	6	0.088	13	0.030	12	0.025	12	-	-	-	-
Sept.	0.034	2	0.048	6	-	-	-	-	0.034	8	-	-	-	-
Oct.	0.060	18	0.089	33	0.074	3	-	-	0.027	44	-	-	-	-
Nov.	-	-	0.009	10	0.032	4	0.020	18	0.030	13	-	-	-	-
Dec.	0.026	3	0.025	18	0.031	5	-	-	0.015	5	0.012	4	-	-
Mean	0.103	218	0.083	265	-	-	-	-	0.046	280	-	-	-	-
Summer	0.128	92	0.103	116	0.085	24	0.070	61	0.040	78	0.028	16	0.169	44
Winter	0.084	64	0.053	68	0.032	9	-	-	0.038	100	0.026	41	-	-
Sp/Aut.	0.085	62	0.078	81	-	-	-	-	0.056	102	-	-	-	-
1978														
Jan.	-	-	-	-	0.001	1	-	-	-	-	-	-	-	-
Feb.	0.010	3	0.036	26	0.085	31	-	-	-	-	-	-	-	-
Mar.	0.085	4	0.047	76	0.021	7	0.017	8	-	-	-	-	-	-
Apr.	0.046	30	0.056	78	0.040	13	-	-	-	-	-	-	-	-
May	0.126	37	0.162	69	0.109	45	0.078	26	-	-	-	-	-	-
Jun.	0.094	26	0.058	46	0.074	21	0.087	39	-	-	-	-	-	-
Jul.	0.060	9	0.054	44	0.090	11	0.073	69	-	-	-	-	-	-
Aug.	0.165	22	0.057	52	0.095	18	-	-	-	-	-	-	-	-
Sept.	0.038	20	0.042	40	0.030	5	-	-	-	-	-	-	-	-
Oct.	0.099	9	0.081	14	0.156	3	-	-	-	-	-	-	-	-
Nov.	0.069	12	0.070	36	0.007	1	-	-	-	-	-	-	-	-
Dec.	-	-	0.042	18	0.006	6	-	-	-	-	-	-	-	-
Mean	0.090	172	0.068	499	0.081	162	-	-	-	-	-	-	-	-
Summer	0.120	94	0.091	211	0.096	95	0.078	134	-	-	-	-	-	-
Winter	0.063	19	0.050	156	0.061	46	-	-	-	-	-	-	-	-
Sp/Aut.	0.051	59	0.054	132	0.054	21	-	-	-	-	-	-	-	-
1977-78														
Summer	0.124	186	0.095	327	0.094	119	0.075	195	-	-	-	-	-	-

town on the east coast makes its climate essentially continental but modified slightly by the sea. It is at the meeting point of air masses from the south, southwest, and west which pass through the United States and therefore yield large  $\tau_a$  values.

TABLE 4.8: MEAN  $\tau_a$  VALUES FOR HAMILTON AND WOODBRIDGE FOR THE SAME DAYS

	14.5.77	21.5.77	22.5.77
	$\bar{\tau}_a$		
Hamilton	0.089	0.222	0.256
Woodbridge	0.033	0.184	0.189
	No. of hrs.		
Hamilton	11	7	10
Woodbridge	4	11	7

The mean values (0.169) for Hamilton for the period 14 May to 22 June 1977 is comparable to 0.182 and 0.117 for Montreal and Woodbridge for the same period. Average values for Hamilton and Woodbridge for 3 days during the period reveal the close agreement (Table 4.8). High values for Hamilton are consistent with its size and large industries and its proximity to other large urban areas (Buffalo, Detroit). The largest value of  $\tau_a$  during the period is 0.41 which is similar to values reaching 0.45 measured by McArthur (1976).

The few months of data for Vancouver suggest that  $\tau_a$  values are large in summer and low in winter. The summer mean of 0.075 for 1977-78 is nearer the mean value of Montreal than that of Woodbridge. Since the data set is small and Vancouver is almost entirely dependent on internal sources of particulates (Section 4.1.1.1), it is inappropriate to rank Vancouver with Montreal and Woodbridge.

For Winnipeg, the maximum monthly mean value (in April) and minimum (in December) compare with monthly mean values for the same year at Woodbridge and Montreal, but the rest of the months are much lower. The mean value of 0.046 for 1977 is lower than the latitudinal estimate of 0.16 for wavelength of 0.5  $\mu\text{m}$  (Toon and Pollack, 1976) for global 'background' aerosol. The measurement site is at the International Airport about 24 kilometers upwind to the west of the city. This suggests little urban influence, hence the low turbidity. In addition, section 4.1.4 will show that 1977 was a year with low turbidity in Canada.

#### 4.1.3 Sal - Tropical Desert Aerosol Location

##### 4.1.3.1 Mean $\tau_a$

Using measurements of direct beam irradiance (Carlson, 1975), mean values of  $\tau_a$  were calculated for Sal for 7 days in July and August, 1974. The mean value of 0.644 for the 7 days compares well with 0.684 measured at wavelength of 0.5  $\mu\text{m}$  by Prospero et al. (1979) at Sal between May and September, 1974. It also falls within 0.50 to 1.0 at wavelength of 0.5  $\mu\text{m}$  reported by Carlson and Benjamin (1980) for 'normal' amounts of

dust over the eastern Atlantic. Turbidity at Sal is comparable with those at large heavily industrialized cities with annual averages of 0.30 to 0.75 (WMO, 1974) and 0.55 proposed by Unsworth and Monteith (1972).

TABLE 4.9: VALUES OF  $\tau_a$  FOR SAL AND OTHER LOCATIONS COMPARED

Station	1974	1974	1968-78	1968 - 1978		1968 - 1978	
	Jul/ Aug	May/ Aug	May/ Aug	Maximum summer	All season	Minimum summer	All season
Sal	0.644	-	-	1.450 (1974)		0.39 (1974)	
Woodbridge	0.089	0.131	0.155	0.588	0.588	0.003	0.001
Montreal	0.175	0.173	0.141	0.637	0.637	0.007	0.001
Goose	-	0.046	0.054	0.142	0.142	0.003	0.0005
	Jun/ Sep						
*Dakar	0.806						
*Sal	0.684						
*Barbados	0.299						
*Miami	0.230						

\* Prospero et al. (1979) for wavelength, 0.5  $\mu\text{m}$ .

Table 4.9 portrays the extreme contrast in values between Sal and the Canadian stations. The maximum for Woodbridge and Montreal are less than the average for Sal and the minimum at Sal exceeds, by far, the maximum at Goose. Most values cluster around  $\sim 0.05$  (Figure 4.6) for the Canadian stations. Even the 'background' aerosol value of 0.25 (Carlson, 1979) is larger than the mean value for any of the Canadian locations.

The differences between Sal and the Canadian stations can be explained in terms of the origin and nature of the particulates and the manner of their transportation. The particulates in Montreal and Wood-

bridge are composed of mainly heterogeneous anthropogenic emissions from the cities themselves and also from foreign sources. The particulates also include limited amounts of soil and other natural matter from the rural areas. On the other hand, particulates at Sal (Prospero et al., 1976; Kondratyev et al., 1976) are of natural origin made up almost entirely of homogenous Saharan desert soil plus small amounts of sea salt. Large amount of Saharan dust is continually present in the atmosphere over Sal but between May and October, upper easterly winds carry successive outbreaks of extremely dusty air about once in 4 to 5 days from the Sahara across the north Atlantic to Florida (Prospero et al., 1979). As the dust decreases along its route through Dakar, turbidity also decreases (Table 4.9). In Canada, the tropical air mass transports the particulates northwards in summer but in winter the polar air mass 'flushes' out most of them. Unlike Canada, there is no counterpart of the polar air to 'purify' the air over Sal. Whereas in Canada, the particulates are mixed fairly evenly from the surface upwards, in Sal the dust is transported mainly in a 5 - 6 km thick layer about 1 - 1.5 km above the surface (Carlson and Prospero, 1972). The dust actually reaching Sal is transported downwards by gravitation and mixing through convective erosion of the base of the layer. This can be illustrated by the concentration of about  $550 \mu\text{g}/\text{m}^3$  at the surface (Carlson and Caverly, 1977) and  $2000 \mu\text{g}/\text{m}^3$  or more near the 70 kPa pressure surface during dust outbreaks (Carlson, 1979). Mean surface concentration for Toronto is about  $129 \mu\text{g}/\text{m}^3$  (Munn, 1973).

#### 4.1.3.2 Daily Variation

To assess the validity of calculating  $\tau_a$  by forcing spectrally integrated irradiance into a Beer's law framework,  $\tau_a$  values were plotted



against turbidity values measured at wavelength of  $0.5 \mu\text{m}$  (Carlson, 1975) for the same optical air mass (Figure 4.7a). The agreement is good with a correlation coefficient of 0.993. The mean daily  $\tau_a$  and sunphotometer measurements and their standard deviations are compared in Figure 4.7b. The symmetrical agreement between them underlines the good correlation between the two sets of values. The agreement shown in the plots suggests that  $\tau_a$  is an acceptable measure of aerosol turbidity.

The largest variations in  $\tau_a$  values at Sal occur on the days of heavy dust outbreak as was the case on 30th July (Figure 4.7b). Similar variations occur in values of  $\tau_a$  when tropical air masses pass over Canada. The maximum value on 30th July, was 1.45 compared with 1.5 at wavelength of  $0.66 \mu\text{m}$  inferred from satellite photographs on that day (Carlson, 1979) but less than the reported maximum of 3.2 at wavelength of  $0.55 \mu\text{m}$  (Levin et al., 1980) during dust storms (Khamsims) in Israel. However, Carlson (1979) inferred values up to 3.5 at wavelength of  $0.66 \mu\text{m}$  from satellite photographs.

Surface winds at Sal have mainly northern component and so have little effect on turbidity as the bulk of the dust is carried overhead by upper easterly winds. This contrasts with Canadian stations where  $\tau_a$  and surface wind direction are correlated (section 4.1.4.1).

#### 4.1.4 Dependence of $\tau_a$ Values on Meteorological Parameters

The dependence of turbidity on synoptic air mass types and weather patterns have been reported by Flowers et al., (1969), Unsworth

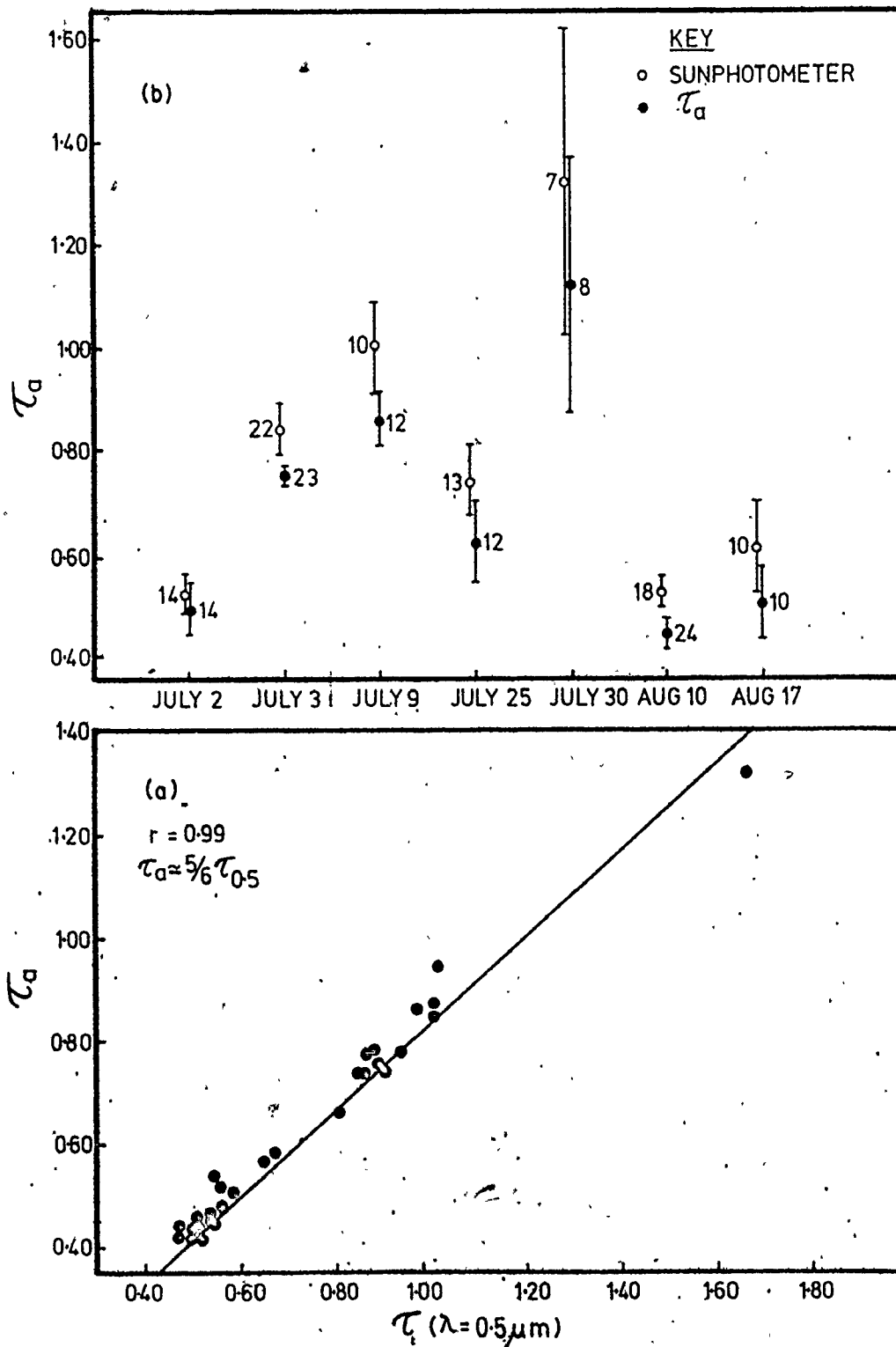


Figure 4.7.  $\tau_a$  values compared with sunphotometer measurements at Sal (1974): (a) correlation (b) mean daily values and  $\pm$  one standard deviation about the mean.

and Monteith (1972), and McArthur (1976). In this study, values of  $\tau_a$  are compared with locally observed meteorological parameters - dew point, dry and wet bulb temperatures; relative humidity; visibility; wind speed and direction. Apart from visibility measured at the nearby airports - Dorval (Montreal) and Toronto (Woodbridge), all the others were measured simultaneously with the solar irradiances. The  $\tau_a$  - visibility relationship will be treated in more detail (Section 4.2).

#### 4.1.4.1 Dependence on Surface Wind Speed and Direction

The concentration of pollutants from a steady continuous point source, in a stationary turbulent flow is inversely related to the wind speed (Neumann, 1977). In real atmospheres, pollutant sources are not continuous and also wind speed and direction are not only dependent on the synoptic situation but also on the surface geometry of the location.

To study the relationship between values of  $\tau_a$  and wind speed and direction, mean seasonal and annual values were calculated for four classes of wind speed (Table 4.10) and for eight classes of wind direction for Montreal and Woodbridge. Also, the diurnal relationship was examined for two days in Montreal (Figure 4.8a).

TABLE 4.10: MEAN SEASONAL  $\tau_a$  AND NUMBER OF HOURLY VALUES IN FOUR CLASSES OF WIND SPEED AT MONTREAL (1968-78)

	Wind speed (meters per second)			
Annual	< 6	7 - 12	13 - 17	> 17
Mean $\tau_a$	0.117	0.111	0.107	0.096
Total hours	409	500	469	799
Winter	< 3	4 - 6	7 - 9	> 9
Mean $\tau_a$	0.083	0.062	0.049	0.045
Total hours	295	256	160	34
Spring/Autumn	< 2	3 - 4	5 - 6	> 6
Mean $\tau_a$	0.113	0.083	0.075	0.061
Total hours	247	219	97	83
Summer	1 - 5	6 - 10	11 - 15	> 15
Mean $\tau_a$	0.137	0.123	0.142	0.169
Total hours	116	176	260	304

Except for summer, the inverse relationship between values of  $\tau_a$  and wind speed is shown both on seasonal and daily basis. Combining wind direction indicates that large values occur with low mean wind speed associated with southerly winds (Figure 4.8b) while small values are obtained from high mean wind speed associated with winds from between north and west quadrants.

Figures 4.9 and 4.10 indicate the relationship between mean seasonal values of  $\tau_a$  and wind direction at Montreal and Woodbridge. At both stations, the foreign sources of particulates are mainly the industrial areas in the United States in the south and so southerly winds

especially in summer are associated with large values. The location of the measurement site with respect to the local sources of particulates, change this simple directional pattern.

The city of Toronto is the main source of local particulates from the southeast for Woodbridge. The importance of this direction shows up clearly in winter and spring/autumn (Figure 4.10, a, b). At Montreal, since the measurement site is near the downtown area, additional particulates can be associated with winds from any direction but perhaps more especially from east of a north-south line in which the greater portion of the city and most of the industries (e.g. petroleum refineries) are located. In winter, larger  $\tau_a$  values are associated with winds from east of this north-south line (Figure 4.9b). The orientation of the St. Lawrence valley in a southwest - northeast direction which channels most of the wind in the area (Powe, 1969) and in which most of the heavy industries lie, seem to affect the values of  $\tau_a$ . The alignment of slightly larger  $\tau_a$  values in this direction in spring/autumn (Figure 4.9a) and summer (Figure 4.9c) is probable evidence of this influence.

#### 4.1.4.2 Dependence on Dew Point Temperature and Relative Humidity

Hänel (1976) and Shettle and Fenn (1979) have shown that aerosol particulates grow in size with increase in relative humidity and that the largest changes occur within the range, 60 - 95%. For relative humidity > 95%, the particles not only increase their size but also change their shape. To study the effect of relative humidity on  $\tau_a$  values, annual and seasonal mean values were calculated for 4 classes of relative humidity

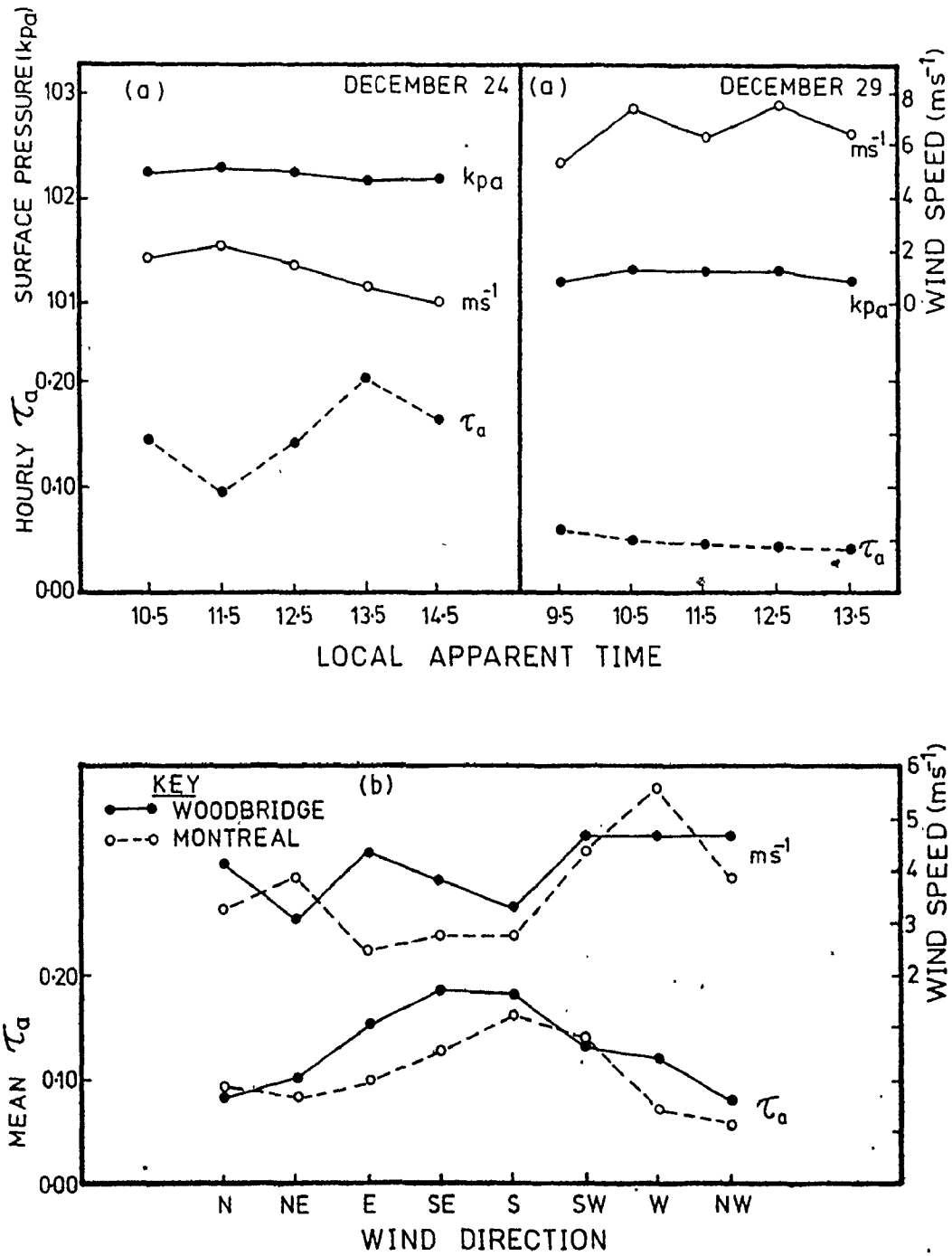


Figure 4.8. The inverse relationship between values of  $\tau_a$  and wind speed: (a) at Montreal for two days (b) at Montreal and Woodbridge, 1968-78.

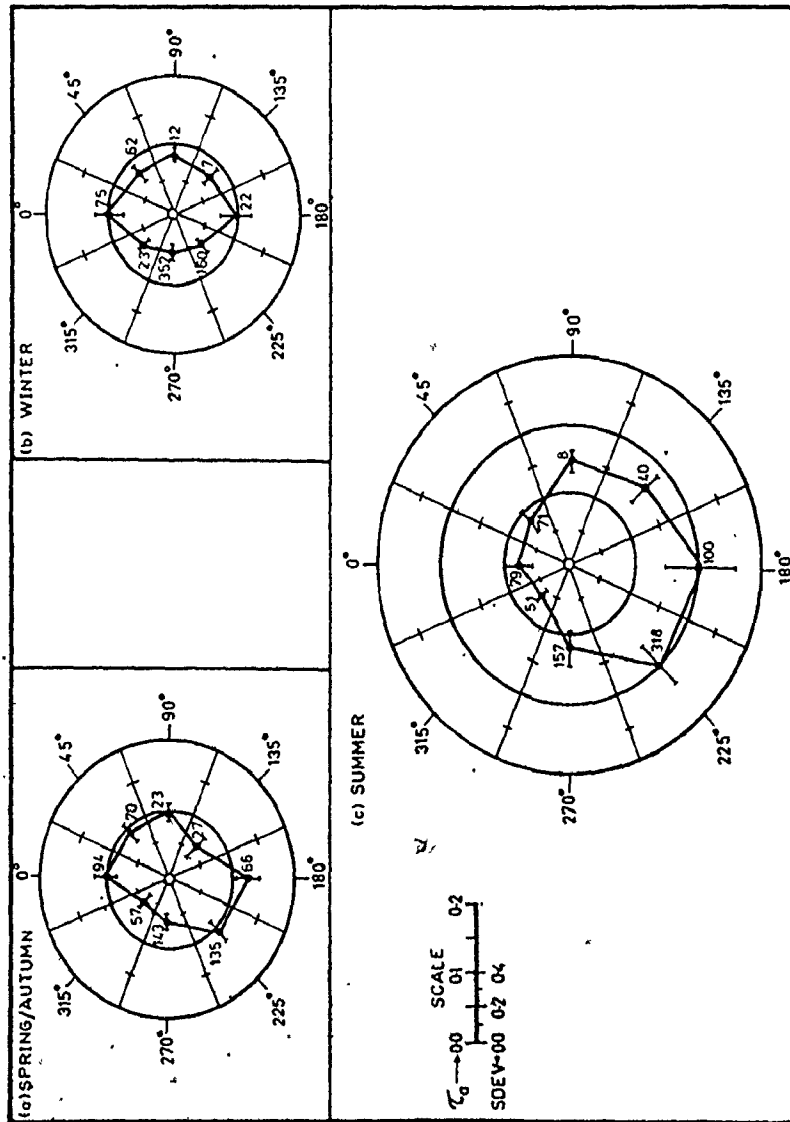


Figure 4.9. Polar plot of mean values of  $\tau_a$  along the radial axis vs wind direction at Montreal, 1968-78.

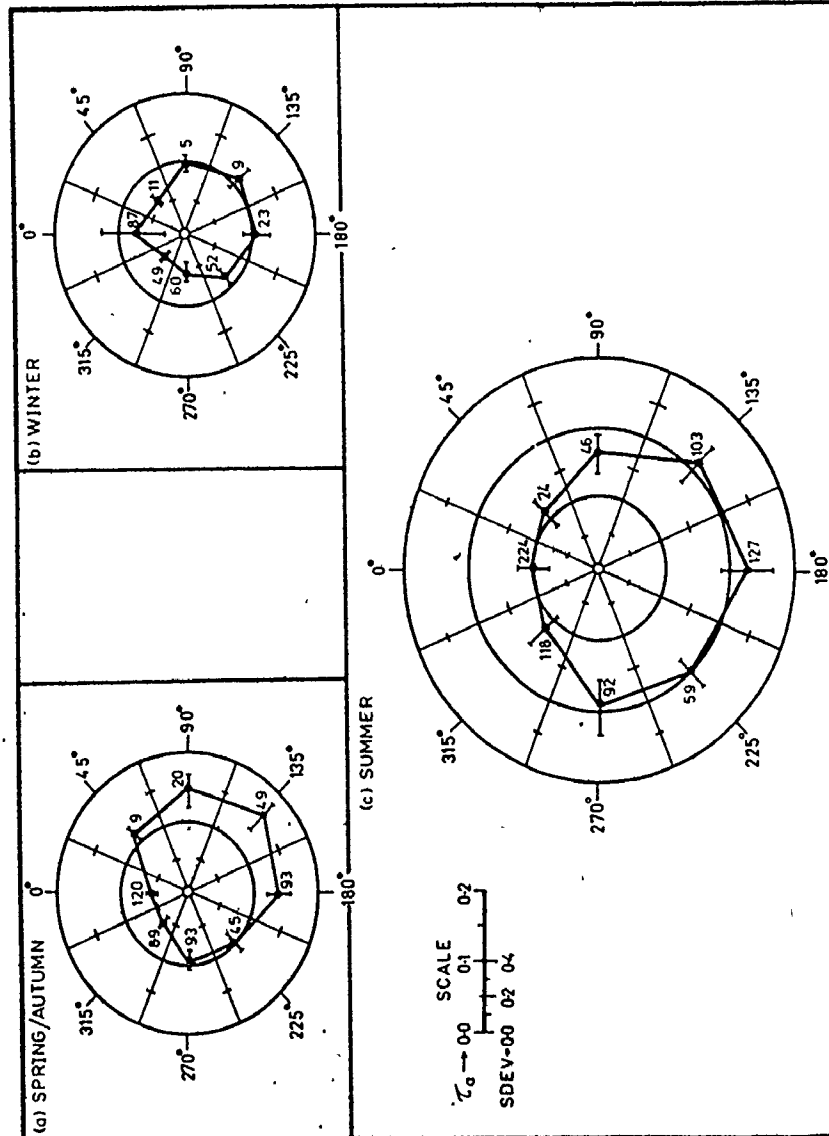


Figure 4.10. Polar plot of mean values of  $\tau_a$  along the radial axis vs wind direction at Woodbridge, 1968-78.



at Montreal and Woodbridge (Table 4.11). In general, values for Montreal are positively and directly dependent on relative humidity < 85% but above 85% the relationship is not clear. For Woodbridge, the same positive and direct relationship exists in winter but for other seasons, dependence on relative humidity is less clear.

Values of  $\tau_a$  were correlated with dew point temperatures in a two-way frequency distribution of the number of occurrences of corresponding  $\tau_a$  and dew point values by season of the year (Table 4.12) for Montreal (1968-78). As Peterson et al. (1981) found for Raleigh, the  $\tau_a$  - dew point relationship was the most significant of the meteorological parameters considered in this analysis. For all seasons, values of  $\tau_a$  increase with dew point temperature and in the frequency groups, values are least in winter and largest in summer. This emphasizes the relative 'cleanliness' of Tropical (summer) and Arctic (winter) air masses with different dew point temperatures. Monthly linear correlation coefficients were highest in summer (> 0.50) and lowest in winter (< 0.40). Peterson et al. (1981), on the other hand, obtained lowest coefficients in summer (< 0.44) and highest in November (0.63). Similar calculations with wet-bulb and dry-bulb temperatures show results like those for dew point temperature (Appendix 5: a,b).

#### 4.2 Turbidity and Visibility

Two aspects of turbidity - visibility relationship were investigated. Firstly, values of  $\tau_a$  and visibility were correlated. Secondly, turbidity values,  $\tau_{ak}$  were calculated with Koschmieder formula and then compared with  $\tau_a$ .

TABLE 4.11: MEAN SEASONAL  $\tau_a$  AND NUMBER OF HOURLY VALUES IN FOUR CLASSES OF RELATIVE HUMIDITY AT MONTREAL AND WOODBRIDGE (1968-78)

	Relative humidity (percent)			
	0 - 40	41 - 70	71 - 85	> 85
<b>Montreal</b>				
<b>Annual</b>				
Mean $\tau_a$	0.085	0.103	0.132	0.107
Total hours	321	1428	342	86
<b>Summer</b>				
Mean $\tau_a$	0.097	0.158	0.169	0.115
Total hours	161	483	168	44
<b>Spring/Autumn</b>				
Mean $\tau_a$	0.080	0.086	0.117	0.108
Total hours	119	413	89	25
<b>Winter</b>				
Mean $\tau_a$	0.052	0.065	0.082	0.083
Total hours	43	585	99	18
<b>Woodbridge</b>				
<b>Annual</b>				
Mean $\tau_a$	0.096	0.134	0.118	0.110
Total hours	248	970	344	107
<b>Summer</b>				
Mean $\tau_a$	0.107	0.180	0.151	0.121
Total hours	143	478	150	74
<b>Spring/Autumn</b>				
Mean $\tau_a$	0.087	0.102	0.086	0.091
Total hours	92	329	105	24
<b>Winter</b>				
Mean $\tau_a$	0.021	0.061	0.100	0.090
Total hours	15	182	97	11

TABLE 4.12: SEASONAL FREQUENCY DISTRIBUTION OF THE NUMBER OF OCCURRENCES OF CORRESPONDING  $\tau_a$  AND DEW POINT TEMPERATURE VALUES FOR MONTREAL (1968-1978).

Season/ $\tau_a$	Dew Point Temperature ( $^{\circ}\text{C}$ )				Total Hours
	< 4	4 - 9	10 - 15	> 15	
<b>Annual</b>					
< 0.129	1258	219	193	14	1684
0.13 - 0.229	103	65	85	52	305
0.23 - 0.349	14	8	18	72	112
> 0.35	9	1	16	50	76
Total hours	1384	293	312	188	2177
Mean $\tau_a$	0.077	0.093	0.124	0.302	
<b>Summer</b>					
	< 9	9 - 14	15 - 20	> 20	
< 0.129	319	188	25	0	532
0.13 - 0.229	54	42	60	9	163
0.23 - 0.349	5	8	55	26	94
> 0.35	3	9	43	12	67
Total hours	379	247	183	47	856
Mean $\tau_a$	0.094	0.099	0.270	0.335	
<b>Spring/Autumn</b>					
	< 1	1 - 6	7 - 12	> 12	
< 0.069	247	56	33	3	339
0.07 - 0.089	59	10	8	1	78
0.09 - 0.129	62	13	15	4	94
> 0.13	28	45	29	33	135
Total hours	396	124	85	41	646
Mean $\tau_a$	0.070	0.105	0.112	0.194	
<b>Winter</b>					
	< -10	-10 to -6	-5 to 0	> 0	
< 0.049	321	17	20	6	364
0.05 - 0.089	187	19	16	2	224
> 0.09	115	23	11	8	157
Total hours	623	59	47	16	745
Mean $\tau_a$	0.062	0.079	0.095	0.141	

#### 4.2.1 $\tau_a$ and Visibility

$\tau_a$  and visibility values were analyzed in three ways. Firstly,  $\tau_a$  was correlated with visibility in a two-way frequency distribution of the number of occurrences of corresponding  $\tau_a$  and visibility values by season of the year (Table 4.13). Secondly, for each wind direction, mean  $\tau_a$  and visibility values were evaluated (Figure 4.11). Thirdly, because equation 2.44 suggests an inverse relationship between  $\tau_a$  and visibility, values of  $\tau_a$  and the inverse of visibility were calculated for each season (Appendix 6 and Figure 4.12).

Figure 4.11 shows the inverse relationship between  $\tau_a$  and visibility.  $\tau_a$  values are largest with southerly winds when visibility is lowest and are least with northerly winds when visibility is highest. Table 4.13 indicates that dependence of values of  $\tau_a$  on visibility becomes tenuous for visibility less than 8 to 10 km but clearer beyond 10 km. Figure 4.12 clarifies this relationship and suggests that two regimes exist. For visibility less than about 10 km,  $\tau_a$  is independent of visibility but shows a strong linear relationship with the inverse visibility greater than 10 km. This result is comparable to the observed relation between incident ultra-violet (UV) irradiance and visibility in which for visibilities  $> 12$  km, the UV ratio at two stations in Los Angeles basin appears to be slightly dependent on visibility but strongly related to visibility below about 10 km (Peterson et al., 1978). The high correlation coefficients (Table 4.14) confirm the strong dependence of  $\tau_a$  on visibility more than 10 km. These results echo the good correla

TABLE 4.13: SEASONAL FREQUENCY DISTRIBUTION OF THE NUMBER OF OCCURRENCES OF CORRESPONDING  $\tau_a$  AND VISIBILITY VALUES FOR MONTREAL (1968-1978).

Season/ $\tau_a$	Visibility (kilometers)				Total Hours
	< 8	8 - 10	11 - 13	> 13	
<b>Annual</b>					
< 0.129	22	28	19	1577	1646
0.13 - 0.229	25	23	32	245	325
0.23 - 0.349	17	21	27	61	126
> 0.35	16	24	13	27	80
Total hours	80	96	91	1910	2177
Mean $\tau_a$	0.255	0.259	0.226	0.085	
<b>Summer</b>					
< 0.129	8	8	2	495	513
0.13 - 0.229	6	7	10	153	176
0.23 - 0.349	10	17	23	48	98
> 0.35	11	20	12	26	69
Total hours	35	52	47	722	856
Mean $\tau_a$	0.330	0.334	0.292	0.114	
<b>Spring/Autumn</b>					
< 0.069	6	1	3	321	331
0.07 - 0.089	1	0	4	74	79
0.09 - 0.129	1	7	3	86	97
> 0.13	15	20	22	82	139
Total hours	23	28	32	563	646
Mean $\tau_a$	0.177	0.220	0.171	0.076	
<b>Winter</b>					
< 0.049	15	0	0	336	351
0.05 - 0.089	4	6	2	219	231
> 0.09	19	14	9	121	163
Total hours	38	20	11	676	745
Mean $\tau_a$	0.139	0.152	0.117	0.060	

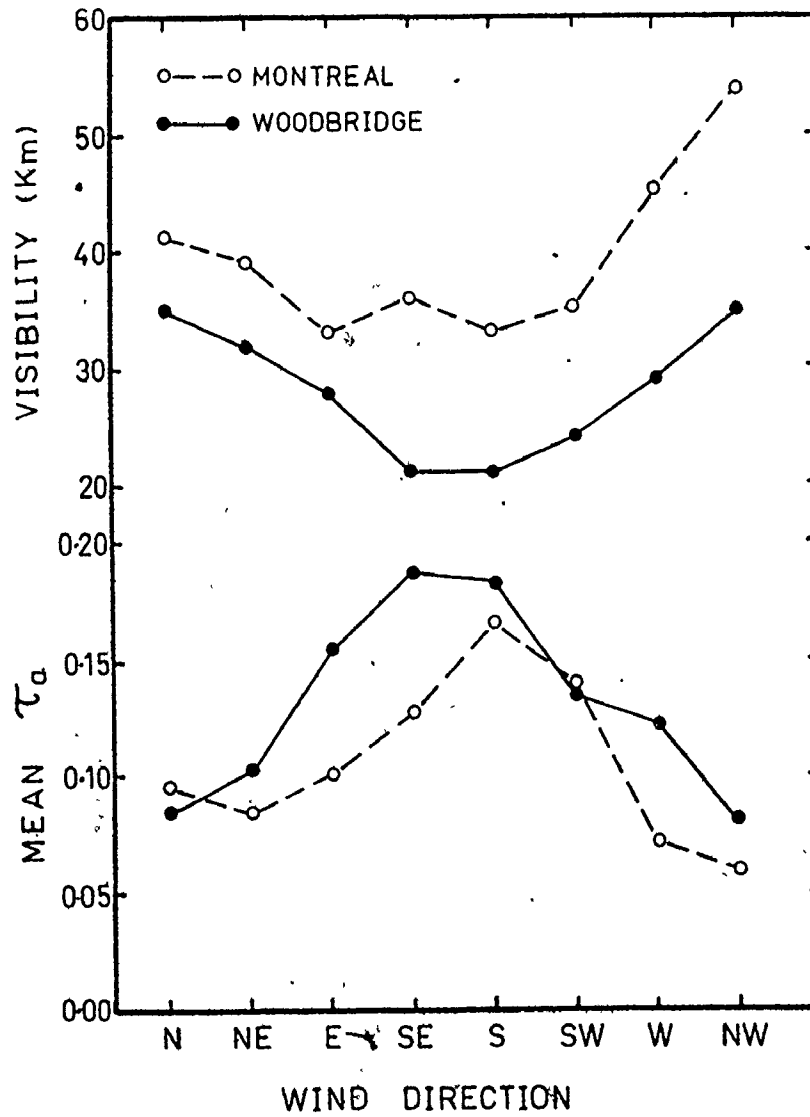


Figure 4.11. The inverse relationship between values of  $\tau_a$  and visibility (km) for eight classes of wind direction at Montreal and Woodbridge, 1968-78.

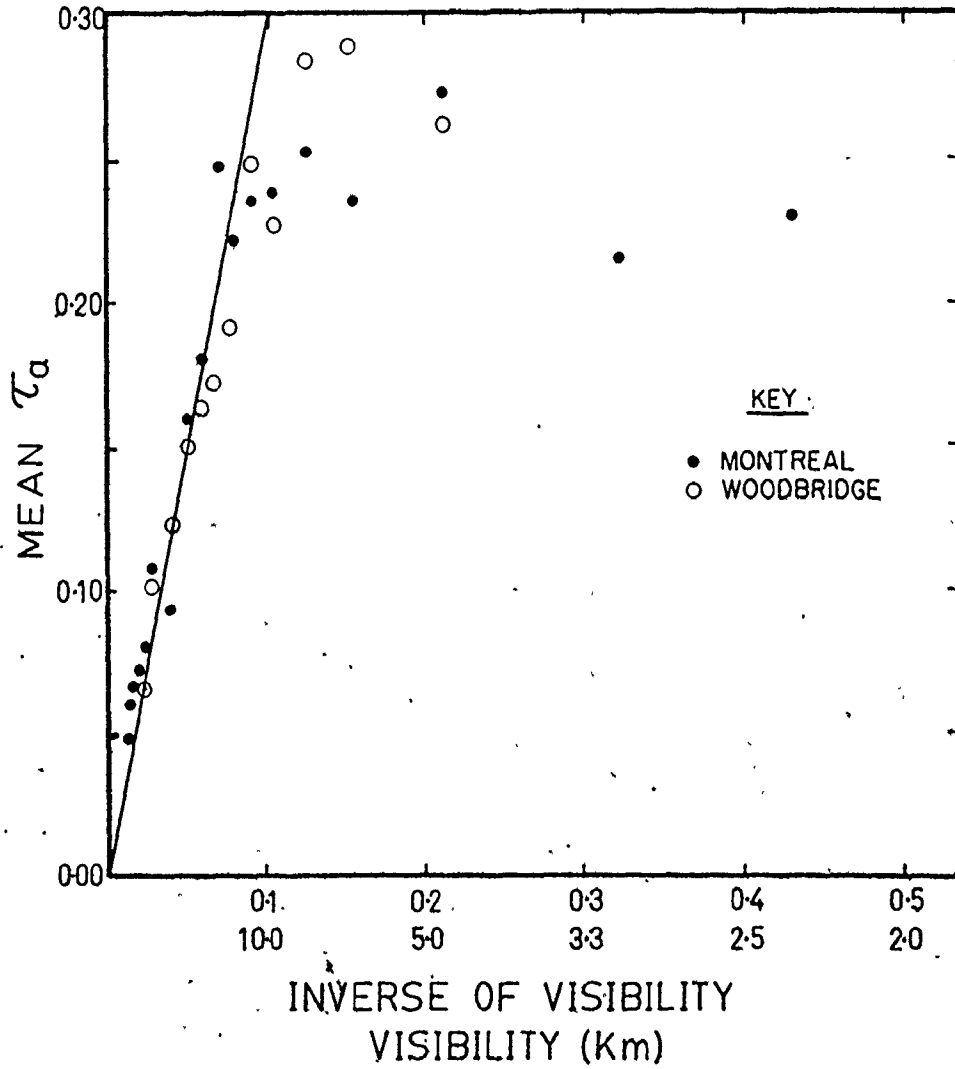


Figure 4.12. Two regime relationship between values of  $\tau_a$  and the inverse of visibility at Montreal and Woodbridge, 1968-78.

tion reported between spectral optical depths and visibility (Pitts et al., 1977) and between spectrally averaged optical depth and aerosol scattering coefficient at the Equator (Feigelson et al., 1975). Peterson et al. (1981) showed good correlation between  $\tau_a$  and visibility.

TABLE 4.14: CORRELATION BETWEEN VALUES OF  $\tau_a$  AND INVERSE VISIBILITY AT MONTREAL (1968-78)

	All season	Summer	Winter	Spring/autumn
Correlation Coefficient ( $v > 10\text{km}$ )	0.97	0.97	0.93	0.94
Correlation Coefficient (all $v$ )	0.61	0.28	0.88	0.68

#### 4.2.2 $\tau_{ak}$ Calculated with Koschmieder Formula

Using equation 2.44, aerosol attenuation coefficient  $\tau_{ak}$  was calculated for altitudes 0.5 to 1.50 km and scale heights 1 to 1.50 km. As expected,  $\tau_{ak}$  increases as visibility decreases whatever the combination of scale height and altitude. The rate of increase is noticeably high for visibility less than 10 km. If, from equation 2.44,  $\tau_{ak}$  is differentiated with respect to visibility and the derivative normalized with  $\tau_{ak}$ , the quotient (the rate of change of  $d\tau_{ak}$  per unit  $dv$ ) is independent of the scale height  $H_p$  and altitude  $Z$  but is inversely related to visibility. At 5 km visibility, the rate is 20% compared with 2% at 50 km. If  $\tau_{ak}$  (equation 2.44) is differentiated with respect to scale height and then with respect to altitude, it can be shown that the rates of change per unit  $d\tau_{ak}$  are independent of visibility. For  $H_p = Z = 1.25$



km, the rate of change for  $H_p$  is 33% compared with 47% for  $Z$  and if  $H_p = Z = 1.50$  km the rates are 28% for  $H_p$  and 39% for  $Z$ . The rates, therefore, decrease with increase in height of  $H_p$  and  $Z$  and are slightly larger for  $Z$ . The rate of change per unit  $d\tau_{ak}$  will then be substantial in cases where aerosol layer is quite close to the surface as in large urban locations.

Plots of  $\tau_{ak}$  for  $H_p = Z = 1.5$  km and for  $H_p = 1$ ,  $Z = 1.5$  km, and  $\tau_a$  appropriate to the measured visibilities are shown in Figure 4.13. There is good agreement between  $\tau_a$  and  $\tau_{ak}$  to within  $\leq 15\%$  for visibility more than 10 km. The best results are for scale height and altitude lying between 1 and 1.5 km which is the same range suggested by Kriebel (1978) for the homogeneous aerosol layer applicable to urban areas.

Apart from the good correlation between spectrally averaged optical depth and aerosol scattering coefficient and also the turbidity - visibility study of Peterson et al. (1981), most other published studies relate spectral optical depth to scattering coefficient or visibility. Despite the fact that visibility is a subjective horizontal estimate while  $\tau_a$  is a vertical measurement, and also that visibility strictly applies to the visible wavelengths, these results show good agreement between turbidity and visibility more than 10 kilometers.

#### 4.3 Turbidity Trends

Values of  $\tau_a$  for Montreal and Woodbridge (1968-78) and Goose (1968-77) were analyzed for year to year variation. Even though records

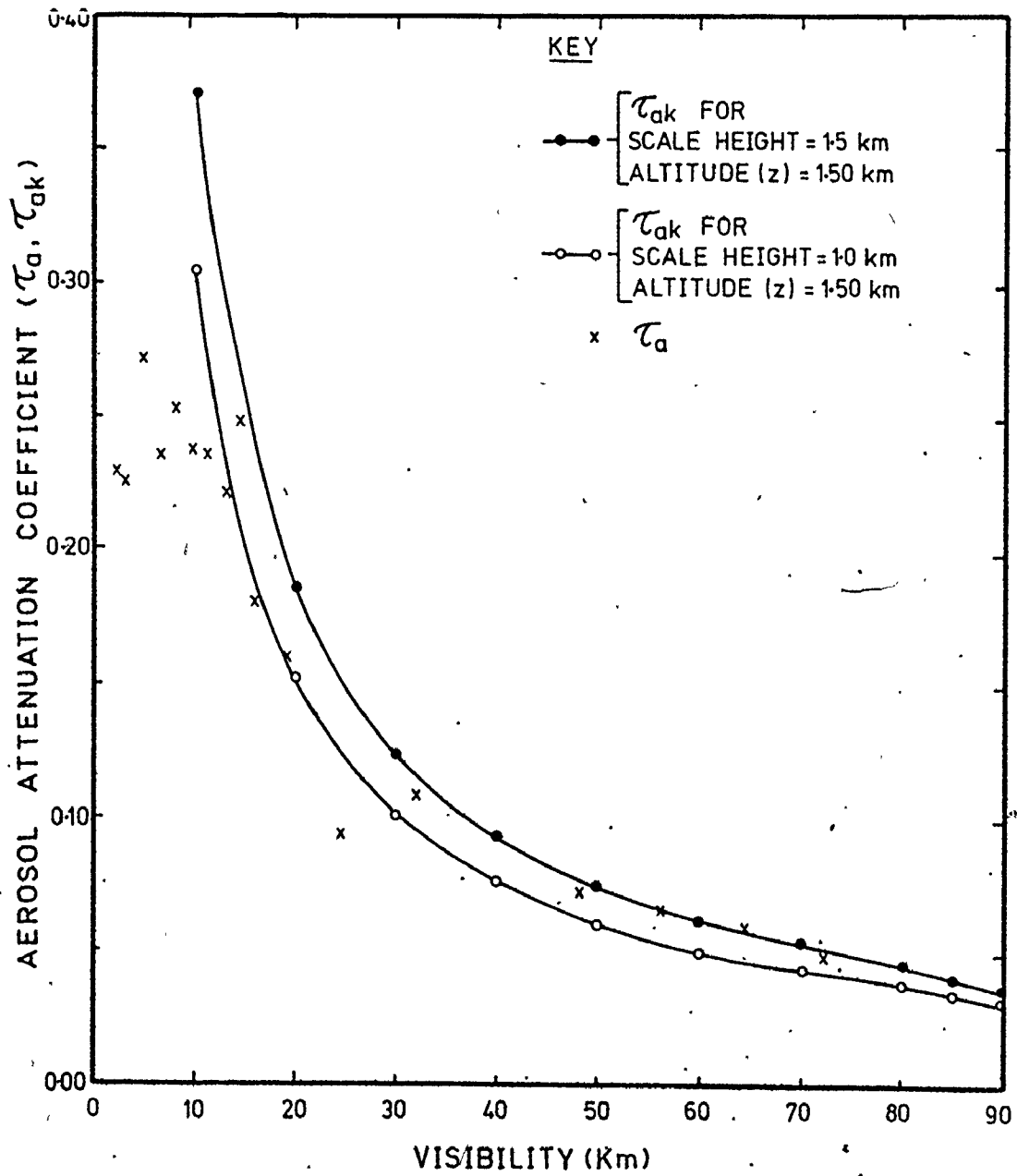


Figure 4.13. Values of  $\tau_a$  and  $\tau_{ak}$  compared for two sets of aerosol scale height and altitude for Montreal, 1968-78.

are available for Goose and Montreal before 1968, the first full year of records for Woodbridge began in 1968 and so to cover the same period at all 3 stations, analysis of data started with 1968. The analysis was done in two ways. First, from the hourly values, mean monthly values were computed for each year. Second, mean seasonal and annual values were calculated from the hourly values for each year (Appendix 7).

The summertime peak values and the mean annual and seasonal values (Figure 4.14), except winter at Woodbridge, show a decrease in mean values at all the stations since 1968. To test whether the trends are significant, a one-sided Cox's test (Bradley, 1968) for trend was applied to the values plotted in Figure 4.14. The mean values were arranged from 1 (1968) to  $n = 11$  (1978; Montreal and Woodbridge) and to  $n = 10$  (1977; Goose). The sign of  $1-n$ ,  $2-(n-1)$ , and so on were considered and the sum  $S$  of the 'difference - scores' was calculated by

$$S = 9h_{1,n} + 7h_{2,n-1} + 5h_{3,n-2} + 3h_{4,n-3} + h_{5,n-4} \quad (4.3)$$

$$\text{Here, } h_{1,n} = \begin{cases} +1 & \text{if first observation} > n^{\text{th}} \\ 0 & \text{if first observation} < n^{\text{th}} \end{cases} \quad \text{and } h_{2,n-1} \text{ etc.,}$$

are defined similarly.

Using the mean of the maximum score  $E(S)$  and the variance  $\text{var}(S)$ , the ratio  $R = \{S - E(S)\} / \{\text{var}(S)\}^{1/2}$  was evaluated from the group of observations (Table 4.15). The distribution of  $R$  is asymptotically standard normal for large  $n$ . Thus for a one-sided test, the critical value of  $R$  for a test at the 5% level of significance with 10 observations is 1.64. The test has the advantage of being non-parametric and thus requires no assumption about linearity and normality of the original data. A minor

criticism is the loss of the middle observation in case of odd number of observations as for Montreal and Woodbridge. The results and further explanations are presented in Table 4.15. They show that the trends are significant at all 3 locations except summer and winter at Woodbridge. It is not clear why winter values at Woodbridge are out of phase with the others but for summer, 1969 was the only year without data in July -- a month usually associated with large  $\tau_a$  values. This reduced the mean value for the month to its lowest during the 1968-78 period and was mainly responsible for the insignificant trend.

TABLE 4.15: COX'S TEST FOR  $\tau_a$  TREND AT MONTREAL, WOODBRIDGE AND GOOSE

Station	Season	*S	**R	Results
Montreal	All	25	1.95	Significant
	Winter	25	1.95	Significant
	Summer	24	1.79	Significant
	Spr/Aut	24	1.79	Significant
Woodbridge	All	25	1.95	Significant
	Winter	9	-0.54	Not Significant
	Summer	17	0.70	Not Significant
	Spr/Aut	25	1.95	Significant
Goose	All	24	1.79	Significant
	Winter	24	1.79	Significant

\*S = No. of difference-scores. For 10 observations (ignoring the middle observation for Montreal and Woodbridge),  $0 < S < 25$ .

$$E(S) = n^2/8 = 25/2 = 12.5$$

$\text{var}(S) = n(n^2 - 1)/24$ , where  $n = 10$  is the number of observations.

$$**R = (S - n^2/8) / \{n(n^2 - 1)/24\}^{1/2}$$

For one-sided test,  $R > 1.64$  is necessary for trend to be significant.

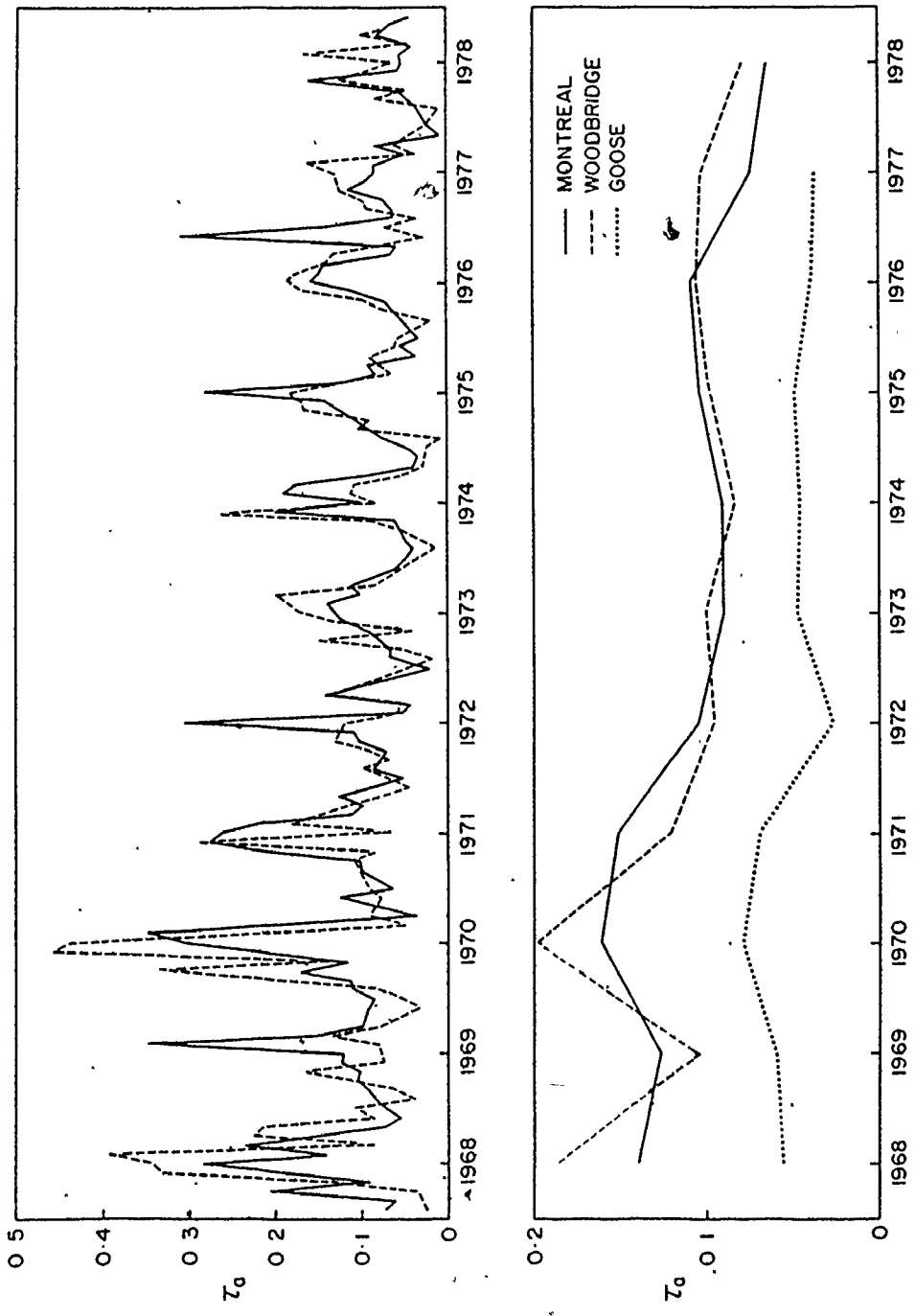


Figure 4.14. Trends in monthly and seasonal values of  $\tau_a$  at Montreal, Woodbridge and Goose.

This general trend suggests a decrease in particulates which has been reported for urban areas in the United States (1957-66: - Ludwig et al. 1971; 1960 - 71: - Bach, 1976; 1930-79: - Eisenbud, 1980; Peterson et al.; 1978) and in England (Wood, 1973). Particulate reduction has been attributed to air control regulations and changes toward cleaner fuels.

For rural areas in the United States, Bach (1976) found no discernible trend in particulate loading (1960-71) but Ludwig et al., (1971) reported an upward trend for 20 non-urban sites in the United States from 1957-66. The non-urban sites were subject to urban influences but this may be minimal for Goose. Since a downward trend in mean  $\tau_a$  values occurs at Goose as well as at Montreal and Woodbridge, there must be an alternative explanation besides air control regulations and use of cleaner fuels.

In Canada, an increase in the incidences of 'clean' Arctic air masses is another possibility for the reduction in particulates. When this air mass dominates,  $\tau_a$  is small. Larger values are associated with tropical air masses. For example in 1972, mean  $\tau_a$  values were below the average values for the 1968-78 period at all 3 locations. This was a particularly cold year (Hare and Thomas, 1974) when Arctic air was dominant throughout most of the summer. Hare and Thomas also recognized a downward trend in the average air temperature near the surface in Canada from 1955 to 1972. Jones and Jiusto (1980) reported not only a decrease in temperature but also an increase in snowfall for 3 cities in New York State from 1940 to 1975.

Recently, Peterson et al. (1981) found an upward trend for turbidity values at Raleigh, Greensboro and Raleigh - Durham in the United States from 1965 to 1979. This finding is at variance with the result of this study. The differences in the two studies may be due to the following:

- (a) The Canadian stations and the American stations are differently located with respect to sources of particulates. The American stations lie in that part of the continent where particulate levels are high as a result of heavy industrialization and urbanization. The Canadian centres on the other hand receive their major supply of particulates from the United States (Clark, 1980) but because of their more northerly location there is greater influence of clean Arctic air masses.
- (b) The methods of evaluating turbidity factors differ. Peterson et al. used values measured with Volz G sunphotometer. The accuracy of the instrument, especially in measuring turbidity in air with small aerosol extent (e.g. Arctic air mass), is controversial (Unsworth and Monteith, 1972; Laulainen and Taylor, 1974, 1975; Russel and Shaw, 1975; Volz, 1975). Peterson et al. (1981) cautioned also that for turbidities near 0.092 (0.04 decadic) the measurement error is +10% and even in the field, the use of the instrument may not yield this level of accuracy because the long - term stability of the instrument is uncertain.

#### 4.4 Turbidity Coefficients Compared

The turbidity factors proposed by Linke (1942) and Polavarapu (1978) were calculated from equations 2.29 and 2.35. Results for Hamilton and Woodbridge are plotted along with  $\tau_a$  values (Figure 4.15).

All the three turbidity factors show similar variation throughout the day. The influence of water vapour on Linke's turbidity factor  $T$  is shown by the much larger values. Polavarapu's aerosol factor  $T_p$  is more in phase with  $\tau_a$  than  $T$  is with it. The use of the MAC model to calculate  $I_0$  in the evaluation of Linke's turbidity factor for dust free atmosphere  $T_{dfm}$  reduces the value of  $T_p$  and further improves the agreement between  $\tau_a$  and  $T_p$ . To examine the extent of improvement of  $T_p$  by the use of  $T_{dfm}$  instead of  $T_{df}$ , the ratios:  $T_p/\tau_a$ ,  $T_{pm}/\tau_a$ , and  $T_{df}/T_{dfm}$  were evaluated for three days in Hamilton and plotted in Figure 4.16.

But for some variations on 14th May,  $T_p/\tau_a$  increases with optical air mass and is constant for a given air mass. The use of  $T_{dfm}$  instead of  $T_{df}$  removes these variations and makes  $T_{pm}/\tau_a$  the same value for a given air mass (Appendix 8).

$T_{dfm}$  is always constantly greater than  $T_{df}$  as the ratio  $T_{df}/T_{dfm}$  is less than unity (Figure 4.16). This suggests that the models used in calculating  $T_{df}$  and  $T_{dfm}$  compare well. The real difference lies in the fact that whereas  $T_{dfm}$  is obtained by using an equation,  $T_{df}$  is obtained from graphs (Section 3.3.5).



Since these results show that Polavarapu's aerosol factor is in good agreement with  $\tau_a$ , his graphical evaluation of  $I_0$  can probably be replaced with the MAC model.

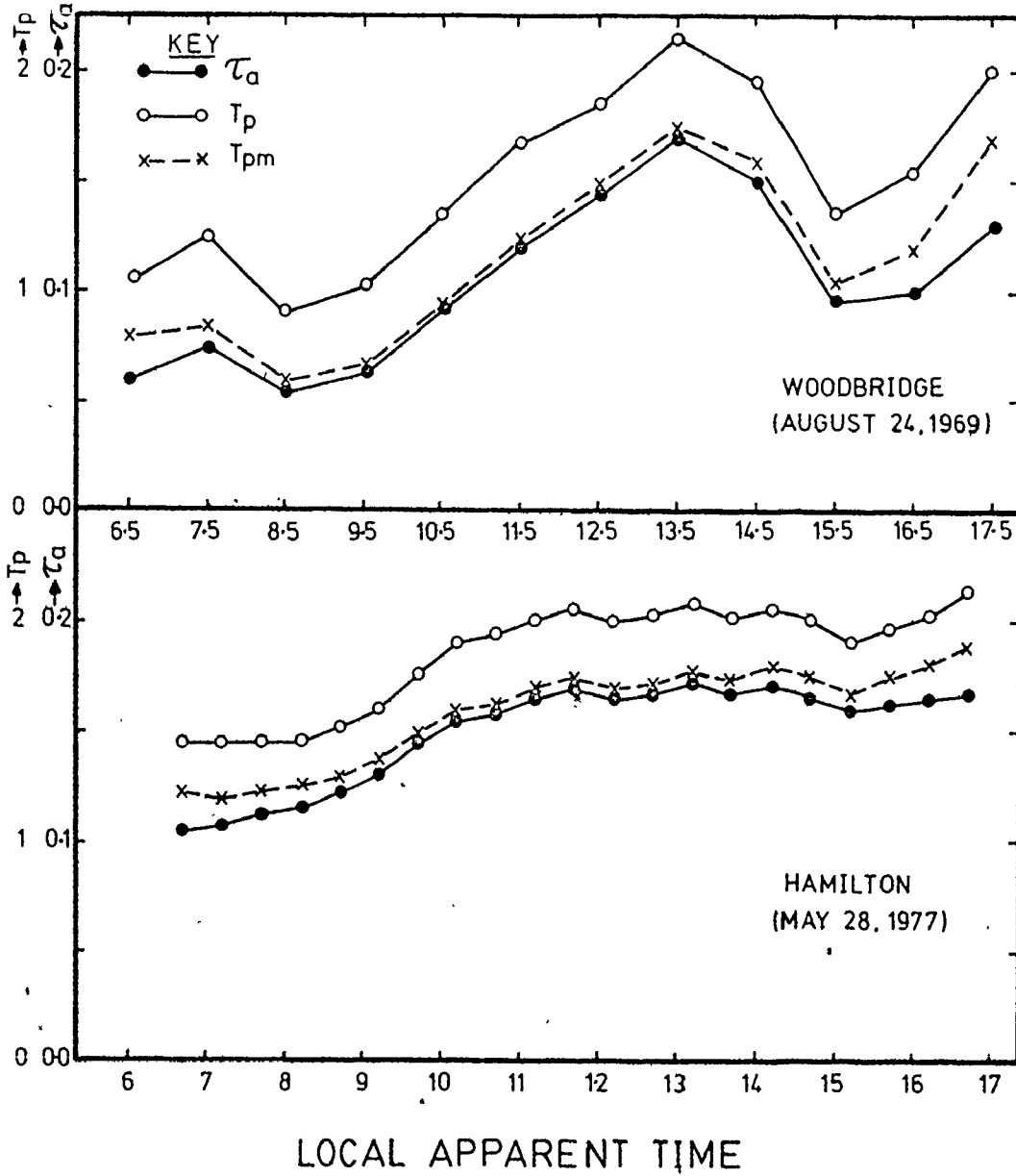


Figure 4.15. Values of  $\tau_a$  and  $T_p$  compared.

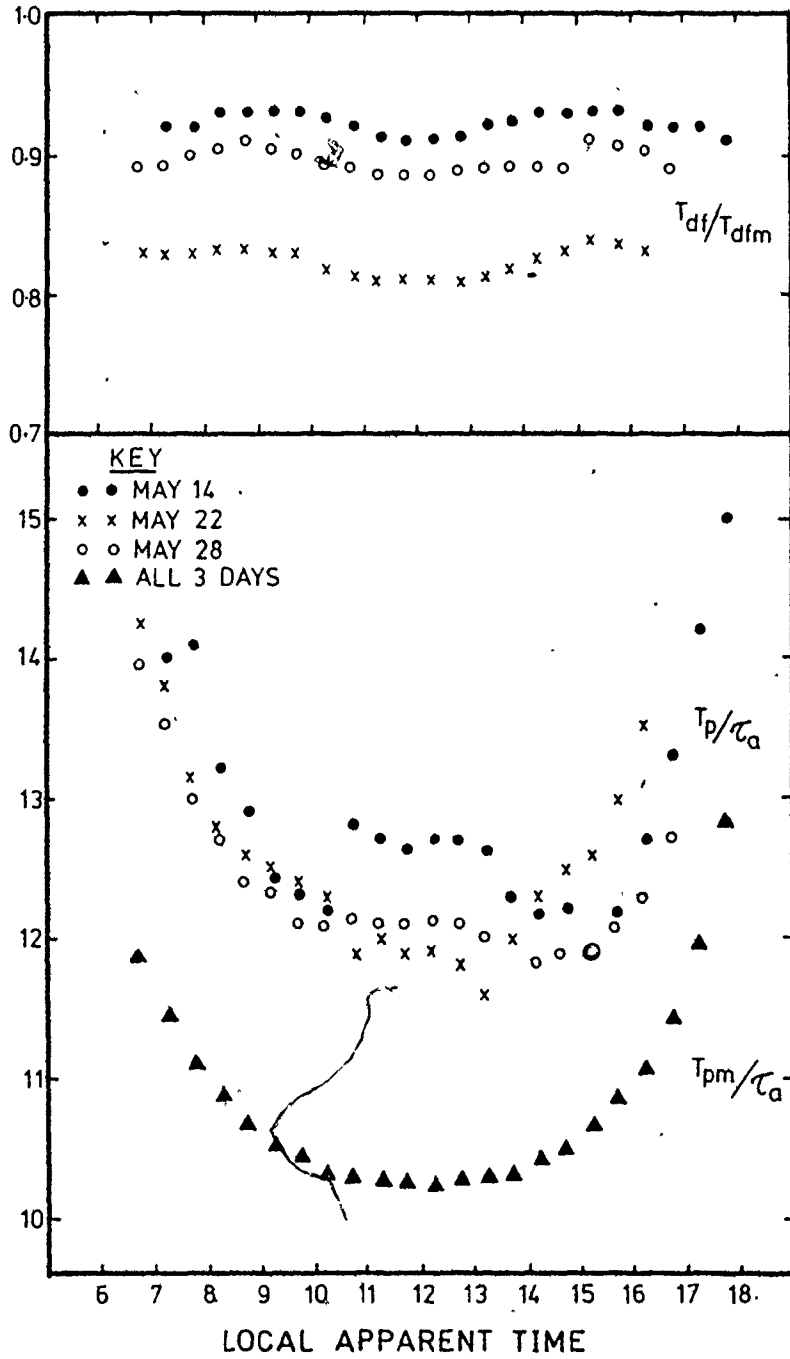


Figure 4.16. Ratios of  $T_p/\tau_a$ ,  $T_{df}/T_{dfm}$  for 3 days at Hamilton.

## BULK SCATTERING AND ABSORPTION PROPERTIES

5.1 Introduction

Estimates of aerosol scattering and absorption depend on measured and calculated diffuse and global irradiances and, Robinson's (1962) ratio of forward to backscatter (Table 2.1). Despite the uncertainties of obtaining backscatter to total scatter ratio (Section 2.1.2), Robinson's values compare well with values obtained from other work (Figure 2.1; Joseph and Wolfson, 1975) and have been widely used (Robinson, 1966; Hamilton and Collingbourne, 1967; Forbes and Hamilton, 1971; Unsworth and Monteith, 1972; Drummond and Robinson, 1974; Wesely and Lipschutz, 1976; Davies and Hay, 1980). Joseph and Wolfson (1975) assigned an error of 15% to Robinson's values.

On cloudless days the diffuse component contributes less than 20% of the global irradiance (Davies, 1980). Diffuse irradiance is measured beneath an occulting ring and measured values are corrected for the portion of the sky hemisphere which is obscured by the ring (Section 3.3.4). Measured global and diffuse irradiances in the AES network are assumed to be correct within 2%.

$G_0$  and  $D_0$  were calculated with the MAC model. To test the validity of the calculated irradiances, the values were compared with results from the Braslau and Dave (1973) model B atmosphere (Section 4.1). The results compare to within 1% (Table 5.1; Davies and Hay, 1978). The

calculated  $G_0$  and  $D_0$  values are assumed to be correct within 2% over a wide range of zenith angles and surface reflection. In the absence of aerosol, diffuse and global irradiances can be calculated with very good accuracy.

TABLE 5.1: GLOBAL AND DIFFUSE IRRADIANCES FOR THE BRASLAU AND DAVE (1973) MODEL B ATMOSPHERE (B + D) and MAC MODEL COMPARED (After Davies and Hay, 1980)

$\alpha_s$	0°		30°		60°		80°		
	B+D	MAC	B+D	MAC	B+D	Mac	B+D	MAC	
Diffuse									
0.0	4	5	5	6	7	8	12	14	
0.1	5	6	5	6	7	9	13	14	
0.2	5	6	6	7	8	9	13	15	
0.8	10	10	10	10	12	12	16	18	
Global									
0.0	80	80	79	79	74	74	62	61	
0.1	81	81	80	79	75	74	62	61	
0.2	81	81	80	80	75	75	63	62	
0.8	85	85	84	83	79	78	65	64	

## 5.2 Scattering and Absorption

Forward scatter and absorption were calculated by equations 2.45 and 2.46 and backscatter by dividing equation 2.45 by  $f/b$ . The relative errors in  $f$ ,  $b$  and  $a$  are about 2%, 15%, and 2.5% which indicate that the error in  $a$  depends virtually on those of the global irradiances since the contribution of  $b$  is usually small as will be shown in this section.

Hourly values of  $f$ ,  $b$ , and  $a$  were evaluated and expressed as fractions of the appropriate extraterrestrial irradiances. For 10° intervals of zenith angle, mean values were calculated (Table 5.2). The

mean from all hourly values are presented in Table 5.3. For comparison, data for Montreal and Woodbridge were also evaluated for the periods represented by Hamilton, Charlottetown, Winnipeg, and Vancouver data.

At any location, extinction is defined as the sum of total scattering and absorption while the sum of backscattering and absorption is the loss in solar irradiance. Paltridge and Platt (1976) suggested that for unit optical air mass and an atmosphere with Ångström turbidity coefficient  $\sim 0.15$  at  $\lambda = 1 \mu\text{m}$ , that is,  $\tau_a \sim 0.369$  at  $\lambda = 0.5 \mu\text{m}$ , the reduction in direct beam irradiance by dust is of order 20%. Compared with the Canadian locations (Tables 5.2 and 5.3), Sal is unique in the extinction of solar irradiance. Except for small zenith angles ( $< 15^\circ$ , Table 5.2b) at Sal, the sum of total scatter and absorption exceeds I and is, on average, equivalent to about 40% of the extraterrestrial irradiance (Table 5.3) or a loss of about 18% (due mainly to absorption) of the incident radiation. This is comparable to 20-25% loss reported by Carlson and Caverly (1977) for Sal. Mean values calculated from publications of Robinson (1962) and Joseph and Wolfson (1975) (Appendix 9), show similar reductions at Lerwick, Malta, and Bet-Dagan but larger ones at Kew, Bracknell, Vienna, and Jerusalem. Even though radiation losses are about the same, Tables 5.3 and Appendix 9 reveal that absorption is far more important at those locations than at Sal.

Canadian stations show smaller reductions at all zenith angles (Table 5.2). On average, in summer, reductions are about 10% in G and 11-15% in I except at Charlottetown and Vancouver with reductions of about 5% in G and 7% in I. Since these reductions for Charlottetown and

TABLE 5.2(a): MEAN VALUES OF ABSORPTION, SCATTERING AND SOLAR IRRADIANCES AS FRACTIONS OF EXTRATERRESTRIAL IRRADIANCE FOR RANGE OF ZENITH ANGLES

Station	Parameter	Range of zenith angles of the sun					
		< 25	25-34	35-44	45-54	55-64	65-78.5
<b>Montreal</b>							
$\alpha_s = 0.15$	G	0.755	0.748	0.756	0.723	0.702	0.648
	D	0.142	0.147	0.132	0.148	0.153	0.176
	I	0.613	0.601	0.624	0.575	0.549	0.472
	f	0.081	0.084	0.064	0.074	0.067	0.068
	b	0.008	0.009	0.009	0.014	0.018	0.032
	a	0.045	0.051	0.045	0.059	0.055	0.052
	b+f	0.089	0.093	0.073	0.088	0.085	0.100
	a+b+f	0.134	0.144	0.118	0.147	0.140	0.152
<b>Woodbridge</b>							
$\alpha_s = 0.15$	G	0.748	0.749	0.745	0.722	0.689	0.618
	D	0.160	0.154	0.146	0.152	0.170	0.194
	I	0.588	0.595	0.599	0.570	0.519	0.424
	f	0.099	0.091	0.079	0.078	0.085	0.087
	b	0.010	0.010	0.010	0.014	0.024	0.041
	a	0.054	0.052	0.050	0.049	0.047	0.055
	b+f	0.109	0.101	0.089	0.092	0.109	0.128
	a+b+f	0.163	0.153	0.139	0.141	0.156	0.183
↓							
<b>Goose</b>							
$\alpha_s = 0.55$	G	-	-	0.835	0.820	0.797	0.737
	D	-	-	0.141	0.138	0.159	0.182
	I	-	-	0.694	0.682	0.638	0.555
	f	-	-	0.047	0.039	0.046	0.048
	b	-	-	0.007	0.007	0.015*	0.024*
	a	-	-	0.008	0.012	0.015*	0.017*
	b+f	-	-	0.054	0.046	0.061	0.072
	a+b+f	-	-	0.062	0.058	0.076	0.089
<b>Winnipeg</b>							
$\alpha_s = 0.15$	G	-	-	0.750	0.768	0.720	-
	D	-	-	0.170	0.141	0.190	-
	I	-	-	0.580	0.627	0.530	-
	f	-	-	0.103	0.068	0.107	-
	b	-	-	0.014	0.012	0.028	-
	a	-	-	0.048	0.030	0.035	-
	b+f	-	-	0.117	0.080	0.135	-
	a+b+f	-	-	0.165	0.110	0.170	-

\*b > a

TABLE 5.2(b): MEAN VALUES OF ABSORPTION, SCATTERING AND SOLAR IRRADIANCES AS FRACTIONS OF EXTRATERRESTRIAL IRRADIANCE FOR RANGE OF ZENITH ANGLES

Station	Parameter	Range of zenith angles of the sun						
		< 25	25-34	35-44	45-54	55-64	5-78.5	
Charlottetown								
$\alpha_s = 0.10$	G	-	0.784	0.758	0.738	0.716	0.640	
	D	-	0.108	0.118	0.132	0.135	0.174	
	I	-	0.676	0.640	0.606	0.581	0.466	
	f	-	0.046	0.052	0.058	0.048	0.071	
	b	-	0.005	0.007	0.011	0.015	0.031	
	a	-	0.023	0.028	0.029	0.025	0.046	
	b+f	-	0.051	0.059	0.069	0.063	0.102	
	a+b+f	-	0.074	0.087	0.098	0.088	0.148	
Vancouver								
$\alpha_s = 0.15$	G	-	0.784	0.768	0.743	0.708	0.632	
	D	-	0.124	0.123	0.134	0.147	0.174	
	I	-	0.660	0.645	0.609	0.561	0.458	
	f	-	0.059	0.054	0.058	0.060	0.063	
	b	-	0.007	0.008	0.011	0.017	0.031	
	a	-	0.009	0.014	0.020	0.027	0.038	
	b+f	-	0.066	0.062	0.069	0.077	0.094	
	a+b+f	-	0.075	0.076	0.089	0.104	0.132	
Hamilton								
$\alpha_s = 0.15$	G	0.742	0.724	0.714	0.679	0.650	-	
	D	0.150	0.159	0.154	0.166	0.163	-	
	I	0.592	0.565	0.560	0.513	0.487	-	
	f	0.089	0.095	0.086	0.091	0.076**	-	
	b	0.007	0.010	0.012	0.017	0.023	-	
	a	0.057	0.065	0.064	0.073	0.077**	-	
	b+f	0.096	0.105	0.098	0.108	0.099	-	
	a+b+f	0.153	0.170	0.162	0.181	0.176	-	
Sal								
$\alpha_s = 0.20$		<15°	15-24°					
	G	0.725	0.718	0.701	0.664	0.624	0.590	0.489
	D	0.329	0.350	0.347	0.354	0.380	0.371	0.381
	I	0.396	0.368	0.354	0.310	0.244	0.219	0.108
	f	0.268	0.287	0.280	0.282	0.300	0.281	0.268
	b	0.024	0.028	0.031	0.040	0.058	0.078*	0.126*
	a	0.058	0.057	0.064	0.080	0.085	0.078*	0.081*
	b+f	0.292	0.315	0.311	0.322	0.358	0.359	0.394
a+b+f	0.350	0.372	0.375	0.402	0.443	0.437	0.475	

\*\*a &gt; f

\*b &gt; a



TABLE 5.3: MEAN VALUES OF ABSORPTION, SCATTERING AND SOLAR IRRADIANCES AS FRACTIONS OF EXTRATERRESTRIAL IRRADIANCE

Station	Period	Parameters										No. of records					
		$\alpha$	$s$	G	I	D	f+b	f	b	a	f+b+a		b+a	f/b	f+b/a		
Montreal	Summer	0.15															
	1968-78			0.71	0.56	0.15	0.09	0.07	0.02	0.05	0.14	0.07	4.2	1.8	394		
	1978			0.72	0.58	0.14	0.09	0.07	0.02	0.05	0.14	0.07	4.2	1.8	81		
	1977			0.71	0.53	0.18	0.12	0.10	0.02	0.05	0.17	0.07	5.0	2.4	29		
Woodbridge	1968-78	0.15		0.71	0.55	0.16	0.10	0.09	0.02	0.04	0.15	0.07	4.7	2.5	406		
	1978			0.73	0.60	0.13	0.07	0.06	0.01	0.03	0.10	0.04	6.0	2.3	50		
	1977			0.71	0.55	0.16	0.11	0.09	0.02	0.04	0.15	0.06	4.5	2.8	34		
	1975			0.72	0.56	0.16	0.10	0.08	0.02	0.04	0.12	0.06	4.0	2.5	50		
Charlottetown	1977-78	0.10		0.75	0.62	0.12	0.06	0.05	0.01	0.03	0.09	0.04	5.1	2.0	38		
Hamilton	1975	0.15		0.71	0.55	0.16	0.10	0.09	0.01	0.07	0.17	0.08	6.8	1.4	66		
Winnipeg	1977	0.15		0.74	0.57	0.17	0.11	0.09	0.02	0.04	0.15	0.06	4.7	2.8	18		
Vancouver	1977-78	0.15		0.73	0.59	0.14	0.07	0.06	0.02	0.02	0.10	0.04	3.9	3.5	213		
Sal	1974	0.20		0.66	0.30	0.36	0.33	0.28	0.05	0.07	0.40	0.12	5.6	4.7	100		
Goose	Winter																
	1968-77	0.55		0.78	0.61	0.17	0.06	0.05	0.017	0.015	0.08	0.03	2.7	4.2	68		
	1968-77	0.70		0.79	0.62	0.17	0.07	0.05	0.018	0.016	0.08	0.03	2.6	4.1	44		
Montreal	1968-78	0.30		0.75	0.60	0.14	0.05	0.04	0.01	0.04	0.09	0.05	2.6	1.5	89		
Woodbridge	1968-78	0.50		0.79	0.65	0.14	0.05	0.04	0.01	0.02	0.07	0.03	4.0	2.4	47		

Vancouver are similar to those for Woodbridge for the same period, their long term averages may well be the same. The mean Canadian values are less than the 20% reduction in I suggested by Paltridge and Platt (1976) but are comparable to 10% reductions in I for low cases of turbidity at Argonne (Wesely and Lipschutz, 1976) and in G for Denver (DeLuisi et al., 1977). In winter when air is cleaner, reduction of solar energy is smaller in Canada. Montreal reveals its urban character with losses of .7 and 8% for G and I compared with 4 and 5% for Woodbridge and Goose. Like Sal, on average, scattering dominates over absorption in Canada, hence the ratio of total scatter to absorption exceeds unity (Table 5.3). Sal and Goose have the largest values of about 5 which are similar to those found by direct measurements over the English Channel by Roach (1961). Hamilton and Montreal have values of about 1.5 while the other locations have values between 2 and 3.5. These ratios emphasize the relative importance of total scattering and absorption. At Sal and Goose, total scattering always exceeds absorption. Hamilton, Montreal, and Woodbridge show evidence of stronger aerosol absorption. Occasionally, absorption equals or exceeds total scattering (Table 5.4) and the ratio  $(f + b + a)/a$  lies within the range (0.5 to 0.9) derived from the publications by Robinson (1962, 1966) and Joseph and Wolfson (1975) (Appendix 9). By direct measurements, Waldram (1945, in industrial haze) and Paltridge and Platt (1973, in continental aerosol plus carbon smoke particles) found that absorption and total scattering contributed equally to the extinction of solar irradiance.

TABLE 5.4: SOME DAYS WHEN ABSORPTION EXCEEDS TOTAL SCATTERING AT MONTREAL AND WOODBRIDGE

Station	Date	b + f	a	(b + f)/a
Montreal				
	16.4.68	0.037	0.062	0.62
	23.8.68	0.043	0.065	0.66
	19.3.70	0.049	0.072	0.68
	29.5.70	0.050	0.062	0.80
	26.3.71	0.045	0.069	0.66
	25.5.72	0.022	0.044	0.50
	01.7.78	0.027	0.047	0.57
Woodbridge				
	22.9.69	0.056	0.069	0.80
	1.10.71	0.052	0.062	0.84
	08.9.76	0.091	0.111	0.82
	24.6.78	0.032	0.037	0.87

Forward scattering is on average, the most dominant extinction process at Sal and the Canadian locations (Table 5.5) except for few occasions when absorption was equal or exceeded it (Table 5.4; Table 5.2,  $z = 55$  to  $64^\circ$  for Hamilton). With the exception of Sal, where it contributes about 43 of the 61% extinction (due to aerosols) of the incident radiation, its contribution in general lies within the range 6 - 17% as Canadian and other sites indicate (Table 5.5).

Backscattering is remarkably constant at 2 - 3% (Robinson, 1962, found 2%) for most stations. The ratio  $b/(f + b)$ , analogous to Sagan and Pollack's  $\beta$  (1967), lies between 0.10 and 0.20 suggested by them (Sagan and Pollack), Chýlek and Coakley (1974), and Weiss et al. (1977). On the average, backscatter is less than absorption except occasionally at Sal, Goose, and at zenith angles larger than  $60^\circ$ . For example on 25 July 1974 at Sal, backscatter exceeded absorption in about 67% of the observations

TABLE 5.5: RELATIVE CONTRIBUTIONS OF ABSORPTION, FORWARD AND BACKSCATTERING TO THE EXTINCTION OF GLOBAL IRRADIANCE

Station	$\alpha_s$	$XG = \frac{f+b+a}{G}$ (%)	$\frac{a}{f+b+a} \cdot XG$ (%)	$\frac{f}{f+b+a} \cdot XG$ (%)	$\frac{b}{f+b+a} \cdot XG$ (%)	Sources
Montreal	0.15	19.6	7.3	9.9	2.4	PS
Woodbridge	0.15	21.5	7.1	11.9	2.5	PS
Hamilton	0.15	23.7	9.3	12.5	1.8	PS
Winnipeg	0.15	20.4	5.0	12.7	2.7	PS
Vancouver	0.15	13.0	2.9	8.1	2.0	PS
Charlottetown	0.10	11.9	3.6	6.8	1.3	PS
Goose	0.55	10.0	1.9	5.9	2.2	PS
Sal	0.20	60.9	10.7	42.5	7.6	PS
Denver (2)*	0.49	-19.5	6.0	9.1	4.4	D+
Jerusalem (5)*	0.25	44.1	24.2	17.4	2.5	J&W
Bet Dagan (5)*	0.26	31.6	13.7	15.9	2.0	J&W
Kew (5)**	0.15	41.6	28.7	10.5	2.4	RB
Vienna (14)**	0.15	41.3	27.6	10.4	3.3	RB
Lerwick (5)*	0.15	32.4	15.5	13.7	3.2	RB
Malta (5)*	0.15	26.0	14.4	9.3	2.3	RB
Bracknell (2)*	0.15	36.7	24.6	9.7	2.4	RB
Quartzite (14)*	0.16		7.1			D+
Big Spring (14)*	0.08		3.5			D+
Rice (14)*	0.20		3.2			D+

PS = Present Study; D+ = DeLuigi et al.; J&W = Joseph and Wolfson; RB = Robinson.

\* indicates number of days in the sample.

\*\* indicates number of years in the sample.

and the average  $b/a$  was 1.5. The hours when  $b$  was larger than  $a$  had zenith angles larger than  $58^\circ$ . This occurrence may be related to sensor errors which are largest at these angles (King, 1979).

These differences in the relative contributions of scattering and absorption may be explained in terms of the size and complex index of refraction of the particles. Sal differs markedly from the Canadian sites. The size of particles at Sal vary from  $r \sim 0.1$  to  $20 \mu\text{m}$  (Schütz, 1980) with the most effective scattering radius about  $5 \mu\text{m}$  (Carlson and Caverly, 1977; Hansen and Travis, 1974). The complex refractive index is  $1.54 - 0.005i$  (Carlson and Caverly, 1977). In Canada, the particle size ranges from  $0.01 \mu\text{m}$  to  $1 \mu\text{m}$  radius with the most effective scattering radius of  $\sim 0.1 \mu\text{m}$  and complex index of refraction of  $1.50 - 0.01i$  for locations with moderate aerosol absorption (Halpern and Coulson, 1976). For Goose, the imaginary part of the complex index may be taken as  $\sim -0.001$ .

With a Junge distribution, scattering is dominated by particles with  $r \sim \lambda$  and in the Rayleigh region is proportional to  $r^6$  (Twomey, 1977). Mie theory (van de Hulst, 1957) shows that as the particle size increases,  $Q_{\text{ext}} \rightarrow 2$ . The most efficient hemispheric backscatters are particles with radii between  $0.1$  and  $0.3 \mu\text{m}$  (Chýlek et al., 1975). Thus the large, almost non-absorbing particles, which are found over Sal, scatter strongly in the forward direction but are ineffective backscatters. This has been shown in this study. In the Rayleigh region absorption is proportional to  $r^3$  (Twomey, 1977) and  $Q_{\text{abs}} > Q_{\text{sca}}$ . For atmospheric aerosols, the most important particle sizes for the extinc-

tion of solar irradiance lie between 0.1  $\mu\text{m}$  to 1.0  $\mu\text{m}$  radius (Bullrich, 1964; Leaderer and Stolwijk, 1980). Bergstrom (1973) has shown that an increase in the absorption index of the refractive index greatly increases the contribution of small particles ( $r < 0.1 \mu\text{m}$ ) but has little effect on large particles ( $r > 5 \mu\text{m}$ ) for wavelength of 0.55  $\mu\text{m}$ . Absorption by small particles exceeds absorption by larger particles by a factor of 4 to 32, while the mass of the small fraction exceeds that of the larger fraction by a factor of 2 to 4 (Weiss et al., 1977). Canadian urban areas have highly absorbing particles like carbon and ash, a greater variety of other small absorbing particles, and so the extinction characteristics of the aerosols differ from those at Sal. The vertical structure of the aerosols over Sal and the Canadian locations also add to the differences in scattering and absorption properties. In Canada, particle concentration decreases from near the surface towards the top of the boundary layer and so extinction of solar irradiance is greatest near the surface. The same condition applies to Sal under normal conditions when there is no Saharan dust outbreak (Kondratyev et al., 1976). During the dust outbreaks the effect is reversed. The smaller and more optically active particles ( $r = 0.1 - 1.0 \mu\text{m}$ ) are concentrated near the top of the dust layer while the large and giant particles fall out towards the surface. Hence the strongest absorption of solar irradiance occurs near the top of the dust layer and decreases towards the surface while aerosol backscatter increases at a more uniform rate from the surface upwards (Kondratyev et al., 1976).

### 5.3 Recovery Rate $R_a$

The Wesely and Lipschutz analysis (Section 2.4.2, equation 2.48)

is sensitive to measurement errors in I and D (sections 4.1 and 5.1) and also to changes in surface albedo and water vapour content of the atmosphere.  $R_a$  is more sensitive to  $\alpha_s$  than to  $mU_w$  and errors increase with increase in optical air mass. Errors due to  $\alpha_s$  exceed 10% only at optical air mass more than 2 and  $\alpha_s$  is more than 0.40. Instantaneous  $R_a$  is not only sensitive to I and D but also to  $I_0$  and  $D_0$ . The relative error in  $R_a$  from equation 2.49 is about 6%.

$R_a$  was calculated for Montreal, Woodbridge, Vancouver, and Sal because it was possible to obtain sizeable data for specified zenith angles. For Montreal, Woodbridge, and Vancouver, zenith angles were selected to within about  $\pm 0.7$  degree but for Sal analysis was only possible with zenith angles  $\pm 3$  degrees. These zenith angles cover a wider range than zenith angles of  $\pm 0.03$  degree used by Wesely and Lipschutz (1976). The differences arise from the fact that integrated hourly values were used in this study whereas Wesely and Lipschutz used data recorded continuously on strip charts and so were able to select sizeable data within small range of a specified zenith angle. Diffuse radiation in the AES network is measured with a shade ring but Wesely and Lipschutz used a disc which is considered to yield a better estimate of diffuse irradiance. Comparisons with their work and some others should be done with care since  $R_a$  is zenith angle dependent and  $R_a$  determined by regression represents the mean over the period of time. Mean values of hourly  $R_a$  were calculated for the same periods and zenith angles covered by the regression analysis.

There is good agreement between  $R_a$  value by regression ( $-dD/dI$ ) and the mean hourly value  $\bar{R}_a$  over the same time period (Table 5.6).  $-dD/dI$  values for Sal are larger than those for Montreal, Woodbridge, and Vancouver and are nearest the Argonne values despite the larger deviations from the mean zenith angles for Sal (Figure 5.1). The high values for Sal compare with values of 75% reported for stratospheric aerosols (Dyer and Hicks, 1965). The result for Sal is consistent with the low absorptivity of the aerosols, a feature also of stratospheric aerosols (Cadle and Grams, 1975), and the highly forward-peaked scattering shown by the Robinson method (section 5.2) and reported also by Carlson and Caverly (1977). Values of  $-dD/dI$  for Montreal, Woodbridge, and Vancouver are also consistent with results in section 5.2 which indicate that, relative to aerosol loading, Montreal absorbs more solar irradiance than Sal and other Canadian locations. Both  $-dD/dI$  and  $\bar{R}_a$  values for all the sites support Wesely and Lipschutz results which show that  $R_a$  decreases almost linearly with increase in optical air mass.

Variation of hourly  $R_a$  values for Canadian stations (Table 5.7) encompasses the ranges of 35-50% for urban and 45-60% for non-urban Canadian sites reported by Barlow (1979). Table 5.7 also indicates that the hourly  $R_a$  values for Hamilton, Montreal, and Woodbridge compare (except for values < 30%) with the ranges inferred by Wesely and Lipschutz (1976) from the data of Unsworth and Monteith (1972) (21% at  $\theta = 65^\circ$  to 61% at  $z = 37.5^\circ$ ) and Robinson (1962) (~30%).



TABLE 5.6: REGRESSION AND MEAN HOURLY VALUES OF  $R_a$  COMPARED

Station/ $\alpha_s$	mean zenith angle	$-dD/dI$	$\bar{R}_a$	Intercept	Data Size
Montreal					
$\alpha_s = 0.15$	24.6	0.71	0.68	686	17
	29.7	0.66	0.63	617	12
	34.0	0.61	0.59	557	10
	46.4	0.52	0.54	418	13
	55.6	0.47	0.51	316	13
	69.9	0.41	0.44	167	26
Woodbridge					
$\alpha_s = 0.15$	23.6	0.70	0.70	706	12
	29.8	0.67	0.64	640	18
	38.5	0.60	0.61	528	20
	48.8	0.57	0.59	427	26
	58.7	0.53	0.54	306	17
	62.6	0.50	0.53	265	11
	71.1	0.46	0.45	169	10
Vancouver					
$\alpha_s = 0.15$	31.8	0.69	0.70	647	19
	49.3	0.62	0.63	444	17
	59.0	0.51	0.53	300	24
	68.8	0.43	0.43	177	22
Sal					
$\alpha_s = .20$	<9	0.79	0.76	835	12
	10 - 16	0.74	0.75	787	11
	20 - 26	0.73	0.78	751	11
	29 - 35	0.70	0.73	648	8
	34 - 40	0.68	0.73	618	10
	42 - 48	0.65	0.70	519	9
	52 - 58	0.64	0.65	394	10
Argonne	37.5	0.70		592	
$\alpha_s = 0.17$	45	0.68		508	
(Weesely and	55	0.62		377	
Lipschutz (1976)	65	0.58		256	

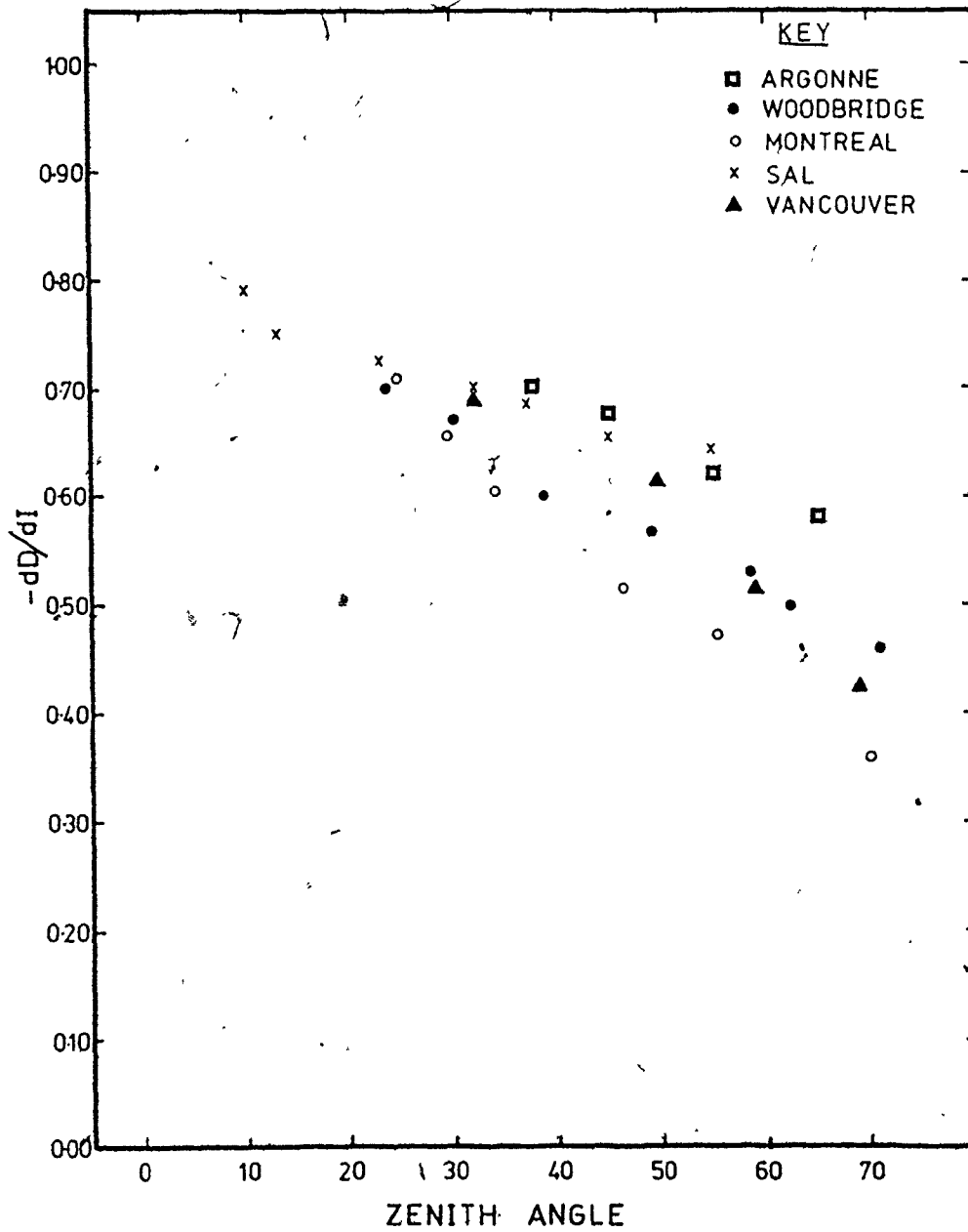


Figure 5.1. Aerosol recovery rates.

TABLE 5.7: MAXIMUM AND MINIMUM VALUES OF HOURLY  $R_a$  FOR CANADIAN SITES

Station	$Z \leq 35^\circ$ ( $\leq 45^\circ$ for Goose)		$Z = 65^\circ$		$\alpha_s$
	Maximum $R_a$ (%)	$Z^\circ$	Minimum $R_a$ (%)	$Z^\circ$	
Montreal	71	29.0	36	65.2	0.15
Woodbridge	78	23.2	37	65.6	0.15
Hamilton	67	23.2	33	68.1	0.15
Charlottetown	68	33.0	41	63.7	0.15
Vancouver	87	32.6	43	65.5	0.15
Goose	77	41.3	57	65.9	0.55

#### 5.4 Bulk Scattering Albedo $W_b$

For the calculation of the diffuse component using the MAC model,  $W_b$  is an important parameter. In practice values have been chosen (Davies, 1980). Therefore for the MAC model and other similar models (e.g. DeLuisi et al., 1977), the values of  $W_b$  presented here may be useful.  $W_b$  indicates the bulk absorption and scattering properties of particulates over an area.

Values of  $W_b$  were calculated from hourly  $R_a$  values and the ratio  $F$  derived from Table 2.1. The relative error in  $W_b$  is about 7% which is closely related to the error in  $R_a$  (section 5.3). To test the appropriateness of this approach, values of  $W_b$  were compared with  $w_o$  values calculated with the Delta-Eddington Approximation (Joseph et al., 1976). The Delta-Eddington ( $\delta$ -Edd) method is spectral and uses a two-stream approximation. It approximates the phase function by a Dirac delta function forward scatter peak which is suitable for highly asymmetric phase functions typical of particulate scattering (Joseph et al., 1976; Paltridge and Platt, 1976).

For a given zenith angle, the  $\delta$ -Edd programme (Wiscombe, 1977) involves the solution of a pair of ordinary differential equations framed in terms of  $\tau$ ,  $w_0$ , and  $g$ . In this particular exercise,  $\alpha_s$  was set to zero so that the reflectance calculated with the  $\delta$ -Edd programme was due only to the aerosol layer. For a fixed zenith angle and a typical value of  $\tau_a$ , appropriate values of  $g \pm 0.015$  and  $W_b \pm 0.005$  were selected. Values of  $g$  were calculated in terms of  $F$  from equation 2.18. For the same zenith angle and  $\tau_a$ , values of  $a/b$  were calculated for the various combinations of  $g$  and  $W_b$ . From the output, values of  $a/b$  within  $\pm 5\%$  of the original value calculated previously were delineated (Table 5.8).

TABLE 5.8: RANGE OF VALUES OF  $a/b \pm 5\%$  OF THE ORIGINAL VALUE OF 3.21 for  $Z = 0^\circ$  AND  $\tau_a = 0.478$  AT SAL (10.8.74)

$w_0 \rightarrow$ $g$ $\downarrow$	0.875	0.880	0.885	0.890	0.895
0.800	2.66	2.53	2.41	2.28	2.15
0.825	3.09	2.94	2.79	2.65	2.51
0.830	3.19	3.04	2.88	2.73	2.59
0.834	3.28	3.12	2.96	2.81	2.66
0.837	3.34	3.18	3.02	2.86	2.71
0.840	3.41	3.25	3.08	2.92	2.77
0.843	3.48	3.32	3.15	2.99	2.82
0.846	3.56	3.39	3.22	3.05	2.89
0.850	3.67	3.49	3.31	3.14	2.97

From these values, the nearest to the original value of  $a/b$  was chosen. For the chosen value, the corresponding values of  $g$  and  $\omega_0$  were selected. These values of  $a/b$ ,  $g$ , and  $\omega_0$  from the  $\delta$ -Edd programme are compared with the original values of those parameters in Table 5.9. The values of  $\omega_0$  from the  $\delta$ -Edd programme are invariably slightly larger than the original  $W_b$  values. However the high correlation between  $\omega_0$  and  $W_b$  and the small standard error of the difference indicate that the  $W_b$  values calculated in this study are acceptable.

Mean values of  $W_b$  for the stations are presented in Table 5.10. Sal and Goose have higher mean and minimum values than the other sites which suggest low aerosol absorptivity as results in sections 5.2 and 5.3 also indicate. Values for Goose compare well with Barlow's (1979) value of 0.91 for high latitude Resolute. The mean value of Sal is comparable with the spectral value of Carlson and Benjamin (1980). Values of  $W_b$  are lower at Sal when there is no dust outbreak from the Sahara, e.g. the minimum value of 0.67 occurred on 10th August - one of the clearest days in Summer, 1974 (Carlson, 1975). On such days the smaller and more abundant optically active ferric oxide (haematite) particles probably increase the absorption of solar irradiance especially in the visible spectrum (Kondratyev et al., 1976). The lower values for Jerusalem illustrate the effect of entrainment of urban aerosol with high index of absorption  $\sim -0.02i$  to 0.05i (Levin et al., 1980) in normally low absorbing desert aerosol like the Saharan over Sal.

The high maximum values of  $W_b$  for the other Canadian stations show that on some occasions aerosols can be as low absorbing as those at

TABLE 5.9: VALUES OF  $w_b$ ,  $a/b$  AND  $g$  USED IN THIS STUDY FOR SAL COMPARED WITH THOSE CALCULATED WITH DELTA-EDDINGTON APPROXIMATION

$\mu \sim 1.0$	Present Study				$\delta$ -Edd Approximation		
Date	$\tau_a$	$g$	$a/b$	$w_b$	$\omega_0$	$a/b$	$g$
10.08.74	0.445	0.83	3.64	0.77	0.86	3.64	0.83
	0.453	0.84	3.57	0.78	0.87	3.56	0.84
	0.461	0.84	3.20	0.80	0.88	3.21	0.85
	0.478	0.83	3.21	0.79	0.89	3.22	0.85
02.07.74	0.502	0.83	3.03	0.80	0.88	3.04	0.84
	0.581	0.83	2.21	0.86	0.91	2.20	0.83
25.07.74	0.661	0.84	1.40	0.90	0.94	1.40	0.83
03.07.24	0.736	0.83	2.70	0.82	0.89	2.71	0.83
	0.750	0.83	2.51	0.83	0.90	2.52	0.84
09.07.74	0.781	0.83	2.00	0.86	0.92	2.00	0.84
	0.812	0.83	2.03	0.86	0.92	2.01	0.84
30.07.24	0.819	0.84	1.49	0.89	0.94	1.50	0.84
	0.843	0.84	2.99	0.81	0.90	2.98	0.85
	0.872	0.83	2.92	0.80	0.90	2.91	0.84
Mean				0.826	0.899		
Standard deviation				0.041	0.025		
Standard error				0.011	0.007		
Standard error of difference				= 0.013			

TABLE 5.10: VALUES OF  $W_b$  AND  $\omega_o$  COMPARED

Site	Period	$W_b$	$\omega_o \lambda$	$W_b(z < 60^\circ)$ max. min.		$\alpha_s$	Data Size	source/ authors
Urban			0.6-0.8 ( $\lambda=0.3+3\mu\text{m}$ )					
Montreal	1968-78	0.60		0.85	0.40	0.15	394	PS
	1978	0.60		0.76	0.40	0.15	100	PS
	1977	0.66		0.82	0.41	0.15	40	PS
Wood- bridge	1968-78	0.65		0.92	0.40	0.15	406	PS
	1978	0.65		0.89	0.43	0.15	50	PS
	1977	0.68		0.79	0.41	0.15	42	PS
Hamilton	1977	0.59		0.84	0.42	0.15	66	PS
	1977	0.65					122	BAP
	1979	0.77		0.90	0.68	0.123	20	R&B
Charlotte town	1977-78	0.70		0.81	0.47	0.10	38	PS
Winnipeg	1977	0.75		0.92	0.40	0.15	18	PS
Vancouver	1977-78	0.78		0.97	0.41	0.15	213	PS
Goose	1968-77	0.81		0.99	0.54	0.55	68	PS
	1974	1.00					17	BA
Resolute	1974	0.91					65	BA
Grimsby	1969	0.72					42	BA
Sal	1974	0.83		0.99	0.67	0.20	100	PS
	1980		0.86 ( $\lambda=.53 \mu\text{m}$ )					C&B
Jerusalem	1968/70	0.46		0.69	0.31	0.25	18	J&W
Bet-Dagan	1968/70	0.56		0.80	0.42	0.26	18	J&W
New York City			0.71 ( $\lambda=0.50 \mu\text{m}$ )					L+
Denver	1973	0.69				0.49		D+
Montreal	1968-78	0.61		0.88	0.49	0.30	89	PS
Wood- bridge	1968-78	0.67		0.97	0.43	0.50	47	PS

B&P = Bergstrom and Peterson; C&B = Carlson and Benjamin; J&W = Joseph and Wolfson; BA = Barlow; R&B = Rouse and Bello; L+ = Lin et al.; D+ = DeLuisi et al.

Goose and Sal. But the change from high to much lower values indicate the variability of aerosol types in urban areas. Mean values of 0.6 to 0.8 fall within the range of 0.53 for polluted areas (Henderson, Colorado) and 0.86 for 'clean sites' (Hall Mountain, Arkansas) for seven U.S. sites reported by Weiss et al., (1977) for  $\lambda = 0.50 \mu\text{m}$ .

#### 5.5. Radiative Significance of Absorption and Scattering

The ratio of absorption to backscatter  $a/b$  has been used by several authors to determine the radiative effect of aerosols on solar radiation (section 2.5). Using the errors in  $a$  and  $b$  (section 5.2), the relative error in  $a/b$  is about 15%. The probable error (Table 5.12) is lower compared with  $\pm 3$  and  $\pm 4$  given by Joseph and Wolfson (1975) for Jerusalem and Bet-Dagan. Values of  $a/b$  are also sensitive to the surface albedo (Table 5.11). This is mainly because multiple reflection increases the path length of solar radiation and consequently absorption.

TABLE 5.11: SENSITIVITY OF  $a/b$  TO SURFACE ALBEDO AT VANCOUVER (31 JULY, 1978)

zenith angle	3.6°	43.2°	61.7°	71.5°
$\alpha_s = 0.10$	1.99	1.27	1.30	1.34
$\alpha_s = 0.15$	2.63	1.59	1.55	1.51
% change in $a/b$	+32	+25	+19	+13

Using equation 2.52 hourly values of  $a/b$  were calculated. Mean values for all zenith angles and for intervals of  $10^\circ$  were also evaluated. Critical values were obtained from equations 2.57 and 2.58 and used



to clarify  $a/b$ . Mean values for all angles and the critical values along with values from other authors are shown in Table 5.12 and Figure 5.2. For Montreal, Woodbridge, and Goose calculations were made for different surface albedos.

The results show that aerosols over Montreal, Woodbridge, Hamilton, and Goose could induce warming of the Earth-atmosphere system while those at Sal, Vancouver, Charlottetown, and Winnipeg could lead to cooling of the system. The results for Montreal, Woodbridge, and Hamilton are consistent with their low values of  $W_b$  and also compare well with results from similiar urban areas (Table 5.12 and Figure 5.2). Rouse and Bello's (1979) results for Hamilton show a cooling tendency for the city. This may be because their model did not include multiple reflections due to the surface which would have increased the absorption and therefore the value of  $a/b$ . Also their data may have represented periods when the aerosols were less absorbing (and so small  $a/b$  values) as revealed in this study (some hours on 21st and 22nd May, 1977). Values for Goose illustrate the fact that surface albedo is important in determining the cooling/warming tendency in the system. For high surface albedo ( $\alpha_s > 0.30$ , Wang and Domoto, 1974;  $\alpha_s > 0.40$ , Herman and Browning, 1975) aerosols induce warming of the system. Despite the high values of  $W_b$  for Goose, the mean  $a/b$  values for  $\alpha_s = 0.35, 0.55, \text{ and } 0.70$  show a warming tendency. For  $\alpha_s = 0.25$ , the mean value indicates cooling (Figure 5.2).

The cooling of the system shown for Sal is in agreement with its high value of  $W_b$  and perhaps illustrates a situation where the aerosol layer not only reduces solar irradiance but is also not in radiative

contact with the surface. When there is a dust outbreak, the aerosol layer reinforces the inversion (due to large scale subsidence of Hadley Cell circulation) in which the surface is influenced by cool trade winds (Carlson and Caverly, 1977; Kondratyev et al., 1976). This condition resembles that in urban areas where aerosols promote temperature inversions and thereby stabilize the air against convection (Toon and Pollack, 1980).

The calculations for intervals of  $10^\circ$  zenith angle show that values of  $a/b$  are not only dependent on  $\alpha_s$  but also upon zenith angle. Values of  $a/b$  decrease also linearly with increase in zenith angle (Figure 5.3). The main reason for the zenith angle dependence of values of  $a/b$  is because backscattering increases faster than absorption as the angle increases and solar irradiance decreases. Except for the combination of zenith angle  $> 65^\circ$  and  $\alpha_s = 0.15$ , results for Montreal and Woodbridge indicate a warming tendency for the system for all zenith angles and surface albedo  $> 0.15$ . Similarly, Goose results indicate a warming of the system for surface albedo  $> 0.25$  except for a combination of zenith angle  $> 55^\circ$  and  $\alpha_s = 0.25$ .

TABLE 5.12: MEAN VALUES OF a/b COMPARED

Station	Period	$\alpha_s$	a/b	Sample Size			Probable error	Source/author
				1*	2*	all		
Montreal	1968-78	0.15	5.0	96	93	394	$\pm 0.46$	PS
	1978	0.15	5.7			108		PS
	1977	0.15	4.1			40		PS
	1968-78	0.30	2.9	4	22	89	$\pm 0.38$	PS
	1968-78	0.50	2.5	3	34	109		PS
Wood- bridge	1968-78	0.15	4.7	116	100	406	$\pm 0.43$	PS
	1978	0.15	4.7			50		PS
	1977	0.15	3.6			42		PS
	1968-78	0.30	4.3	3	23	57	$\pm 0.47$	PS
	1968-78	0.50	3.3	2	23	47	$\pm 0.32$	PS
Hamilton	1977	0.15	6.1	4	29	66	$\pm 0.66$	PS
	1979	0.12	2.8			20		R&B
Charlotte- town	1977-78	0.10	3.5	25	0	38	$\pm 0.41$	PS
Winnipeg	1977	0.15	2.5	9	0	18	$\pm 0.28$	PS
Vancouver	1977-78	0.15	1.9	151	3	213	$\pm 0.21$	PS
Goose	1968-77	0.35	1.6	7	5	39	$\pm 0.19$	PS
	1968-77	0.55	1.1	2	4	68	$\pm 0.13$	PS
	1968-77	0.70	1.2	4	6	44	$\pm 0.14$	PS
Sal	1974	0.70	1.8	43	0	100	$\pm 0.21$	PS
Urban	1971	0.20	4.0					E+
Desert	1971	0.30	( $\lambda=0.5\mu\text{m}$ )					E+
			( $\lambda=0.5\mu\text{m}$ )	2.3				
Jerusalem	1968/70	0.25	11.5					J&W
Bet-Dagan	1968/70	0.26	8.5					J&W
Kew	1965	0.15	12.1					RB
Bracknell	1965	0.15	9.0					RB
Vienna	1938-50	0.15	11.3					RB
South- England	1962	0.20	4.0					RB
English Channel	1962	0.08	3.0					RB
Halley Bay	1956-58	0.65	4.3					RB
Denver	1973	0.49	1.4					D+

PS = Present study; R&B = Rouse and Bello; E+ = Ensor et al.; J&W = Joseph and Wolfson; RB = Robinson; D+ = LeLuisi et al.

$$1^* \quad (a/b)_{\text{crit}^1} = a/b < (1 - \alpha_s)^2 / 2\alpha_s$$

$$2^* \quad (a/b)_{\text{crit}^2} = a/b > (1 + \alpha_s^2) / \alpha_s$$

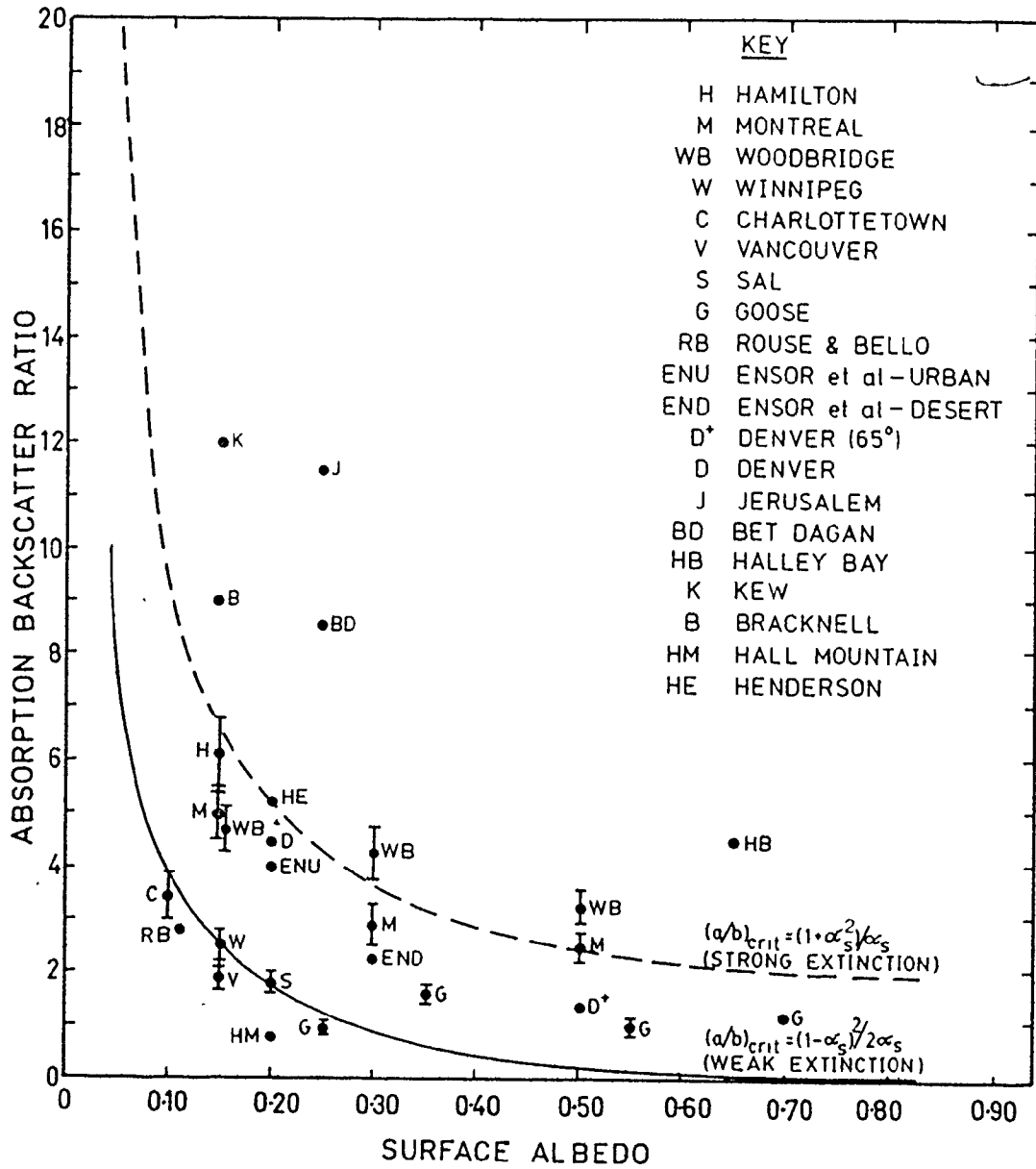


Figure 5.2. Absorption to backscatter ratio as a function of surface albedo.

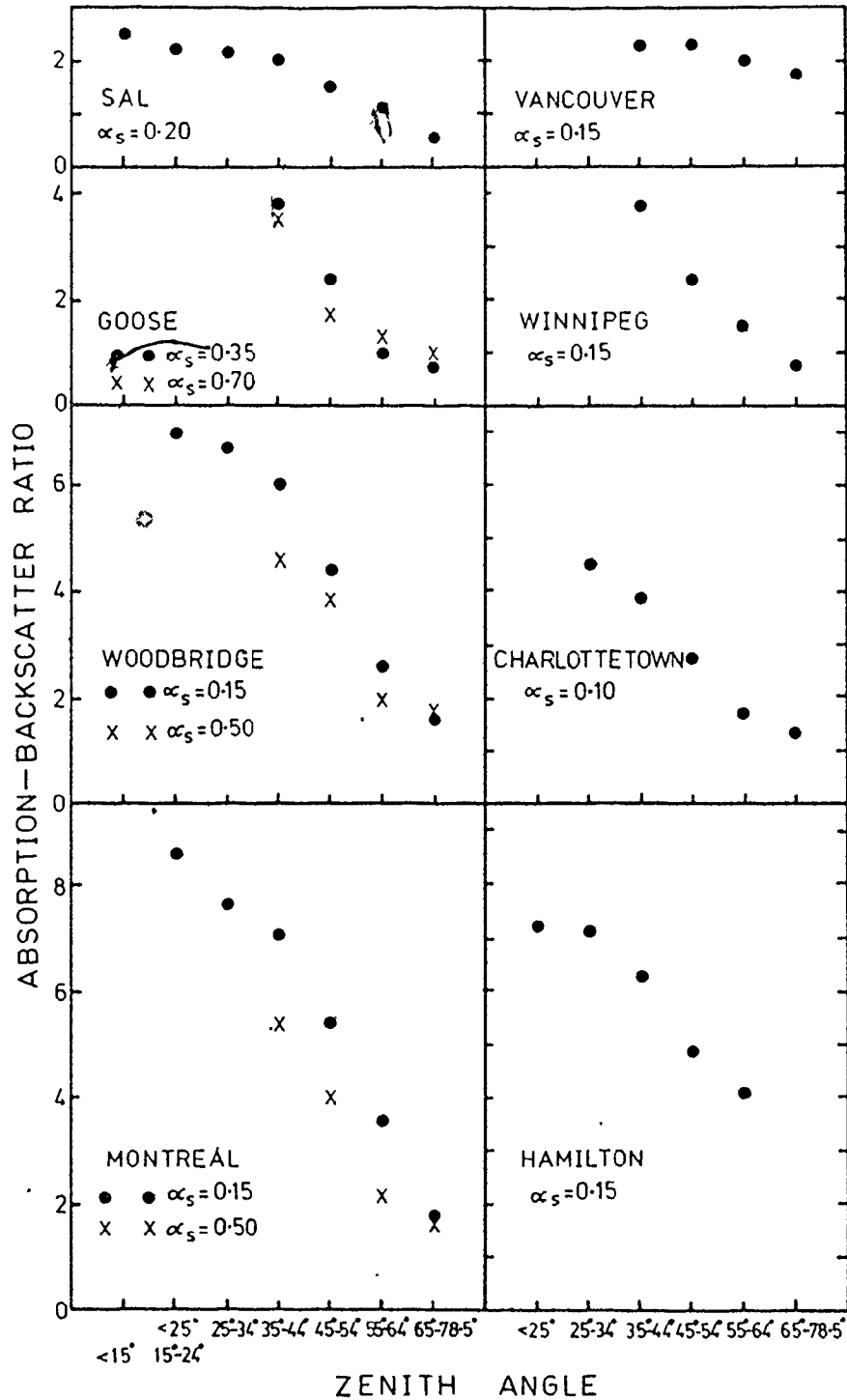


Figure 5.3. Absorption to backscatter ratio as a function of zenith angle.

## CHAPTER SIX

### SUMMARY AND CONCLUSIONS

Aerosol attenuation effects in Canadian urban areas were determined for Montreal, Woodbridge (Toronto), Hamilton, Vancouver, Charlottetown, and Winnipeg and compared with non-urban locations of Goose and Sal. Because available solar radiation and meteorological data in the AES network do not justify rigorous radiative transfer calculations, simpler empirical models were used. The following conclusions may be drawn:

Cloudless sky direct beam irradiances calculated with the MAC model and also estimated from measured global and diffuse irradiances have been used to evaluate values of  $\tau_a$ . The values compare well with turbidity coefficients obtained with other methods.

Values for Montreal, Woodbridge, and Goose indicate a downward trend in cloudless sky turbidity since 1968. This implies either an increased incidence of cleaner air mass or a decrease in particulates or a combination of both factors. Further studies are needed to examine this question. Since the Polar regions may be more sensitive to significant changes in turbidity than other regions of the world, this result can be of interest to Canada with territory extending beyond the Arctic circle.

For visibility more than 10 km, there is a strong linear relationship between  $\tau_a$  and the inverse of visibility but for less than 10 km,  $\tau_a$  is independent of visibility. This may be related to increase in particle size due to increase in relative humidity at low visibility.

Measured and calculated cloudless sky global and diffuse irradiances have been used to determine aerosol scatter, absorption, recovery rate, bulk scattering albedo, and the ratio of absorption to backscatter. Values compare well with those from other methods.

Absorption is as important in large Canadian urban areas as in United States cities (Davies and McKay, 1981, Davies and McArthur, 1980; Rouse et al., 1973). It is generally accepted that absorption and emission of long wave radiation by Carbon dioxide warms the Earth-atmosphere system. Aerosol absorption of short and long wave radiation compliments this warming. The warming tendency at Goose is related to multiple reflection caused by high surface albedo. This result assumes greater significance during winter in Canada especially in areas with absorbing aerosols.

Despite larger turbidity at Sal, aerosol absorption is not as important as in Canada. The absorption within the Saharan air layer reinforces the inversion due to large

scale subsidence in this zone (northern component of descending air in Hadley Cell). Since the dust outbreaks move from land to sea, the effect of change in surface albedo on the absorption/cooling characteristics of the aerosols require study (Joseph and Wolfson, 1975).

The approach used in this study has some limitations. Although aerosol effects are most easily determined in cloudless condition they may not be representative of all conditions as borne out by the records of cloudless periods at the stations (Appendix 2). Solar radiation measurements used here are non-spectral but absorption by some aerosol types are spectrally dependent. Perhaps a way to reconcile a spectral study with the present method is to establish a relationship between simultaneous spectral and global measurements. Even though the effect of aerosols on long wave radiation is generally smaller than on short wave, their effect in the atmospheric window (8 - 14  $\mu\text{m}$ ) below inversions in heavily polluted areas and generally in temperate regions (except in very clear conditions) is not negligible (Grassl, 1974) and so should be investigated. However the long wave effect augments the warming of the system due to aerosol absorption of short wave radiation.

The effect of stratospheric aerosols has not been explicitly included in the study. Since the effect of the stratosphere on the troposphere is mainly radiative (there is no strong convective link between them), the reduction of solar irradiance in the stratosphere can be estimated and incorporated in the MAC model. The importance of stratospheric aerosols increases during and shortly after major volcanic eruptions.



Except for the Fuego eruption in 1974 which might have had little or no effect on the area covered by this study, no major eruption occurred between 1968 and 1978.

Despite the limitations, this study has demonstrated that aerosol effects can be determined using direct beam, diffuse, and global radiation measurements. This approach is capable of wider application since solar radiation and meteorological data are available at many stations in Canada and other parts of the world. To ensure greater accuracy, better estimates of diffuse irradiance can be obtained from measurements of direct beam and global irradiances. It is therefore advisable for the Atmospheric Environment Service to establish an integrated and sustained programme of pyrheliometric measurements to replace the present measurements with diffusograph. This will provide a reliable data bank for monitoring turbidity trend and aerosol attenuation effects in Canada.

APPENDIX 1  
LIST OF SYMBOLS  
UPPER CASE ROMAN

Symbol	Definition	Unit
B	ratio of aerosol backscatter to total scatter	dimensionless
D	diffuse irradiance	$W/m^2$
$D_0$	cloudless sky diffuse irradiance	$W/m^2$
$D_R$	diffuse irradiance due to molecular (Rayleigh) scattering	$W/m^2$
$D_s$	diffuse irradiance due to multiple reflections between ground and atmosphere	$W/m^2$
ET	equation of time	minutes
F	ratio of aerosol forward scatter to total scatter	dimensionless
G	global irradiance	$W/m^2$
$G_0$	cloudless sky global irradiance	$W/m^2$
H	hour angle	degree
$H_p$	aerosol scale height	km
I	direct beam irradiance	$W/m^2$
$I_\lambda$	spectral radiant intensity	$W/m^2/sr/\mu m$
$I_\lambda(0)$	spectral irradiance at top of atmosphere	$W/m^2$
$I_0$	cloudless sky direct beam irradiance	$W/m^2$
$I_*$	extraterrestrial irradiance on a horizontal surface corrected for the Sun-Earth distance	$W/m^2$
LAT	local apparent time	hr
LS	longitude of station	degree
LSM	longitude of standard meridian	degree
LST	local standard time	hr
$N_0$	aerosol concentration at ground level	$\mu g/m^3$
$N_z$	aerosol concentration at height Z	$\mu g/gm^3$
R	actual Sun-Earth distance	km

## APPENDIX 1 CONTINUED

Symbol	Definition	Unit
$\bar{R}$	mean Sun-Earth distance	km
$R_a$	aerosol recovery rate	dimensionless; %
$T$	Linke's turbidity factor	dimensionless
$T_a$	transmittance after extinction by aerosols	dimensionless
$T_{a\lambda}$	spectral transmittance after extinction by aerosols	dimensionless
$T_d$	dew point emperature	°C
$T_{df}$	Linke's turbidity factor for dust free atmosphere	dimensionless
$T_{oz}$	transmittance after absorption by ozone	dimensionless
$T_p$	Polavarapu's aerosol factor	dimensionless
$T_R$	transmittance after scattering by dry air molecules	dimensionless
$Q_{abs}$	Mie absorption efficiency factor	dimensionless
$Q_{bs}$	Mie backscatter efficiency factor	dimensionless
$Q_{ext}$	Mie extinction efficiency factor	dimensionless
$Q_{sca}$	Mie scattering efficiency factor	dimensionless
$U_{oz}$	equivalent ozone depth in the atmosphere	mm
$U_w$	pressure and temperature corrected water path length	mm
$U'_w$	uncorrected water path length	mm
$W_b$	bulk scattering albedo for aerosols	dimensionless
$Z$	altitude	km
$Z$	solar zenith angle	degree
$Z_T$	height of top of atmosphere	km

## APPENDIX 1 CONTINUED

Symbol	Definition	Unit
LOWER CASE ROMAN		
a	aerosol absorption	$W/m^2$
$a_{oz}$	ozone absorptance	dimensionless
$a_w$	water vapour absorptance	dimensionless
b	aerosol backscatter	$W/m^2$
$b_{abs}$	Mie mass absorption coefficient	$m^2/kg$
$b_{abs}$	Mie mass backscatter coefficient	$m^2/kg$
e	vapour pressure	$P_a$
$e_s$	saturation vapour pressure	$P_a$
f	aerosol forward scatter	$W/m^2$
g	spectrally averaged asymmetry factor	dimensionless
g	acceleration due to gravity	$m/s^2$
$g_\lambda$	spectral asymmetry factor	dimensionless
m	optical air mass	dimensionless
$n(r)$	number density of a particle size distribution	$m^{-3}/\mu m$
p	station surface pressure	$kP_a$
$p_\lambda$	spectral scattering phase function	dimensionless
$p_0$	standard sea level pressure	$kP_a$
q	specific humidity	$k_g/k_g$
v	particle radius	$\mu m$
v	visibility	km
x	Mie size parameter	dimensionless

## APPENDIX 1 CONTINUED

Symbol	Definition	Unit
LOWER CASE GREEK		
$\alpha_E$	Earth's effective albedo for clear sky	dimensionless
$\alpha_R$	molecular (Rayleigh) scattering component of the atmospheric albedo	dimensionless
$\alpha_s$	surface albedo	dimensionless
$\beta$	Ångström turbidity coefficient	dimensionless
$\beta_{abs}$	volume absorption coefficient	$\text{km}^{-1}$
$\beta_{ext}$	volume extinction coefficient	$\text{km}^{-1}$
$\beta_m$	volume total scattering coefficient (molecular)	$\text{km}^{-1}$
$\beta_p$	volume total scattering coefficient (particle)	$\text{km}^{-1}$
$\beta_{sca}$	volume total scattering coefficient (general)	$\text{km}^{-1}$
$\delta$	solar declination	degree
$\eta$	complex index of refraction	dimensionless
$k_\lambda$	spectral mass absorption coefficient	$\text{m}^2/\text{kg}$
$\lambda$	wavelength	$\mu\text{m}$
$\mu$	cosine of zenith angle	dimensionless
$\omega_0$	single scattering albedo	dimensionless
$\omega_{0\lambda}$	spectral single scattering albedo	dimensionless
$\phi$	station latitude	degree
$\psi$	scattering angle	degree
$\sigma_{ext}$	extinction cross-section	$\text{m}^2$
$\sigma_\lambda$	spectral mass scattering coefficient	$\text{m}^2/\text{kg}$
$\sigma_{sca}$	scattering cross-section	$\text{m}^2$

## APPENDIX 1 CONTINUED

Symbol	Definition	Unit
$\tau$	optical depth	dimensionless
$\tau_a$	aerosol attenuation coefficient	dimensionless
$\tau_{ak}$	aerosol attenuation coefficient (Koschmieder formula)	dimensionless
$\tau_\lambda$	spectral optical depth	dimensionless

## APPENDIX 2

## TOTAL RECORDS AND DAYS OF DATA AT ALL STATIONS

	Montreal		Woodbdg. Goose		Winnipeg		Charlotte.		Vancouv.		Hamilton			
	hrs	days	hrs	days	hrs	days	hrs	days	hrs	days	recds	days		
Jan	121	43	34	15	89	35	17	6	1	1	-	-	-	-
Feb	190	61	30	17	148	40	22	6	31	7	-	-	-	-
Mar	263	64	171	45	147	34	43	11	7	3	8	1	-	-
Apr	301	74	302	77	86	20	50	12	13	3	-	-	-	-
May	290	65	284	75	46	17	18	5	45	8	26	2	80	4
Jun	178	56	197	59	38	10	22	6	22	6	77	6	12	1
Jul	195	66	179	63	10	5	26	8	21	9	80	7	-	-
Aug	190	54	181	55	15	5	12	5	31	8	12	1	-	-
Sep	133	45	95	32	1	1	8	4	5	3	-	-	-	-
Oct	139	52	125	40	7	4	44	9	6	2	-	-	-	-
Nov	70	24	31	11	8	2	13	5	5	3	18	3	-	-
Dec	102	31	35	13	29	16	25	11	11	2	-	-	-	-
Totals	2172	635	1665	502	624	189	300	88	198	55	221	20	92	5
1968	134	49	85	32	77	22	-	-	-	-	-	-	-	-
1969	181	50	130	38	74	19	-	-	-	-	-	-	-	-
1970	144	45	66	26	28	11	-	-	-	-	-	-	-	-
1971	131	41	95	35	35	11	-	-	-	-	-	-	-	-
1972	145	46	146	34	10	4	-	-	-	-	-	-	-	-
1973	112	42	68	28	63	17	-	-	-	-	-	-	-	-
1974	212	60	190	58	74	21	-	-	-	-	-	-	-	-
1975	124	46	280	77	105	42	-	-	-	-	-	-	-	-
1976	225	64	215	61	94	25	20	7	-	-	-	-	-	-
1977	265	81	218	61	64	17	280	81	36	14	79	8	92	5
1978	499	111	172	52	-	-	-	-	162	41	142	12	-	-
Totals	2172	635	1665	502	624	189	300	88	198	55	221	20	92	5

1974	Sal	
	recds	days
July	69	5
Aug	34	2
Totals	103	7

## APPENDIX 3

THE EFFECT OF CHANGES IN OZONE TRANSMISSION ON  $\tau_a$  AT WOODBRIDGE

Date	LAT	$\tau_{a_1}$	$\tau_{a_2}$	$ \tau_{a_1} - \tau_{a_2} $	$\frac{x}{ oz_1 - oz_2}  \%$
17.4.74		$oz_1 = 3.50$	$oz_2 = 4.15$		
	7.5	0.006	0.004	0.002	0.3
	8.5	0.019	0.017	0.002	0.3
	9.5	0.037	0.035	0.002	0.3
	10.5	0.047	0.045	0.002	0.3
	11.5	0.056	0.054	0.002	0.3
	12.5	0.067	0.065	0.002	0.3
	13.5	0.072	0.070	0.002	0.3
	14.5	0.078	0.076	0.002	0.3
	15.5	0.075	0.073	0.002	0.3
	16.5	0.063	0.061	0.002	0.3
	17.5	0.058	0.056	0.002	0.3
19.3.77		$oz_1 = 3.50$	$oz_2 = 5.60$		
	7.5	0.072	0.077	0.005	0.2
	8.5	0.073	0.079	0.006	0.3
	9.5	0.064	0.070	0.006	0.3
	10.5	0.046	0.052	0.006	0.3
	11.5	0.029	0.036	0.007	0.3
	12.5	0.028	0.035	0.007	0.3
	13.5	0.025	0.032	0.007	0.3
	14.5	0.029	0.036	0.007	0.3
	15.5	0.031	0.037	0.006	0.3
08.6.68		$oz_1 = 3.50$	$oz_2 = 3.20$		
	9.5	0.453	0.454	0.001	0.3
	10.5	0.479	0.480	0.001	0.3
	11.5	0.469	0.470	0.001	0.3
	12.5	0.466	0.467	0.001	0.3
	13.5	0.485	0.486	0.001	0.3
	14.5	0.436	0.437	0.001	0.3
	15.5	0.376	0.377	0.001	0.3
	16.5	0.307	0.308	0.001	0.3

$$x = |\tau_{a_1} - \tau_{a_2}|$$



## APPENDIX 4

MEAN DAILY MAXIMUM AND MINIMUM VALUES OF  $\tau_a$  FOR CANADIAN LOCATIONS

Station	Period	$\tau_a$ (max)	No. of hours	Date	$\tau_a$ (min)	No. of hours	Date	No. of days per period
Montreal	1968-78							
	Jan-Feb	0.087	8	14.2.70	0.037	8	15.2.74	8
	Mar-Apr	0.119	9	11.4.71	0.020	9	22.3.76	26
	May-Jun	0.224	8	21.5.77	0.051	10	15.6.78	14
	Jul-Aug	0.478	9	28.8.74	0.023	11	21.8.78	23
	Sep-Oct	0.329	10	20.9.68	0.020	8	23.10.77	10
	Nov-Dec	0.055	6	19.12.78	0.007	8	5.11.77	10
Woodbridge	1968-78							
	Jan-Apr	0.116	8	17.3.75	0.030	8	23.3.73	23
	May-Jun	0.402	12	5.6.74	0.065	11	24.6.78	22
	Jul-Aug	0.225	11	9.8.70	0.105	12	24.8.69	8
	Sep-Oct	0.202	8	16.10.68	0.031	8	28.9.75	13
	Nov-Dec	0.065	6	30.12.70	0.024	6	13.12.76	6
Goose	1968-77							
	Jan-Feb	0.105	8	27.2.69	0.013	7	22.2.75	17
	Mar-Apr	0.066	8	18.4.75	0.014	8	13.3.77	17
	May-Jun	0.092	9	6.5.75	0.011	11	22.6.77	3
Hamilton	1977							
	May-Jun	0.256	10	22.5.77	0.089	9	14.5.77	4
Vancouver	1977-78							
	Jun-Aug	0.105	11	26.7.77	0.039	12	20.7.78	13
Charlotte- town	1978							
	Feb/Dec	0.181	7	20.2.78	0.007	6	24.12.78	4
	May-Aug	0.061	11	12.5.78	0.054	12	7.5.78	8
Winnipeg	1977							
	Jan-Mar	0.050	7	2.3.77	0.022	7	5.3.77	6
	Oct	0.042	7	19.10.77	0.017	9	2.10.77	5

## APPENDIX 5a

SEASONAL FREQUENCY DISTRIBUTION OF THE NUMBER OF OCCURRENCES OF  
CORRESPONDING  $\tau_a$  AND DRY-BULB TEMPERATURE VALUES FOR MONTREAL  
(1968-78)

Season/ $\tau_a$	Dry Bulb Temperature ( $^{\circ}\text{C}$ )				Total hrs.
	< 10	10 - 15	16 - 21	> 21	
Annual	< 10	10 - 15	16 - 21	> 21	
< 0.129	1053	243	200	160	1656
0.13 - 0.229	71	57	79	110	317
0.23 - 0.349	8	8	21	87	124
> 0.35	8	0	8	64	80
Total hours	1140	308	308	421	2177
Mean $\tau_a$	0.070	0.087	0.116	0.204	
Summer	< 15	15 - 20	21 - 26	> 26	
< 0.129	213	163	141	13	530
0.13 - 0.229	26	46	56	38	166
0.23 - 0.349	0	12	38	43	93
> 0.35	1	4	35	27	67
Total hours	240	225	270	121	856
Mean $\tau_a$	0.090	0.105	0.168	0.286	
Spring/Autumn	< 5	5 - 10	11- 16	> 16	
< 0.069	149	94	64	33	340
0.07 - 0.089	33	20	19	6	78
0.09 - 0.129	29	29	20	16	94
> 0.13	9	25	38	62	134
Total hours	220	168	141	117	646
Mean $\tau_a$	0.067	0.078	0.099	0.141	
Winter	< -20	-19 to -10	-9 to 0	> 0	
< 0.049	88	149	96	33	366
0.05 - 0.089	38	91	63	31	223
> 0.09	9	67	45	35	156
Total hours	135	307	204	99	745
Mean $\tau_a$	0.060	0.063	0.064	0.095	

## APPENDIX 5b

SEASONAL FREQUENCY DISTRIBUTION OF THE NUMBER OF OCCURRENCES OF  
CORRESPONDING  $\tau_a$  AND WET-BULB TEMPERATURE VALUES FOR MONTREAL (1968-78)

Season/ $\tau_a$	Wet-Bulb Temperature ( $^{\circ}\text{C}$ )				Total hrs.
	< 5	5 - 10	11 - 16	> 16	
Annual	< 5	5 - 10	11 - 16	> 16	
< 0.129	1034	247	294	82	1657
0.13 - 0.229	59	67	72	116	314
0.23 - 0.349	6	12	15	93	126
> 0.35	8	0	10	62	80
Total hours	1107	326	391	353	2177
Mean $\tau_a$	0.069	0.091	0.100	0.235	
Summer	< 5	5 - 10	11 - 16	> 16	
< 0.069	86	107	246	77	516
0.13 - 0.229	2	25	45	101	173
0.23 - 0.349	0	3	7	88	98
> 0.35	1	0	9	59	69
Total hours	89	135	307	325	856
Mean $\tau_a$	0.083	0.087	0.093	0.238	
Spring/Autumn	< 3	3 - 8	9- 14	> 14	
< 0.069	198	105	39	10	352
0.07 - 0.089	43	18	12	2	75
0.09 - 0.129	41	28	19	3	91
> 0.13	12	39	39	38	128
Total hours	294	190	109	53	646
Mean $\tau_a$	0.070	0.086	0.112	0.177	
Winter	< -12	-2 to -7	-6 to -1	> -1	
< 0.049	208	106	20	29	363
0.05 - 0.089	122	47	35	21	225
> 0.09	68	32	36	21	157
Total hours	398	185	91	71	745
Mean $\tau_a$	0.063	0.056	0.085	0.097	

## APPENDIX 6

CORRELATION BETWEEN VALUES OF  $\tau_a$  AND INVERSE OF VISIBILITY AT  
MONTREAL (1968-78)

v(km)	1/v	$\tau_a$	All size	$\tau_a$	Summer size	$\tau_a$	Winter size	$\tau_a$	Spring/Autumn size
2.32	0.431	0.231	10	0.109	2	0.262	8	-	-
3.10	0.323	0.215	4	-	-	0.382	1	0.159	3
4.75	0.211	0.272	16	0.433	5	0.146	4	0.229	7
6.40	0.156	0.235	43	0.296	24	0.129	11	0.196	8
8.00	0.125	0.252	40	0.294	22	0.194	10	0.209	8
9.70	0.103	0.237	57	0.313	29	0.105	11	0.195	17
11.30	0.088	0.236	22	0.371	8	0.117	5	0.182	9
12.90	0.078	0.222	69	0.274	39	0.118	6	0.162	24
14.50	0.069	0.247	4	0.284	3	-	-	0.137	1
16.10	0.062	0.180	92	0.207	54	0.128	23	0.161	15
19.30	0.052	0.161	112	0.197	58	0.087	22	0.145	32
24.60	0.041	0.093	422	0.128	164	0.062	166	0.083	96
32.20	0.031	0.107	150	0.152	44	0.080	52	0.095	56
40.20	0.025	0.078	271	0.110	81	0.065	154	0.064	40
48.30	0.021	0.072	240	0.100	77	0.046	110	0.082	59
56.30	0.018	0.066	112	0.088	16	0.046	61	0.090	35
64.40	0.016	0.059	79	0.074	28	0.045	23	0.055	30
72.40	0.014	0.047	428	0.052	208	0.041	79	0.044	143

## APPENDIX 7

ANNUAL CHANGES IN VALUES  $\tau_a$  AT MONTREAL, WOODBRIDGE, AND GOOSE

Station	Year	All Season $\tau_a$	size	Summer $\tau_a$	size	Winter $\tau_a$	size	Spring/Autumn $\tau_a$	size
Montreal									
	1968	0.161	134	0.219	40	0.117	46	0.154	48
	1969	0.128	181	0.172	58	0.089	52	0.120	71
	1970	0.146	144	0.214	37	0.107	76	0.162	31
	1971	0.151	131	0.238	49	0.095	48	0.102	34
	1972	0.098	145	0.118	81	0.075	26	0.072	38
	1973	0.093	112	0.121	37	0.067	40	0.094	35
	1974	0.090	212	0.173	56	0.045	111	0.100	45
	1975	0.128	124	0.192	63	0.050	42	0.091	19
	1976	0.100	225	0.145	105	0.058	81	0.066	39
	1977	0.083	265	0.103	116	0.053	68	0.078	81
	1978	0.068	499	0.091	211	0.050	156	0.054	132
	1968-1978	0.103	2172	0.141	853	0.067	746	0.092	573
Woodbridge									
	1968	0.201	85	0.325	32	0.039	14	0.157	39
	1969	0.107	130	0.098	60	0.065	36	0.168	34
	1970	0.224	66	0.281	39	0.074	15	0.227	12
	1971	0.148	95	0.180	52	0.081	5	0.112	38
	1972	0.107	146	0.125	79	0.074	20	0.092	47
	1973	0.103	68	0.131	20	0.049	29	0.157	19
	1974	0.087	190	0.131	91	0.029	40	0.158	59
	1975	0.129	280	0.164	168	0.068	33	0.080	79
	1976	0.133	215	0.166	114	0.051	26	0.111	75
	1977	0.103	218	0.128	92	0.084	64	0.085	62
	1978	0.090	172	0.120	94	0.063	19	0.051	59
	1968-1978	0.121	1665	0.155	841	0.062	301	0.116	504
Goose									
	1968	0.055	77	0.055	15	0.053	58	0.081	4
	1969	0.046	74	0.047	1	0.063	53	0.073	20
	1970	0.058	28	0.075	5	0.056	12	0.065	11
	1971	0.063	35	0.043	2	0.064	33	-	-
	1972	0.026	10	0.048	3	0.017	3	0.017	4
	1973	0.047	63	0.059	7	0.044	51	0.061	5
	1974	0.038	74	0.046	11	0.035	43	0.039	20
	1975	0.047	105	0.082	26	0.029	66	0.066	13
	1976	0.035	94	0.040	23	0.032	61	0.059	10
	1977	0.031	64	0.028	16	0.026	41	0.084	7
	1968-1977	0.047	624	0.054	109	0.043	421	0.061	94

APPENDIX 8

$T_{pm}/\tau_a$  FOR HAMILTON AND WOODBRIDGE

Hamilton			Woodbridge		
$T_{pm}/\tau_a$	$m$	$T_{pm}/\tau_a$	$T_{pm}/\tau_a$	$m$	$T_{pm}/\tau_a$
14.5.77	28.5.77	22.5.77	24.8.69	17.4.74	21.5.77
2.26	11.5	2.66	11.9	2.64	11.8
1.90	11.1	2.17	11.4	2.25	11.4
1.66	10.9	1.83	11.0	1.88	11.1
1.48	10.7	1.62	10.8	1.67	10.9
1.35	10.5	1.45	10.6	1.47	10.6
1.26	10.4	1.32	10.5	1.34	10.5
1.19	10.3	1.23	10.4	1.25	10.4
1.14	10.3	1.17	10.3	1.18	10.3
1.11	10.3	1.12	10.3	1.13	10.3
1.10	10.3	1.09	10.3	1.10	10.3
1.10	10.3	1.08	10.2	1.09	10.3
1.11	10.3	1.08	10.2	1.09	10.3
1.14	10.3	1.09	10.3	1.23	10.4
1.19	10.3	1.11	10.3	1.31	10.5
1.25	10.4	1.16	10.3	1.43	10.6
1.35	10.5	1.22	10.4	1.61	10.8
1.47	10.6	1.29	10.5	1.83	11.0
1.64	10.8	1.41	10.5		
1.88	11.1	1.56	10.7		
2.23	11.4	1.77	10.9		
2.76	12.0	2.08	11.3		
3.66	12.8				
				4.31	13.4
				2.45	11.7
				4.49	13.5
				2.50	11.8
				1.79	11.0
				1.45	10.7
				1.28	10.5
				1.28	10.3
				1.19	10.3
				1.27	10.4
				1.43	10.6
				1.76	11.0
				1.43	10.6
				1.27	10.4
				1.19	10.3
				1.19	10.3
				1.27	10.4
				1.45	10.7
				1.28	10.5
				1.28	10.3
				1.16	10.3
				1.10	10.3
				1.10	10.3
				1.16	10.3
				1.29	10.5
				1.29	10.3
				2.00	11.2
				3.03	12.2
				2.00	11.2
				2.00	11.2
				3.03	12.2

APPENDIX 9: MEAN VALUES OF ABSORPTION, SCATTERING, AND SOLAR IRRADIANCES FROM OTHER SOURCES

Source/ Station	Period	$\alpha_s$	Parameters			f			a	f+bta	bta	f/b	f+b/a	No. of records
			G	I	D	f+b	f	b						
Joseph and Wolfson (1975)														
Jerusalem	1968/70	0.25	0.65	0.48	0.17	0.13	0.11	0.02	0.16	0.29	0.17	7.1	0.82	18
Bet Dagan	1968/70	0.26	0.69	0.52	0.17	0.12	0.11	0.01	0.10	0.22	0.11	7.9	1.31	18
Robinson (1962)														
Halley Bay	1956-58	0.65	0.75	0.63	0.12	0.15	0.01	0.004	0.09	0.10	0.09	2.8	0.18	4
Kew	1947-51	0.15	0.62	0.48	0.14	0.08	0.07	0.02	0.18	0.26	0.19	4.3	0.45	3
Vienna	1938-50	0.15	0.61	0.46	0.15	0.08	0.06	0.02	0.17	0.25	0.19	3.2	0.49	4
Lwiro	Jan/56	0.15	0.75	0.66	0.09	0.04	0.04	0.008	0.08	0.12	0.09	4.5	0.56	5
Pretoria	Nov/56	0.15	0.75	0.66	0.09	0.04	0.04	0.007	0.08	0.12	0.09	4.8	0.53	5
Windhoek	Oct/55	0.15	0.78	0.69	0.09	0.04	0.03	0.006	0.06	0.10	0.06	5.3	0.70	5
Lerwick	1953/54/60	0.15	0.69	0.52	0.17	0.12	0.09	0.02	0.11	0.22	0.13	4.3	1.08	12
Malta	Jan-Aug/58	0.15	0.70	0.57	0.13	0.08	0.07	0.02	0.10	0.18	0.12	4.1	0.80	12
Robinson (1966)														
Kew	Mar/65	0.15	0.67	0.52	0.15	0.08	0.07	0.02	0.17	0.25	0.18	4.0	0.48	10
Bracknell	Mar/65	0.15	0.67	0.52	0.15	0.09	0.07	0.02	0.17	0.26	0.19	3.8	0.53	10

## REFERENCES

- Alkezweeny, A.J., and N.S. Laulainen, 1981: Comparison between polluted and clean air masses over Lake Michigan. J. Appl. Meteor., 20, 209-212.
- Ångström, A., 1961: Techniques of determining the turbidity of the atmosphere. Tellus, 13, 214-223.
- Atwater, M.A., 1977: Urbanization and pollutant effects on the thermal structure in four climatic regimes. J. Appl. Meteor., 16, 888-895.
- Bach, W., 1976: Global air pollution and climatic change. Rev. Geophys. Space Phys., 14, 429-474.
- Bach, W., and A. Daniels, 1975: Handbook of Air Quality in the United States. Oriental Publishing Company, Honolulu, 235 pp.
- Barlow, F., 1979: Modelling Solar Radiation Components in Aerosol Atmospheres. M.Sc. Thesis, McMaster University, 128 pp.
- Barrett, E.W., 1971: Depletion of short-wave irradiance at the ground by particles suspended in the atmosphere. Solar Energy, 13, 323-337.
- Bergstrom, R.W., 1973: Extinction and absorption coefficients of the atmospheric aerosol as a function of particle size. Contrib. Atmos. Phys., 46, 223-234.
- Bergstrom, R.W., and J.T. Peterson, 1977: Comparison of predicted and observed solar radiation in an urban area. J. Appl. Meteor., 16, 1107-1116.
- Bevington, P.R., 1969: Data Reduction and Error Analysis for the Physical Sciences. McGraw-Hill Book Company, New York, 336 pp.
- Bolle, H.J., ed., 1977: Radiation in the Atmosphere. Science Press, Princeton, 630 pp.
- Bradley, J.V., 1968: Distribution-Free Statistical Tests. Prentice-Hall, Inc., New Jersey, 388 pp.
- Braslau, N., and J.V. Dave, 1973a: Effect of aerosols on the transfer of energy through realistic model atmospheres. Part I: Non-absorbing aerosols. J. Appl. Meteor., 12, 601-615.
- Braslau, N., and J.V. Dave, 1973b: Effect of aerosols on the transfer of energy through realistic model atmospheres. Part II: Partly-absorbing aerosols. J. Appl. Meteor., 12, 616-619.



- Bryson, R.A., 1968: All other factors being constant. Weatherwise, 21, 56-61.
- Bullrich, K., 1964: Scattered radiation in the atmosphere and the natural aerosol. Advances in Geophysics, 10, 99-260.
- Byers, H.R., 1974: General Meteorology. McGraw-Hill Book Company, 461 pp.
- Cadle, R.D., and G.W. Grams, 1975: Stratospheric aerosol particles and their optical properties. Rev. Geophys. Space Phys., 13, 475-501.
- Canada. Atmospheric Environment Service Ozone Data for the World. Toronto.
- Carlson, T.N., J.M. Prospero, and K.J. Hanson, 1973: Attenuation of solar radiation by windborne Saharan dust off the west coast of Africa. NOAA Technical Memorandum, ERL WMPO-7, NHRL 106, 1-27.
- Carlson, T.N., 1975: A Compilation of Solar Radiation Measurements Made on Sal, Cape Verde During GATE. The Pennsylvania State University, Pennsylvania, 160 pp.
- Carlson, T.N., and R.S. Caverly, 1977: Radiative characteristics of Saharan dust at solar wavelengths. J. Geophys. Res., 82, 3141-3152.
- Carlson, T.N., and J.M. Prospero, 1977: Saharan air outbreaks: meteorology, aerosols, and radiation. U.S. GATE Central Program Workshop Report to N.S.F. of workshop held in Boulder, Colorado, 25 July-12 August, 1977. NCAR publ., 57-78.
- Carlson, T.N., and P. Wendling, 1977: Reflected radiance measured by NOAA 3 VHRR as a function of optical depth for Saharan dust. J. Appl. Meteor., 16, 1368-1371.
- Carlson, T.N., 1979: Atmospheric turbidity in Saharan dust outbreaks as determined by analyses of satellite brightness data. Mon. Wea. Rev., 107, 322-335.
- Carlson, T.N., and S.G. Benjamin, 1980: Radiative heating rates for Saharan dust. J. Atmos. Sci., 37, 193-213.
- Chandrasekhar, S., 1960: Radiative Transfer. Dover Publications, Inc., New York, 393 pp.
- Charlock, T.P., and W.D. Sellers, 1980: Aerosol effects on climate: calculations with time-dependent and steady-state radiative-convective models. J. Atmos. Sci., 37, 1327-1341.
- Charlson, R.J., N.C. Ahlquist, and H. Horvath, 1968: On the generality of correlation of atmospheric aerosol mass concentration and light scatter. Atmos. Environ., 2, 455-464.

- Charlson, R.J., and M.J. Pilat, 1969: Climate: The influence of aerosols. J. Appl. Meteor., 8, 1001-1002.
- Chýlek, P., and J.A. Coakley, Jr., 1973: Man-made aerosols and heating of the atmosphere over Polar regions. Climate of the Arctic. ed., G. Weller and S.A. Bowling, Geophysical Institute, University of Alaska, Fairbanks, 159-165.
- Chýlek, P., and J.A. Coakley, Jr., 1974: Aerosols and climate. Science, 183, 75-77.
- Chýlek, P., G.W. Grams, G.A. Smith, and P.B. Russell, 1975: Hemispherical backscattering by aerosols. J. Appl. Meteor., 14, 380-387.
- Clark, T.L., 1980: Annual anthropogenic pollutant emissions in the United States and Southern Canada east of the Rocky Mountains. Atmos. Environ., 14, 961-970.
- Coakley, J.A., Jr., and P. Chýlek, 1975: The two-stream approximation in radiative transfer: including the angle of the incident radiation. J. Atmos. Sci., 32, 409-418.
- Coakley, J.A., Jr., 1977: Aerosols and the Earth's radiation budget. Radiation in the Atmosphere. ed. H.J. Bolle, Science Press, Princeton, 464-468.
- Dalrymple, G.J., and M.H. Unsworth, 1978: Longwave radiation at the ground: IV. Comparison of measurement and calculation of radiation from cloudless skies. Quart. J.R. Met. Soc., 104, 989-997.
- Daniel, H., 1980: Man and Climatic Variability. WMO-No.543, World Meteorological Organization, Geneva, 32 pp.
- Dave, J.V., 1978: Effect of aerosols on the estimation of total ozone in an atmospheric column from the measurement of its ultraviolet radiance. J. Atmos. Sci., 35, 899-911.
- Davies, J.A., P.J. Robinson, and M. Nunez, 1970: Radiation Measurement Over Lake Ontario and the Determination of Emissivity. First Report. Department of Geography, McMaster University, Hamilton, Ontario, 85 pp.
- Davies, J.A., 1980: Models for Estimating Incoming Solar Irradiance. Report to the Atmospheric Environment Service, DSS Contract No. OSU79-00163, 100 pp.
- Davies, J.A., and J.E. Hay, 1980: Calculation of the solar radiation incident on a horizontal surface. Proceedings of the First Solar Radiation Data Workshop, edited by T. Won and J.E. Hay, 32-58.
- Davies, J.A., and L.J.B. McArthur, 1980: Effect of aerosols on climate. The Effects of Aerosols on Atmospheric Processes, edited by R.C. Pierce and J. Young, National Research Council of Canada (in press).

- Davies, J.A., and D.C. McKay, 1981: Evaluation of methods for estimating solar irradiance in Canada. Fourth Conference on Atmospheric Radiation, June 16-18, Toronto. American Meteorological Society, Boston, Massachusetts.
- Deirmendjian, D., 1969: Electromagnetic Scattering by Spherical Polydispersions. American Elsevier, New York, 290 pp.
- DeLuisi, J.J., P.M. Furukawa, D.A. Gillette, B.G. Schuster, R.J. Charlson, W.M. Porch, R.W. Fegley, B.M. Herman, R.A. Rabinoff, J.T. Twitty, and J.A. Weinman, 1976: Results of a comprehensive atmospheric aerosol-radiation experiment in the Southwestern United States. Part I: Size distribution, extinction optical depth and vertical profiles of aerosols suspended in the atmosphere. J. Appl. Meteor., 15, 441-454.
- DeLuisi, J.J., and B.M. Herman, 1977: Estimation of solar radiation absorption by volcanic stratospheric aerosols from Agung using surface-based observations. J. Geophys. Res., 82, 3477-3480.
- DeLuisi, J.J., J.E. Bonelli, and C.E. Shelden, 1977: Spectral absorption of solar radiation by the Denver brown (pollution) cloud. Atmos. Environ., 11, 829-836.
- Drummond, A.J., and G.D. Robinson, 1974: Some measurements of the attenuation of solar radiation during BOMEX. Appl. Opt., 13, 487-492.
- Dyer, A.J., and B.B. Hicks, 1965: Stratospheric transport of volcanic dust inferred from solar radiation measurements. Nature, 208, 131-133.
- Dyer, A.J., and B.B. Hicks, 1968: Global spread of volcanic dust from the Bali eruption of 1963. Quart. J. R. Met. Soc., 94, 545-554.
- Eisenbud, M., 1980: Overview of aerosol research. Ann. N. Y. Acad. Sci., 338, 599-604.
- Elterman, L., 1968: UV, visible and IR attenuation for altitudes to 50 km. Air Force Cambridge Research Laboratories, Environmental Research Paper No. 285.
- Ensol, D.S., W.M. Porch, M.J. Pilat, and R.J. Charlson, 1971: Influence of the atmospheric aerosol on albedo. J. Appl. Meteor., 10, 1303-1306.
- Espencheid, W.F., M. Kerker, and E. Matijevic, 1964: Logarithmic distribution functions for collidal particles. J. Phys. Chem., 68, 3093-3097.
- Feigelson, E.M., V.N. Kapustin, G.N. Martianova, B.A. Semenchko, 1975: Aerosol and water vapour influences on direct solar radiation fluxes in the centre of Equatorial Atlantic. GATE Report No. 14. Preliminary Scientific Results (Vol. 11) of GATE, World Meteorological Organization, Geneva, 290-295.

- Flowers, E.C., R.A. McCormick, and K.R. Kurfis, 1969: Atmospheric turbidity over the United States, 1961-1966. J. Appl. Meteor., 8, 955-962.
- Forbes, A.J., and R.A. Hamilton, 1971: Clear sky radiation measurement at Lerwick. Quart. J. R. Met. Soc., 97, 99-102.
- Friedlander, S.K., 1977: Smoke, Dust and Haze. Fundamentals of aerosol behavior. John Wiley & Sons, New York, 317 pp.
- Gerber, H.E., 1979: Absorption of 632.8 nm radiation by maritime aerosols near Europe. J. Atmos. Sci., 36, 2502-2512.
- Grassl, H., 1973: Separation of atmospheric absorbers in the 8-13 micrometer region. Contrib. Atmos. Phys., 46, 75-88.
- Grassl, H., 1974: Influence of different absorbers in the window region on radiative cooling (and on surface temperature determination). Contrib. Atmos. Phys., 47, 1-13.
- Gulbrandsen, A., 1978: On the use of pyranometers in the study of spectral solar radiation and atmospheric aerosols. J. Appl. Meteor., 17, 899-904.
- Halpern, P., and K.L. Coulson, 1976: A theoretical investigation of the effect of aerosol pollutants on short-wave flux divergence in the lower atmosphere. J. Appl. Meteor., 15, 464-469.
- Hamilton, R.A., and R.H. Collingbourne, 1967: A difficulty in the interpretation of certain solar radiation measurement. Quart. J. R. Met. Soc., 93, 186-194.
- Hänel, G., 1976: The properties of atmospheric aerosol particles as functions of the relative humidity at thermodynamic equilibrium with the surrounding moist air. Advances in Geophysics, 19, 73-188.
- Hänel, G., 1976: The single-scattering albedo of atmospheric aerosol particles as a function of relative humidity. J. Atmos. Sci., 33, 1120-1124.
- Hansen, J.E., and L.D. Travis, 1974: Light scattering in planetary atmospheres. Space Sci. Rev., 16, 527-610.
- Hansen, J.E., A.A. Lacis, P. Lee, and W.C. Wang, 1980: Climatic effects of atmospheric aerosols. Ann. N. Y. Acad. Sci., 338, 575-587.
- Hare, F.K., and M.K. Thomas, 1974: Climate Canada. Wiley Publishers of Canada Limited, Toronto, 256 pp.
- Hay, J.E., and T.R. Oke, 1976: The Climate of Vancouver. B.C. Geographical Series, Number 23, Tantalus Research Limited, Vancouver, 47 pp.
- Herman, B.M., and S.R. Browning, 1975: The effect of aerosols on the Earth-atmosphere albedo. J. Atmos. Sci., 32, 1430-1445.

- Hogan, A.W., 1968: An experiment illustrating that gas conversion by solar radiation is a major influence in the diurnal variation of Aitken nucleus concentrations. Atmos. Environ., 2, 599-601.
- Horvath, H., 1971: On the applicability of the Koschmieder visibility formula. Atmos. Environ., 5, 177-184.
- Idso, S.B., and K.R. Cooley, 1981: Meteorological modification of particulate air pollution and visibility patterns at Phoenix, Arizona. Arch. Meteor. Geophys. Bioklim., Ser. B, 29, 229-237.
- Jones, P.A., and J.E. Jiusto, 1980: Some local climate trends in four cities of New York State. J. Appl. Meteor., 19, 135-141.
- Joseph, J.H., and A. Manes, 1971: Secular and seasonal variations of atmospheric turbidity at Jerusalem. J. Appl. Meteor., 10, 453-462.
- Joseph, J.H., and N. Wolfson, 1975: The ratio of absorption to backscatter of solar radiation by aerosols during Khamsin conditions and effects on the radiation balance. J. Appl. Meteor., 14, 1389-1396.
- Joseph, J.H., W.J. Wiscombe, and J.A. Weinman, 1976: The Delta-Eddington approximation for radiative flux transfer. J. Atmos. Sci., 33, 2452-2459.
- Junge, C.E., 1963: Air Chemistry and Radioactivity. Academic Press, New York, 382 pp.
- Kasten, F., 1966: A new table and approximation formula for the relative optical air mass. Archiv. for Meteor., Geophys. un Bioklim, B14, 206-223.
- King, M.D., 1979: Determination of the ground albedo and the index of absorption of atmospheric particulates by remote sensing. Part II: Application. J. Atmos. Sci., 36, 1072-1083.
- Komp, M.J., and A.H. Auer, Jr., 1978: Visibility reduction and accompanying aerosol evolution downwind of St. Louis. J. Appl. Meteor., 17, 1357-1367.
- Kondratyev, K. Ya., 1972: Radiation Processes in the Atmosphere. WMO-No. 309, World Meteorological Organization, Geneva, 214 pp.
- Kondratyev, K.Ya., O.D. Barteneva, L.I. Chapursky, A.P. Chernenko, V.S. Grishechkin, L.S. Ivlev, V.A. Ivanov, V.I. Korzov, V.B. Lipatov, M.A. Prokofyev, V.K. Tolkatchev, O.B. Vasiliev, and V.F. Zhvaley, 1976: Aerosol in the GATE Area and its Radiative Properties. Atmospheric Science Paper No. 247, Department of Atmospheric Science, Colorado State University, Fort Collins, Colorado, 109 pp.
- Kondratyev, K.Ya., 1977: Summary of Caenex. Radiation in the Atmosphere. ed. H.J. Bolle, Science Press, Princeton, 6-12.

- Konyukh, L.A., F.B. Yurevich, R.D. Cess, and Harshvardham, 1979: Tropospheric aerosols: Effects upon the surface and surface-atmosphere radiation budgets. J. Quant. Spectrosc. Radiat. Transfer, 22, 483-488.
- Kriebel, K.T., 1978: On the determination of the atmosphere optical depth by measurements of the meteorological range. Beitr. Phys. Atmos., 51, 330-337.
- Kuhn, P.M., H.K. Weickmann, and L.P. Stearns, 1975: Longwave radiation effects of the Harmattan haze. J. Geophys. Res., 80, 3419-3424.
- Lacis, A.A., and J.E. Hansen, 1974: A Parameterization for the absorption of solar radiation in the Earth's atmosphere. J. Atmos. Sci., 31, 118-133.
- Laktionov, A.G., V.N. Adnashkin, V.M. Kopchenov, A.Yu. Semova, O.B. Stsiborskiy, 1975: On the relation between optical and aerosol characteristics of the east Atlantic atmosphere. GATE Report No. 14. Preliminary Scientific Results (Vol. 11) of GATE, World Meteorological Organization, Geneva, 296-298.
- Latimer, J.R., 1972: Radiation Measurement. International Field Year for the Great Lakes, Technical Manual Series No. 2, 53 pp.
- Laulainen, N.S., and B.J. Taylor, 1974: The Precision and accuracy of Volz sun-photometry. J. Appl. Meteor., 13, 298-302.
- Laulainen, N.S., and B.J. Taylor, 1975: The precision and accuracy of Volz sun-photometry, II. Causes of systematic error. J. Appl. Meteor., 14, 1214-1217.
- Leaderer, B.P., and J.A.J. Stolwijk, 1980: Optical properties of the urban aerosol and their chemical composition. Ann. N. Y. Acad. Sci., 338, 70-85.
- Leighton, P.A., 1973: Geographical aspects of air pollution. Climate in Review. ed. G. McBoyle, Houghton Mifflin Company, Boston, 226-240.
- Levin, Z., and J.D. Linberg, 1979: Size distribution, chemical composition, and optical properties of urban and desert aerosols in Israel. J. Geophys. Res., 84, 6941-6950.
- Levin, Z., J.H. Joseph, and Y. Mekler, 1980: Properties of Sharav (Khamsin) dust - Comparison of optical and direct sampling data. J. Atmos. Sci., 37, 882-891.
- Lin, Chin-i, Mbaker, and R.J. Charlson, 1973: Absorption coefficient of atmospheric aerosol: a method of measurement. Appl. Opt., 12, 1356-1363.
- Linke, F., 1942: Die sonnenstrahlung und ihre Schwachung in der atmosphäre. Handbuch der Geophysik, 8, Borntrager, Berlin, 239-332.

- London, J., 1977: Observation of the solar flux at the top of the atmosphere -- A brief overview. Radiation in the Atmosphere. ed. H.J. Bolle, Science Press, Princeton, viii-xvii.
- Ludwig, J.H., G.B. Morgan, and T.B. McMullen, 1971: Trends in urban air quality. Man's Impact on the Climate. ed. W.H. Matthews, W.W. Kellogg, and G.D. Robinson. MIT Press, Cambridge, Massachusetts, 321-338.
- McArthur, L.J.B., 1976: Determination and Analysis of Turbidity over Hamilton, Ontario. B.Sc. Thesis, Department of Geography, McMaster University, 124 pp.
- McCartney, H.A., 1975: Spectral Distribution of Solar Radiation Within and Above Crops. Ph.D. Thesis, University of Nottingham, 167 pp.
- McCartney, E.J., 1976: Optics of the Atmosphere; Scattering by Molecules and Particles. John Wiley & Sons, New York, 408 pp.
- McClatchey, R.A., R.W. Fenn, J.E.A. Selby, F.E. Volz, and J.S. Garing, 1970: Optical Properties of the Atmosphere. AFCRL-70-0527, AD 715270.
- McCormick, R.A., and J.H. Ludwig, 1967: Climate modification by atmospheric aerosols. Science, 156, 1358-1359.
- Meador, W.E., and W.R. Weaver, 1980: Two-stream approximations to radiative transfer in planetary atmospheres: A unified description of existing methods and a new improvement. J. Atmos. Sci., 37, 630-643.
- Middleton, P.B., and J.R. Brock, 1977: Modeling the urban aerosol. J. Air. Pollut. Control Assoc., 27, 771-775.
- Miller, J.R., ed., 1980: Prospects for Man: Climatic Change. The Centre for Research on Environmental Quality, Faculty of Science, York University, 253 pp.
- Mitchell, J.M., Jr., 1971: The effect of atmospheric aerosols on climate with special reference to temperature near the earth's surface. J. Appl. Meteor., 10, 703-714.
- Morales, C., ed., 1979: Saharan Dust: Mobilization, Transport, Deposition. SCOPE 14, John Wiley & Sons, New York, 320 pp.
- Munn, R.E., 1973: A study of suspended particulate air pollution at two locations in Toronto, Canada. Atmos. Environ., 7, 311-318.
- Neumann, J., 1977: Averaging for wind speed in a given direction in the concentration equation for pollutants. J. Appl. Meteor., 16, 1097-1100.
- Oke, T.R., 1978: Boundary Layer Climates. Methuen & Co. Ltd., London, 372 pp.
- Oke, T.R., and G.E. Maxwell, 1975: Urban heat island dynamics in Montreal and Vancouver. Atmos. Environ., 9, 191-200.

- Painter, H.E., 1981: The shade ring correction for diffuse irradiance measurements. Solar Energy, 26, 361-363.
- Paltridge, G.W., 1969: A note on the calculation of aerosol absorption from solar radiation measurements. Quart. J. R. Met. Soc., 95, 650-662.
- Paltridge, G.W., 1972: Direct measurement of water vapour absorption of solar radiation in the free atmosphere. J. Atmos. Sci., 30, 156-160.
- Paltridge, G.W., and C.M.R. Platt, 1973: Absorption and scatter of radiation by an aerosol layer in the free atmosphere. J. Atmos. Sci., 30, 734-737.
- Paltridge, G.W., and C.M.R. Platt, 1976: Radiative Processes in Meteorology and Climatology. Elsevier, Amsterdam, 318 pp.
- Patterson, E.M., and D.A. Gillette, 1977: Measurements of visibility vs mass-concentration for airborne soil particles. Atmos. Environ., 11, 193-196.
- Peterson, J.T., E.C. Flowers, and J.H. Rudisill, 1978: Urban-rural solar radiation and atmospheric turbidity measurements in the Los Angeles Basin. J. Appl. Meteor., 17, 1595-1609.
- Peterson, J.T., E.C. Flowers, G.J. Berri, C.L. Reynolds, and J.H. Rudisill, 1981: Atmospheric turbidity over central North Carolina. J. Appl. Meteor., 20, 229-241.
- Pitts, D.E., W.E. McAllum, M. Heidt, K. Jeske, J.T. Lee, D. DeMonbrun, A. Morgan, and J. Potter, 1977: Temporal variations in atmospheric water vapour and aerosol optical depth determined by remote sensing. J. Appl. Meteor., 16, 1312-1321.
- Polavarapu, R.J., 1978: Atmospheric turbidity over Canada. J. Appl. Meteor., 17, 1368-1374.
- Powe, N.N., 1969: Climate of Montreal. Climatological Studies No. 15, Department of Transport, Meteorological Branch, Ottawa.
- Prospero, J.M., R.T. Nees, and D. Savoie, 1976: Atmospheric Aerosol Measurements during GATE. Tech. Rep. No. TR76-5, University of Miami, GATE data archives, 18 pp.
- Prospero, J.M., D.L. Savoie, T.N. Carlson, and R.T. Nees, 1979: Monitoring Saharan aerosol transport by means of atmospheric turbidity measurements. Saharan Dust. ed., C. Morales, SCOPE 14, John Wiley & Sons, New York, 171-186.
- Rasool, S.I., and S.H. Schneider, 1971: Atmospheric carbon dioxide and aerosols: Effects of large increases on global climate. Science, 173, 138-141.
- Reiquam, H., 1970: An atmospheric transport and accumulation model for airsheds. Atmos. Environ., 4, 233-247.



- Roach, W.T., 1961: Some aircraft observations of fluxes of solar radiation in the atmosphere. Quart. J. R. Met. Soc., 87, 346-363.
- Robinson, G.D., 1962: Absorption of solar radiation by atmospheric aerosol, as revealed by measurements at the ground. Arch. Meteor. Geophys. Bioklim., Ser. B, 12, 19-40.
- Robinson, G.D., 1966: Some determinations of atmospheric absorption by measurements of solar radiation from aircraft and at the surface. Quart. J. R. Met. Soc., 92, 263-269.
- Robinson, N., ed., 1966: Solar Radiation. Elsevier Publishing Company, Amsterdam, 347 pp.
- Rouse, W.R., D. Noad, and J. McCutcheon, 1973: Radiation, temperature and atmospheric emissivities in a polluted urban atmosphere at Hamilton, Ontario. J. Appl. Meteor., 12, 798-807.
- Rouse, W.R., and R.L. Bello, 1979: Short-wave radiation balance in an urban aerosol layer. Atmosphere-Ocean, 17, 157-168.
- Russell, P.B., and G.W. Grams, 1975: Application of soil dust optical properties in analytical models of climate change. J. Appl. Meteor., 14, 1037-1043.
- Russell, P.B., and G.E. Shaw, 1975: Comments on "The Precision and Accuracy of Volz Sunphotometry". J. Appl. Meteor., 14, 1206-1209.
- Russell, P.B., and R.D. Hake, Jr., 1977: The post-Fuego stratospheric aerosol: Lidar measurements, with radiative and thermal implications. J. Atmos. Sci., 34, 163-177.
- Sagan, C., and J.B. Pollack, 1967: Anisotropic nonconservative scattering and the clouds of Venus. J. Geophys. Res., 72, 469-477.
- SCEP, 1970: Report of the study of critical environment problems. Man's Impact on the Global Environment. MIT Press, Cambridge, Massachusetts
- Schneider, S.H., 1971: A comment on "Climate: The Influence of aerosols". J. Appl. Meteor., 10, 840-841.
- Schuepp, W., 1949: Die Bestimmung der Komponenten der atmosphärischen Trübung aus Aktrometermessungen. Arch. Meteor. Geophys. Bioklim., B, 1, 257-346.
- Schütz, L., 1980: Long range transport of desert dust with special emphasis on the Sahara. Ann. N. Y. Acad. Sci., 338, 515-532.
- Secret, J.A., and I. Dirmhirn, 1979: Accuracies achievable with indirect measurements of the direct solar irradiance component. Solar Energy, 23, 509-512.

- Shettle, E.P., and R.W. Fenn, 1979: Models for the Aerosols of the Lower Atmosphere and the Effects of Humidity Variations on their Optical Properties. AFGL-TR-79-0214, ERP No. 676, Air Force Geophysics Laboratory, Hanscom, Massachusetts, 94 pp.
- SMIC, 1971: Inadvertent Climate Modification. The MIT Press, Cambridge, Massachusetts, 308 pp.
- Spencer, J.W., 1971: Computer estimation of direct solar radiation on clear days. Solar Energy, 13, 437-438.
- Thekaekara, M.P., and A.J. Drummond, 1971: Standard values for the solar constant and its spectral components. Nature Phys. Sci., 229, 7-9.
- Toon, O.B., and J.B. Pollack, 1976: A global average model of atmospheric aerosols for radiative transfer calculations. J. Appl. Meteor., 15, 225-246.
- Toon, O.B., and J.B. Pollack, 1980: Atmospheric aerosols and climate. American Scientist, 68, 268-278.
- Twitty, J.T., and J.A. Weinman, 1971: Radiative properties of carbonaceous aerosols. J. Appl. Meteor., 10, 725-731.
- Twomey, S., 1977: Atmospheric Aerosols. Elsevier Scientific Publishing Company, Amsterdam, 302 pp.
- Unsworth, M.H., and J.L. Monteith, 1972: Aerosol and solar radiation in Britain. Quart. J. R. Met. Soc., 98, 778-797.
- van de Hulst, H.C., 1957: Light Scattering by Small Particles. John Wiley & Sons, New York, 470 pp.
- Volz, F., 1969: Twilight and stratospheric dust before and after Agung eruption. Appl. Opt., 8, 2505-2517.
- Volz, F., 1975: Precision and accuracy of sunphotometry - A response. J. Appl. Meteor., 14, 1209-1213.
- Waldram, J.W., 1945: Measurement of the photometric properties of the upper atmosphere. Quart. J. R. Met. Soc., 71, 319-336.
- Wang, W., and G.A. Domoto, 1974: The radiative effect of aerosols in the Earth's atmosphere. J. Appl. Meteor., 13, 521-534.
- Weiss, R., R.J. Charlson, A.P. Waggoner, M.B. Baker, D. Covert, D. Thorsell, and S. Yuen, 1977: Application of directly measured aerosol radiative properties to climate models. Radiation in the Atmosphere. ed., H.J. Bolle, Science Press, Princeton, 469-471.
- Wesely, M.L., and R.C. Lipschutz, 1976: An experimental study of the effects of aerosols on diffuse and direct solar radiation received during the summer near Chicago. Atmos. Environ., 10, 981-987.

- Whitby, K.T., R.B. Husar, and B.Y.H. Liu, 1972: The aerosol size distribution of Los Angeles smog. J. Colloid Interface Sci., 39, 177-204.
- Wiscombe, W.J., 1977: The Delta-Eddington Approximation for a Vertically Inhomogeneous Atmosphere. Tech. Note NCAR/TN-121, National Center for Atmospheric Research, Boulder, Colorado, 66 pp.
- Wiscombe, W.J., and G.W. Grams, 1976: The backscattered fraction in a two-stream approximation. J. Atmos. Sci., 33, 2240-2451.
- World Meteorological Organization, 1971: Atmospheric turbidity data for the world, July-December, 1971. U.S. Dept. of Commerce, NOAA, Ashville, North Carolina.
- Wood, C.M., 1973: Visibility and sunshine in greater Manchester. Clean Air, 3, 15-24.
- Won, T., 1977: The Simulation of Hourly Global Radiation from Hourly Reported Meteorological Parameters - Canadian Prairie Area. Paper presented at the Third Conference, Canadian Solar Energy Society Inc., Edmonton, Alberta, 23 pp.
- Yamamoto, G., 1962: Direct absorption of solar radiation by atmospheric water vapour, carbon dioxide and molecular oxygen. J. Atmos. Sci., 19, 182-188.
- Yamamoto, G., M. Tanaka, and K. Arao, 1968: Hemispherical distribution of turbidity coefficient as estimated from direct solar radiation measurements. J. Meteor. Soc. Japan, 46, 278-300.
- Yamashita, S., 1974: A comparative study of turbidity in an urban and a rural environment at Toronto. Atmos. Environ., 8, 507-518.